2F

PNL-4032

UC-71

A Risk Assessment for the Transportation of Radioactive Zeolite Liners

Raymond H. V. Gallucci
Project Coordinator

January 1982

Prepared for the U.S. Department of Energy
under Contract DE-AC06-76RLO 1830

Pacific Northwest Laboratory
Operated for the U.S. Department of Energy
by Battelle Memorial Institute

Battelle

PNL-4032

DISCLAIMER

PACIFIC NORTHWEST LABORATORY
operated by
BATTELLE
for the
UNITED STATES DEPARTMENT OF ENERGY
under Contract DE-AC06-76RLO 1830

Printed in the United States of America
Available from
National Technical Information Service
United States Department of Commerce
5285 Port Royal Road
Springfield, Virginia 22151

NTIS Price Codes
Microfiche A01

Printed Copy

Pages	Price Codes
001-025	A02
026-050	A03
051-075	A04
076-100	A05
101-125	A06
126-150	A07
151-175	A08
176-200	A09
201-225	A010
226-250	A011
251-275	A012
276-300	A013

PNL-4032
UC-71

A RISK ASSESSMENT FOR THE TRANSPORTATION OF RADIOACTIVE ZEOLITE LINERS

Raymond H. V. Gallucci
Project Coordinator

Technical Contributors:

Raymond H. V. Gallucci
Michael J. Budden
Laurin R. Dodd
John R. Friley
Sue L. Sutter

January 1982

Prepared for the U.S. Department of Energy
Under Contract DE-AC06-76RLO 1830

Pacific Northwest Laboratory
Richland, Washington 99352

ACKNOWLEDGMENTS

The authors would like to acknowledge the assistance provided by Robert G. Rau in running the POPCOR program and A. Lynn Franklin with the TRECII program, both from Energy Systems Department. They would also like to thank Garry H. Bryan and Lawrence L. Petkus of the Chemical Technology Department for their assistance in providing input information for the study. Special note goes to Harold Van Tuyl, also of Chemical Technology, for his perceptive review of the draft report. Finally, the authors wish to acknowledge the secretarial efforts of Jenni Farnsworth in preparing this report.

TABLE OF CONTENTS

LIST OF TABLES

LIST OF FIGURES

1.0 SUMMARY

The risk is estimated for the shipment of radioactive zeolite liners in support of the Zeolite Vitrification Demonstration Program currently underway at Pacific Northwest Laboratory (PNL) under the sponsorship of the U.S. Department of Energy. This program will establish the feasibility of zeolite vitrification as an effective means of immobilizing high-specific-activity wastes.

In this risk assessment, it is assumed that two zeolite liners, each loaded around July 1, 1981 to 60,000 Ci, will be shipped by truck around January 1, 1982.[1] However, to provide a measure of conservatism, each liner is assumed to initially hold 70,000 Ci, with the major radioisotopes as follow:

$$^{90}Sr = 3{,}000 \text{ Ci}$$

$$^{134}Cs = 7{,}000 \text{ Ci}$$

$$^{137}Cs = 60{,}000 \text{ Ci}$$

Should shipment take place with essentially no delay after initial loading (regardless of loading date), the shipment loading would be only 2.7% higher than that for the assumed six-month delay. This would negligibly affect the overall risk.

The liners themselves are the ion-exchange columns of the Submerged Demineralizer System (SDS) which has been developed to decontaminate the high-activity-level water inside the containment and primary coolant system of Three-Mile-Island (TMI).[2] One each will be sealed inside a CNS 1-13C, type-B shipping cask mounted on a flatbed trailer. There will be one cask per truck. The shipping route covers approximately 2,600 miles from TMI near Harrisburg, Pennsylvania to PNL at Hanford, Washington. Except for some local routing near TMI and PNL, the shipments will be exclusively over federal highways.

The risk assessment considers radioactive releases resulting from transportation accidents. No potential release is anticipated during

normal (non-accident) transport. Three accident forces, as defined in reference 3, are considered and yield the following five accident scenarios:

1. Fire-only
2. Impact-only
3. Puncture-only
4. Impact-with-fire
5. Puncture-with-fire.

The inhalation pathway for radionuclides is presumed dominant. Thus, all radioactive releases are specified in terms of the amount airborne in the respirable range (10 μm or less).

Failure thresholds are estimated for release from these scenarios. Probabilities and amounts of release are calculated. A summary of these is presented in Table 1.1 for the major radioisotopes (^{90}Sr, ^{134}Cs, and ^{137}Cs). The probability of an airborne, respirable release occurring for any scenario is estimated at 8.4E-5 per shipment (1.7E-4 for two shipments). The results are then combined with models for the following factors to yield risk estimates:

1. Atmospheric dispersal of the radionuclides
2. Dose to the critical organs for the radionuclides
3. Population distribution along the transportation route.

The TRECII program is employed to calculate the risk estimates.[4]

The results are presented in two forms: the complementary cumulative density function and the total risk (expected dose). The risk is measured in terms of the 50-year inhalation dose to the exposed population (along the transport route) for the two shipments. The complementary cumulative density function is shown in Figure 1.1 (base case). The range of values (probabilities and doses) spanned by this curve indicates that the level of risk to the public is insignificant. Likewise, the total risk, a value of 5.3E-7 man-rem for the two shipments, also indicates that no significant risk will be posed to the public.

TABLE 1.1. Estimated Probabilities and Airborne Releases in the Respirable Range for Accident Scenarios

	ACCIDENT SCENARIOS												
	FIRE ONLY			IMPACT ONLY	PUNCTURE ONLY	IMPACT WITH FIRE				PUNCTURE WITH FIRE			
	Fire Duration (Min.)					Fire Duration (Min.)				Fire Duration (Min.)			
	15-30	30-60	60-150			0-15	15-30	30-60	60-150	0-15	15-30	30-60	60-150
PROB. OF RELEASE (PER SHIPMENT)	2.2E-5	3.4E-6	1.1E-6	5.7E-5	1.6E-7	2.1E-7	6.0E-8	9.4E-9	3.1E-9	5.9E-10	1.6E-10	2.6E-11	8.6E-12
SR-90 RELEASE (Ci)	.030	.13	.47	.0016	.0016	.0035	.034	.13	.48	.0020	.030	.13	.48
CS-134 RELEASE (Ci)	.059	.27	.99	7.3E-5	7.3E-5	.0043	.071	.29	1.1	8.8E-4	.061	.27	1.0
CS-137 RELEASE (Ci)	.59	2.7	9.9	6.9E-4	6.9E-4	.042	.71	2.9	11.	.0088	.61	2.7	10.

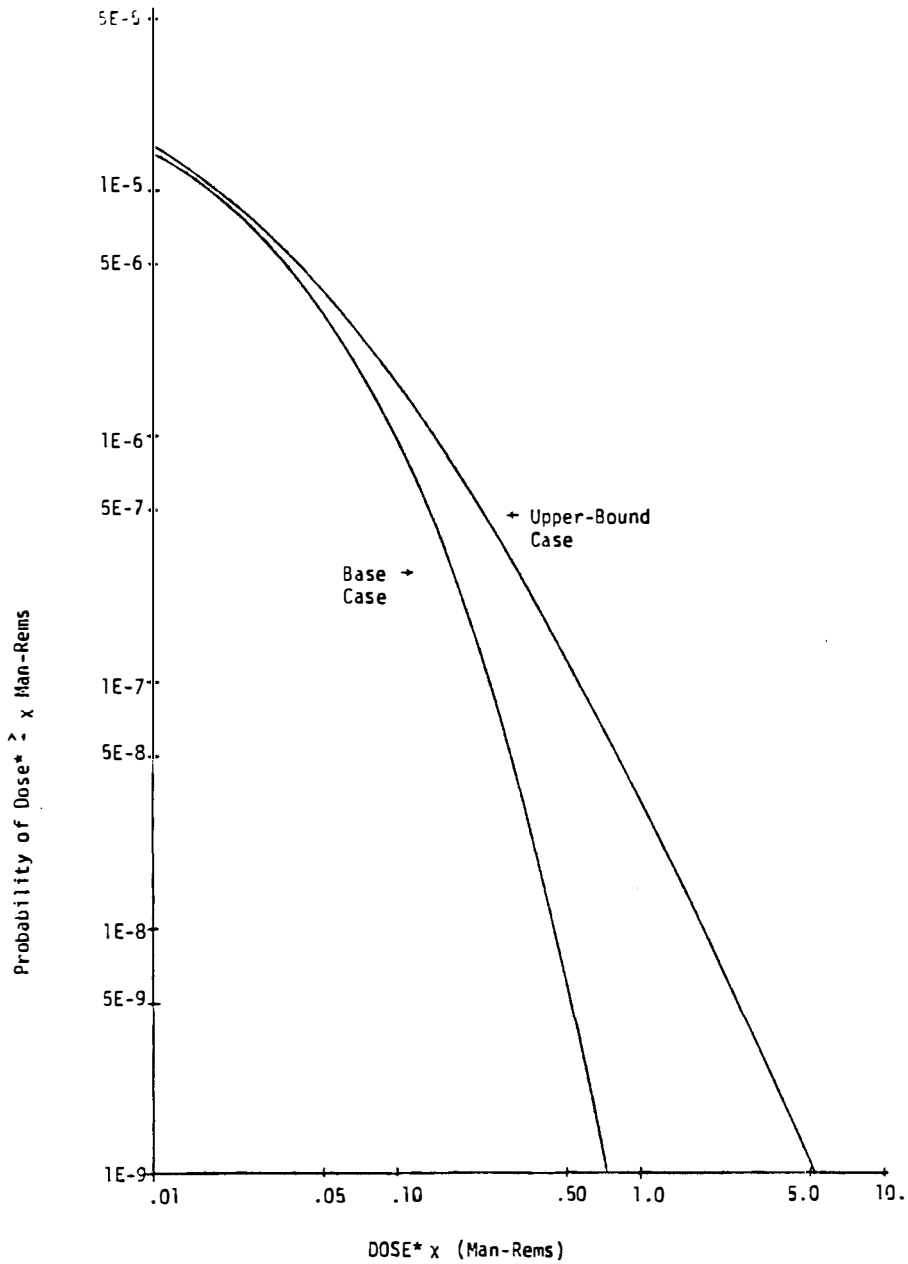

*50-yr inhalation dose to exposed population

FIGURE 1.1. Complementary Cumulative Density Function for Two Shipments

A sensitivity analysis is performed by assuming that the maximum estimable releases (airborne and respirable) of the major radioisotopes occur for the longest fire durations in the scenarios involving fire. The complementary cumulative density function (upper-bound case in Figure 1.1) exhibits an upward shift in probability at a given dose. The fractional shift increases with dose level. However, the range of values (probabilities and doses) spanned by this curve still indicates that the level of risk to the public is insignificant. The maximum dose from the least-likely scenario (5 man-rem at a probability of 1E-9 for two shipments) is only 1.2E-4 of the estimated exposure due to natural background radiation. Likewise, the total risk for the two shipments, while increasing by 28% to 6.8E-7 man-rem, still indicates that no significant risk will be posed to the public. This value is only 5.2E-10 of the estimated exposure due to natural background along the route and only 8.9E-4 of the total risk from accidents for analogous spent fuel shipment.

As a result of this risk assessment, it is concluded that the transport of the radioactive zeolite liners from TMI to PNL by truck can be conducted at an insignificant level of risk to the public.

REFERENCES

1. Evaluation of Increased Cesium Loading on Submerged Demineralizer System (SDS) Zeolite Beds. DOE/NE-0012; U.S. Department of Energy (May 1981).

2. Campbell, D. et al., Evaluation of the Submerged Demineralizer System (SDS) Flowsheet for Decontamination of High-Activity-Level Water at the Three-Mile Island Unit Two Nuclear Power Station. ORNL/TM-7448; Oak Ridge National Laboratory (July 1980).

3. Dennis, A., et al., Severities of Transportation Accidents Involving Large Packages. SAND77-0001; Sandia Laboratories (May 1978).

4. Franklin, A., TRECII: A Computer Program for Transportation Risk Assessment. PNL-3208; Pacific Northwest Laboratory (May 1980).

2.0 INTRODUCTION

The presence of a substantial amount of high-activity-level water in the containment and primary coolant system of the crippled Three-Mile Island (TMI), Unit 2 reactor has been an issue of much concern. The Submerged Demineralizer System (SDS) has been developed to decontaminate this water.[1] Through the use of zeolite ion-exchange columns, the levels of radioactive cesium and strontium in this water will be reduced substantially.

The need remains for safely disposing of the radioactively-loaded zeolite liners. A first step in this process is the immobilization of the radionuclides in a stable form. As part of this effort, Pacific Northwest Laboratory (PNL) has undertaken the Zeolite Vitrification Demonstration Program (ZVDP) which will establish the feasibility of zeolite vitrification as an effective means of immobilizing the TMI wastes. This program is sponsored by the U.S. Department of Energy.

The vitrification demonstration requires shipment of two radioactively-loaded zeolite liners from TMI to PNL. To assure that this shipment can be conducted at a minimal level of risk to the public, this risk assessment is performed as part of the ZVDP. The results are specific to these shipments.

Two zeolite liners, loaded to approximately 60,000 Ci each, will be shipped by truck using the CNS 1-13C, type-B shipping cask as an overpack. There will be one liner per cask, one cask per truck. This study assumes a loading date of July 1, 1981 for the zeolite liners and a shipping date of January 1, 1982.[2] To provide a degree of conservatism, an initial loading of 70,000 Ci, rather than the expected 60,000 Ci, has been assumed for each liner.

This assessment utilizes the results from previous transportation risk assessments in determining the shipping environment.[3-5] Previous studies have indicated that potential releases from non-accident situations (e.g., package closure errors) are negligible. The risk is dominated by

the accident environment. Thus, this study analyzes the risk from transportation accidents only. An analysis is performed for equilibrium conditions inside the liner-cask system during normal (non-accident) transport to ensure that no radioactive release is expected.

Accident scenarios are developed involving fire, impact, and puncture forces. Their probabilities are estimated along with the corresponding radioactive releases. The inhalation pathway for radionuclides is assumed dominant. Thus, these releases are specified in terms of the amounts airborne in the respirable range (10 μm or less). Estimates of the risk are made in terms of the 50-year inhalation dose to the exposed population. Atmospheric dispersion, diffusion climatology, and population distribution along the transport route are factored into the risk estimate. The risk is reported both as a complementary cumulative density function (probability vs. dose) and as a total expected (probabilistically-weighted) dose. A sensitivity analysis is performed by varying the release estimates for certain accident scenarios. Finally, the risk is compared with the level of exposure of the appropriate population due to natural background radiation and with the total risk from accidents for analogous spent fuel shipment.

REFERENCES

1. Campbell, D. et al., Evaluation of the Submerged Demineralizer System (SDS) Flowsheet for Decontamination of High-Activity-Level Water at the Three-Mile Island Unit 2 Nuclear Power Station. ORNL/TM-7448; Oak Ridge National Laboratory (July 1980).

2. Evaluation of Increased Cesium Loading on Sumberged Demineralizer System (SDS) Zeolite Beds. DOE/NE-0012; U.S. Department of Energy (May 1981).

3. McSweeney, T. et al., An Assessment of the Risk of Transporting Plutonium Dioxide and Liquid Nitrate by Truck. BNWL-1846; Pacific Northwest Laboratory (August 1975).

4. Elder, H. et al., An Assessment of the Risk of Transporting Spent Nuclear Fuel by Truck. PNL-2588; Pacific Northwest Laboratory (November 1978).

5. Geffen, C. et al., An Assessment of the Risk of Transporting Uranium Hexaflouride by Truck and Train. PNL-2211; Pacific Northwest Laboratory (August 1978).

3.0 TRANSPORTATION SYSTEM

Transport of the zeolite liners from TMI to PNL will be by truck over the interstate highway system. Each liner will be placed inside a CNS 1-13C, type-B shipping cask and transported on a flatbed trailer, one cask per trailer. Only two liners are expected to be shipped to PNL for the vitrification demonstration phase. Shipment is assumed to take place on January 1, 1982, as indicated in Reference 1.

3.1 ZEOLITE LINERS

The zeolite liners are the ion-exchange columns of the SDS that will be used to decontaminate high-activity-level water from TMI, Unit 2. This water is comprised of approximately 700,000 gal. from the containment building sump and 90,000 gal. from the primary coolant system.

3.1.1 Submerged Demineralizer System

The SDS was designed by Allied General Nuclear Services for Chem-Nuclear Systems, Inc. Reference 2 provides a thorough description of the SDS; only a brief overview is given here. Figure 3.1 is a flowsheet for the SDS. The contaminated water is filtered during transfer into the ion-exchange feed tanks, from which it is pumped through two parallel trains of ion-exchange columns. In each train is a series of three liners containing zeolite (a mixture of Linde Ionsiv IE-96 and A-51). The effluent from these trains passes through two parallel columns of organic cation-exchange resins. Subsequently, this effluent flows through a large polishing column containing cation, anion, and mixed resin layers.

The contaminated water that will be processed by the SDS has the radionuclide composition indicated in Table 3.1. Of these isotopes, the zeolite is primarily effective in removing those of Sr and Cs from the contaminated water. The liners in the first position will be removed after being loaded to approximately 60,000 Ci. The liners in positions two and three will be advanced, with a new liner being placed in the third position. This cycle will be repeated until decontamination is

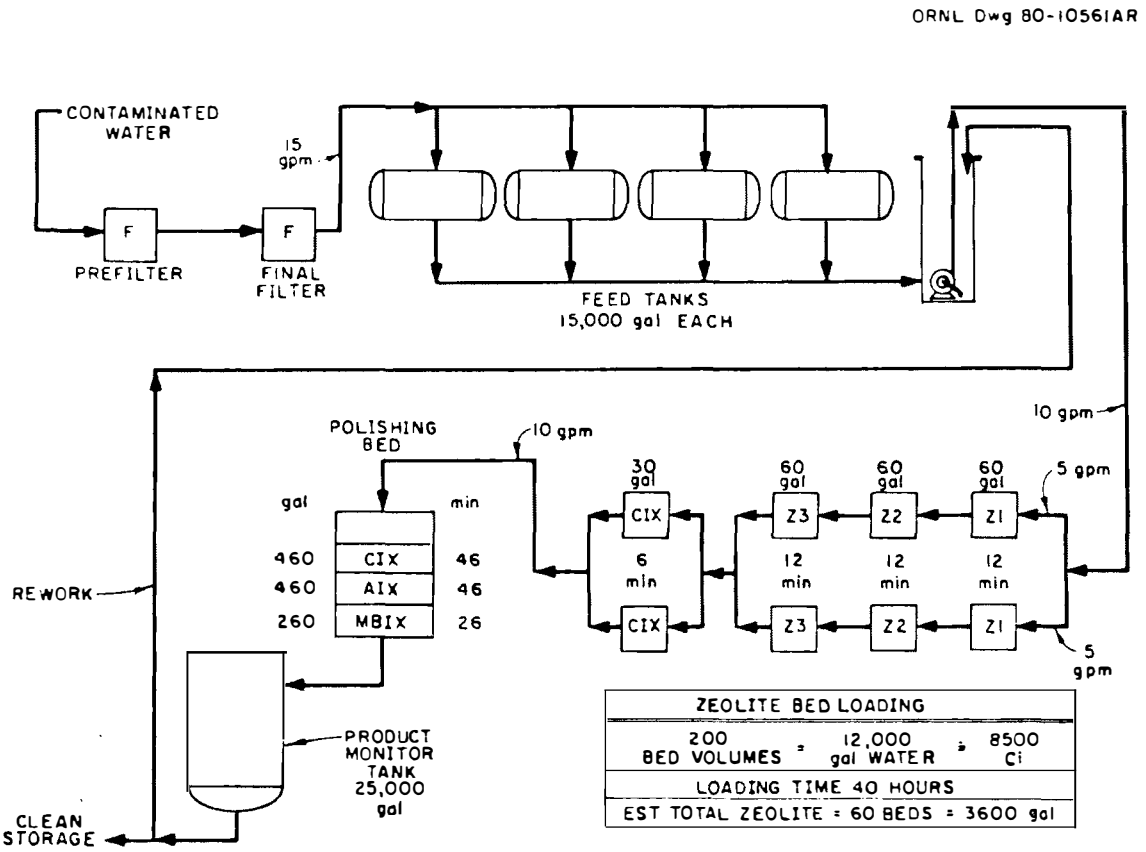

FIGURE 3.1.[2] Submerged Demineralizer System Flowsheet

TABLE 3.1.[2] Composition of Contaminated Water

(Values are corrected for radioactive decay to July 1, 1980).

	Reactor Coolant System	Containment Building Water	Total
Volume	90,000 gal	700,000 gal	790,000 gal
Sodium	1350 ppm	1200 ppm	3600 kg
Boron	3870 ppm	2000 ppm	38,000 kg (as H_3BO_3)
Cesium	1.5 ppm	0.8 ppm	4.8 kg
Strontium	< 0.05 ppm	0.1 ppm	0.4 kg

Nuclide	Conc. (μCi/mL)	Relative Ingestion Hazard[a]	Conc. (μCi/mL)	Relative Ingestion Hazard[a]	Total (Ci)
^{3}H	0.17	60	1.0	300	2,500
^{89}Sr	5[b]	2,000,000	0.53	200,000	3,000
^{90}Sr	25[b]	80,000,000	2.3	8,000,000	14,000
^{106}Ru	0.1	10,000	0.002	200	40
^{125}Sb	0.01	100	0.02	200	50
^{134}Cs	10	1,000,000	26	3,000,000	67,000
^{137}Cs	57	3,000,000	160	8,000,000	410,000
^{144}Ce	0.03	2,000	0.0005	50	10

[a]Expressed as multiples of the concentrations listed in 10 CFR 20, Appendix B, Table II, Column 2.

[b]Values vary, probably because of precipitation.

complete. This process enables the liners to sorb most of the Cs while in the first position. Sr sorption, requiring a longer residence time, will be primarily accomplished by the liners while in the second and third positions.

3.1.2 Structure

Figure 3.2 is a schematic of an individual SDS zeolite liner.[3] It is cylindrical with an overall height of 4 ft. 5 1/2 in. and an outer diameter of 2 ft. The vessel has a 68-gal. capacity and is cylindrical with curved ends. Its wall consists of 3/8 in. thick stainless steel. The vessel has been designed to withstand 350 psig at 400°F, or 15 psig at 850°F. Maximum operating pressure is 100 psig at 100°F. However, it has been hydrostatically tested to 530 psig. When empty, an individual liner weighs 650 lb_m.

3.1.3 Contents

Each SDS liner will contain 8.1 ft^3 of zeolite, an alumino-silicate containing water of hydration.[4] The zeolite will initially contain 17% by weight of water of hydration (henceforth referred to as "bound" water). At a bulk density of 46 lb_m/ft^3, the zeolite weighs 373 lb_m (including the bound water). Also present inside the liner will be "unbound" (non-hydrated, or free) water, 30% by weight of the zeolite. This unbound water weighs 112 lb_m, bringing the total weight of the liner's contents to 485 lb_m. Overall, the liner and its contents weigh 1,135 lb_m.

The total radioactivity of a zeolite liner when fully loaded is expected to be 60,000 Ci (as of July 1, 1981). For conservatism in assessing the risk, an initial loading of 70,000 Ci will be assumed. Table 3.2 lists the isotopic compositions for 10,000 Ci in the liner when loaded (July 1, 1981) and when shipped (January 1, 1982).[1] The isotopic compositions for 70,000 Ci, also listed in this table, are obtained by multiplying those for 10,000 Ci by seven.

Should shipment take place with essentially no delay after the initial loading (regardless of loading date), the shipment loading would be the same as the initial (70,000 Ci). This represents only a 2.7% increase in the assumed shipment loading (68,180 Ci to 70,000 Ci). Any effect upon the overall risk would be negligible.

All wall thicknesses are 3/8".

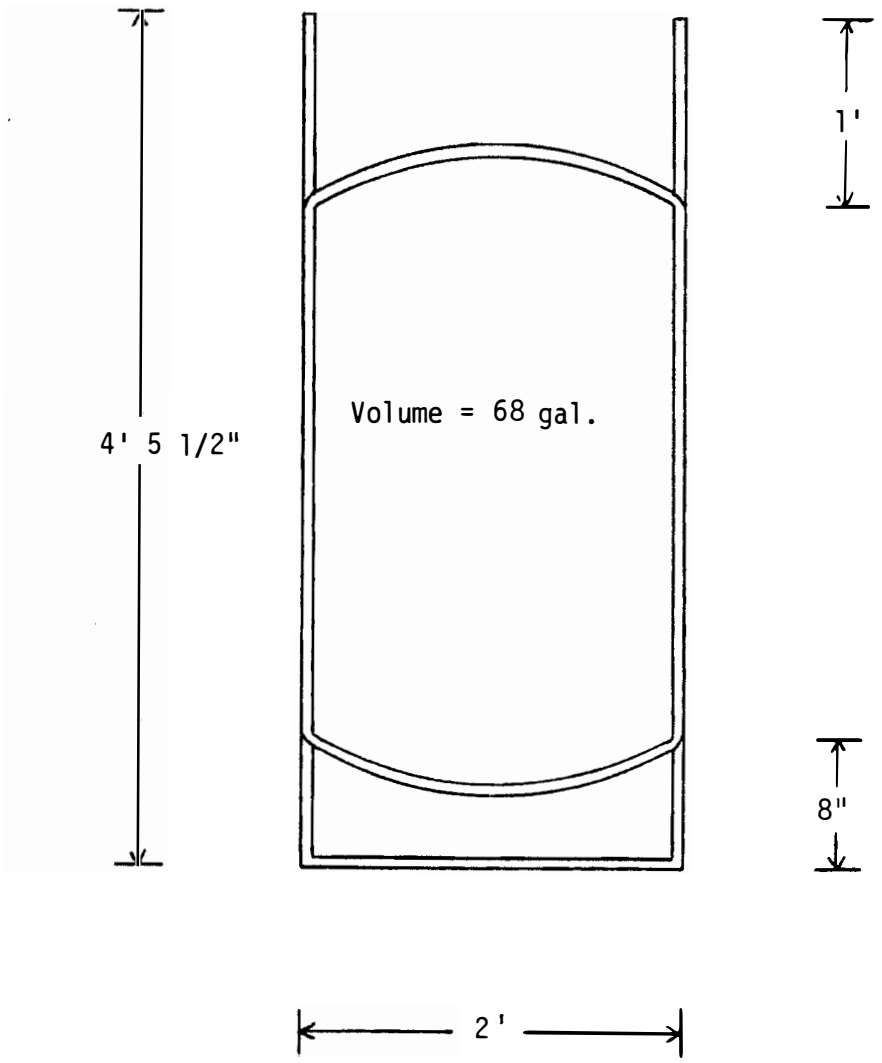

FIGURE 3.2. Simplified Schematic of a Zeolite Liner

TABLE 3.2. Radioisotopic Composition of an SDS Zeolite Liner

	ESTIMATED RADIOACTIVITY (Ci)			
	10,000-Ci INITIAL LOADING		70,000-Ci INITIAL LOADING	
ISOTOPE	As of Loading (7/1/81)	As of Shipment (1/1/82)	As of Loading (7/1/81)	As of Shipment (1/1/82)
^{89}Sr	.5	.04	3.5	.28
^{90}Sr	398.5	393.8	2,790	2,757
^{134}Cs	1,016	858.8	7,112	6,012
^{137}Cs	8,585	8,487	60,100	59,410
TOTAL	10,000	9,740	70,000	68,180

3.2 SHIPPING CASK

The zeolite liners will be shipped from TMI to PNL by truck using CNS 1-13C shipping casks, type-B casks made by Chem-Nuclear Systems, Inc. Each cask will contain one liner; there will be one cask per truck. For selection, this cask had to satisfy the following constraints:

1. it must be certified for type-B shipments[5]
2. its inner dimensions must accommodate the zeolite liner
3. it must provide adequate shielding for the given radioactive loading of the liner
4. it must be compatible with the equipment available at the shipping and receiving facilities
5. it must reject enough decay heat to ensure that no adverse thermal effects upon it or its contents occur.

For a liner loading of 60,000 Ci, the CNS 1-13C cask satisfies these constraints. The details involved in verifying this are discussed in references 1 and 6. This cask is still expected to satisfy these constraints at the assumed loading of 70,000 Ci per liner.

Figure 3.3 is a schematic of the CNS 1-13C cask.[6] It is a steel-encased, lead-shielded cylinder 5 ft. 8 1/16 in. high (without impact limiters) and 3 ft. 3 1/8 in. wide. When attached, the impact limiters raise the overall height to 8 ft. 3 13/16 in. Each limiter has an outer diameter of 5 ft. The cask has a cylindrical inner cavity that is 4 ft. 6 in. high and 2 ft. 2 1/2 in. wide. A zeolite liner will fit snugly into this volume.

The cask's outer wall consists of steel fire protection sheets that are separated from an interior steel plate by 16-gage wires spaced 6 in. apart. Between this interior plate and the innermost steel plate is lead shielding, 5 in. thick around the sides, 6 in. thick in the base and 5 25/32 in. thick in the lid. Twelve 1 1/4-in. bolts attach the steel-plated, plug-type lid to the cask. A silicone gasket ensures positive

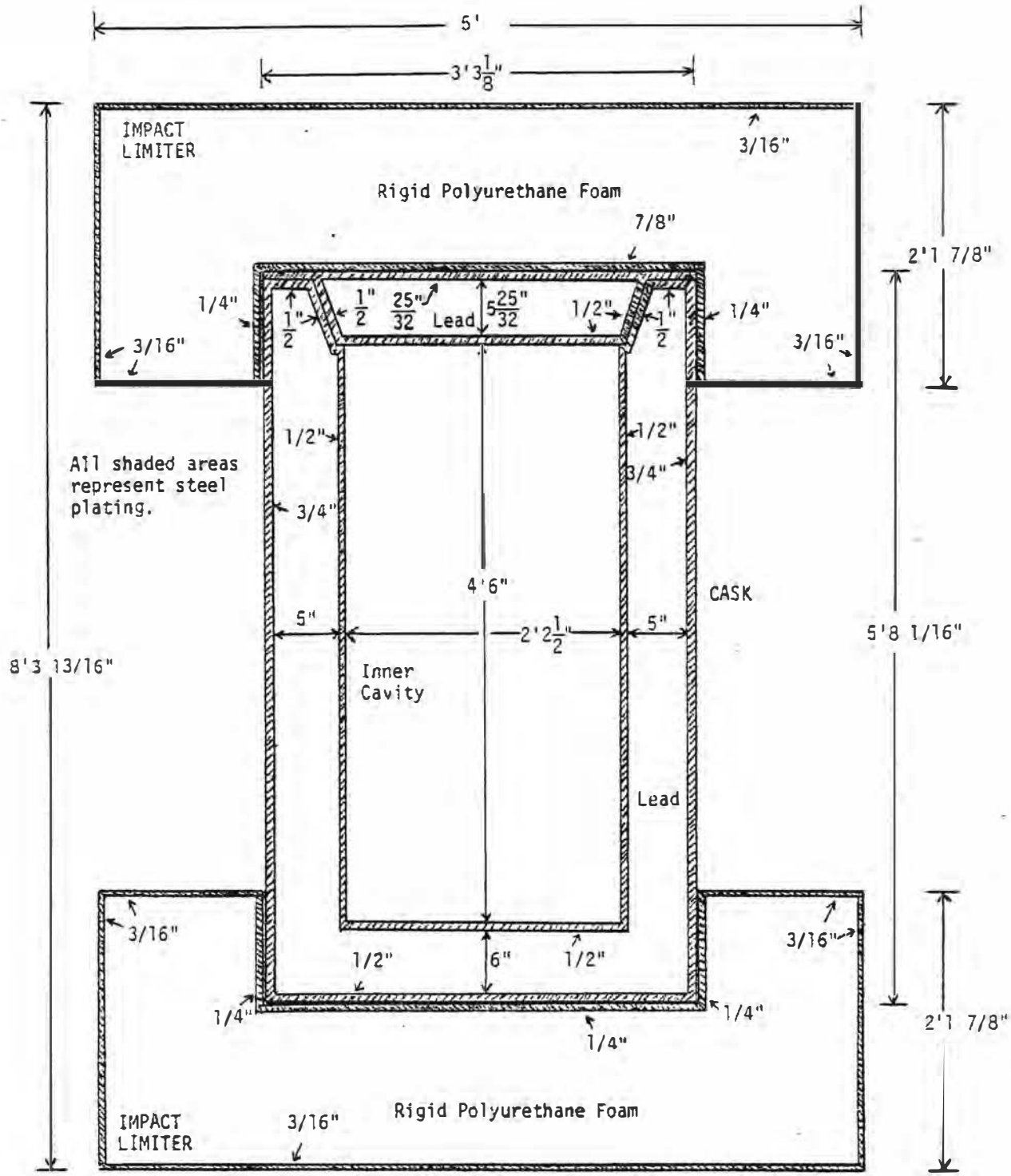

FIGURE 3.3. Simplified Schematic of CNS 1-13C Shipping Cask

closure. The impact limiters, which will be used for the shipments from TMI to PNL, consist of rigid polyurethane foam encased by steel plating. They are locked to one another by six ratchet binders.

When empty, the CNS 1-13C cask with the impact limiters and their binders weighs 24,600 lb_m. Six cables, each connected to a steel arm projecting at a downward angle from the edge of the cask lid, attach the cask to the flatbed trailer. Figure 3.4 illustrates this tie-down arrangement. Reference 6 contains a detailed description of the cask and the analysis performed in obtaining its license. This report is currently being updated to include modifications associated with the use of the impact limiters in the TMI-to-PNL shipments.

3.3 SHIPPING ROUTE

Figures 3.5 through 3.7 present the shipping route for transport of the zeolite liners from TMI to PNL.[7] Except for local routing near TMI and PNL, the federal highway system will be used exclusively. The total distance is approximately 2,600 miles and can be covered in less than one week.

3.4 LINER-CASK EQUILIBRIUM CONDITIONS

It is important to verify that the material being shipped and its containers are stable under "normal" (non-accident) conditions. There should be no threat to the integrity of the zeolite liner nor to that of the CNS 1-13C cask if shipment proceeds without incident. Since zeolite is a chemically stable material, no potential for an adverse reaction is perceived under normal transport conditions. However, the radioactive generation of decay heat during normal transport could potentially lead to adverse structural changes in the zeolite or the lead in the cask's walls depending upon the temperature buildup. Further, the presence of a significant amount of unbound water (112 lb_m) provides a potential for pressure buildup from steam generation. These thermal threats must be investigated.

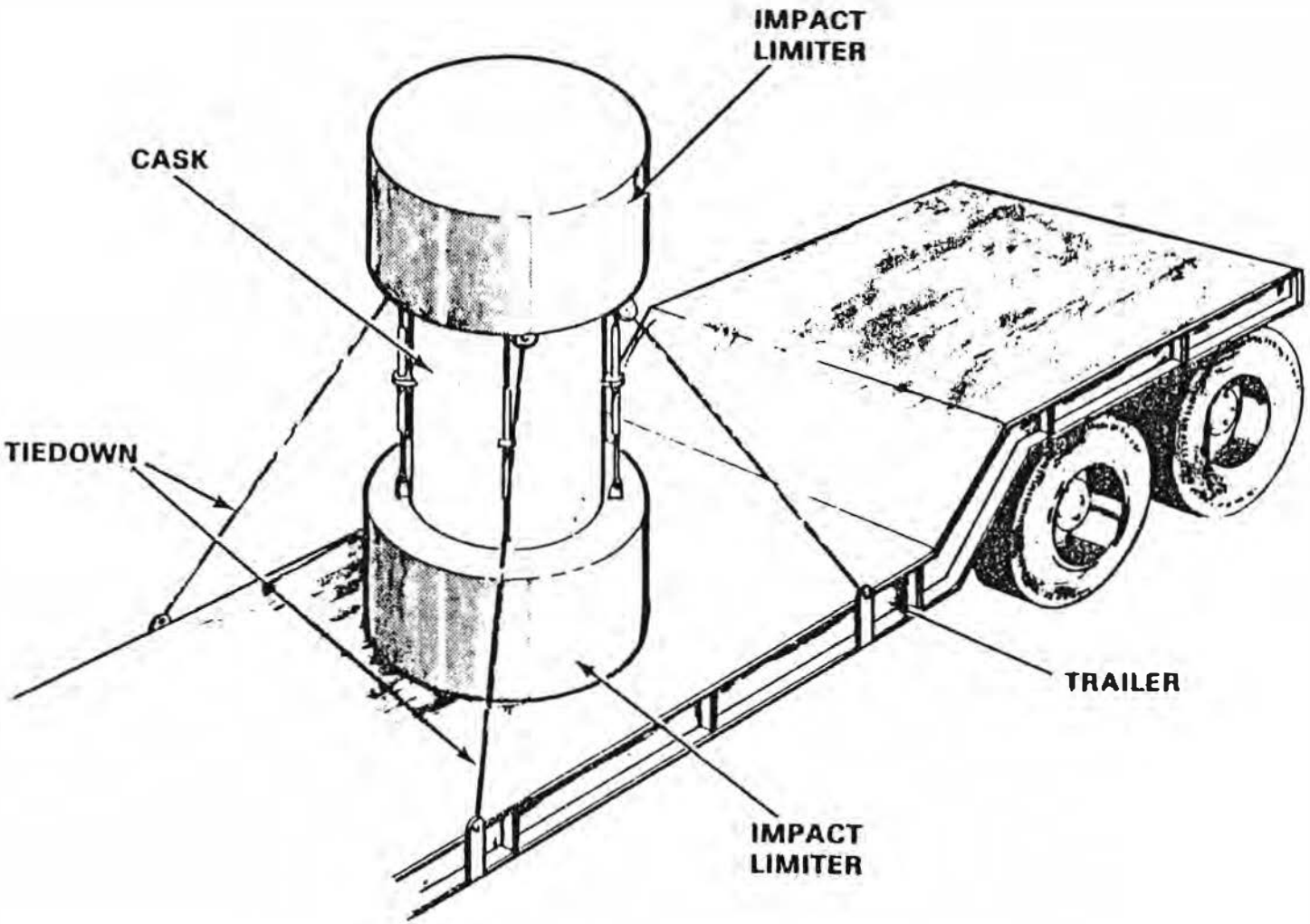

FIGURE 3.4. Tie-Down System for CNS 1-13C Shipping Cask

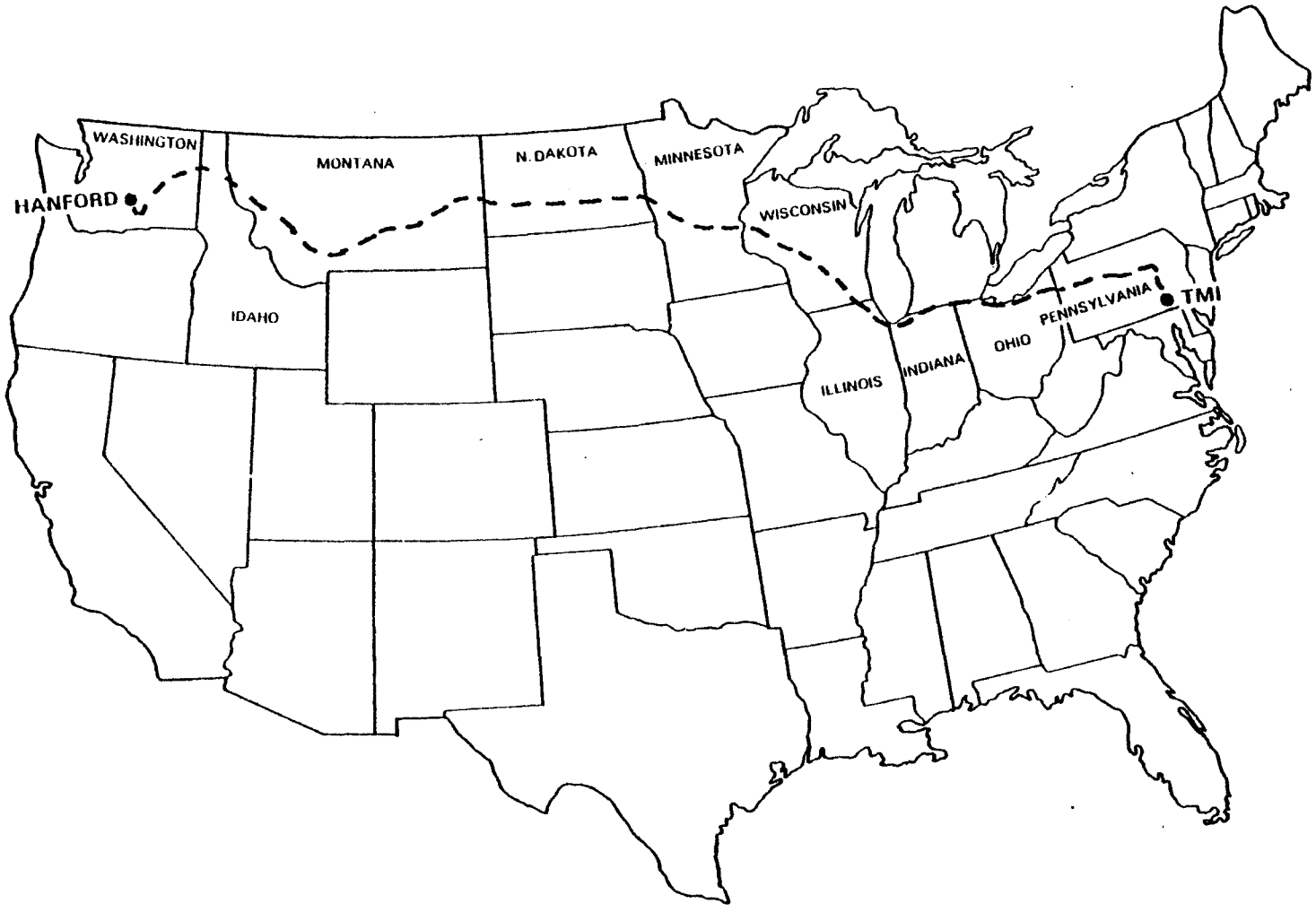

FIGURE 3.5. Transportation Route from TMI to PNL

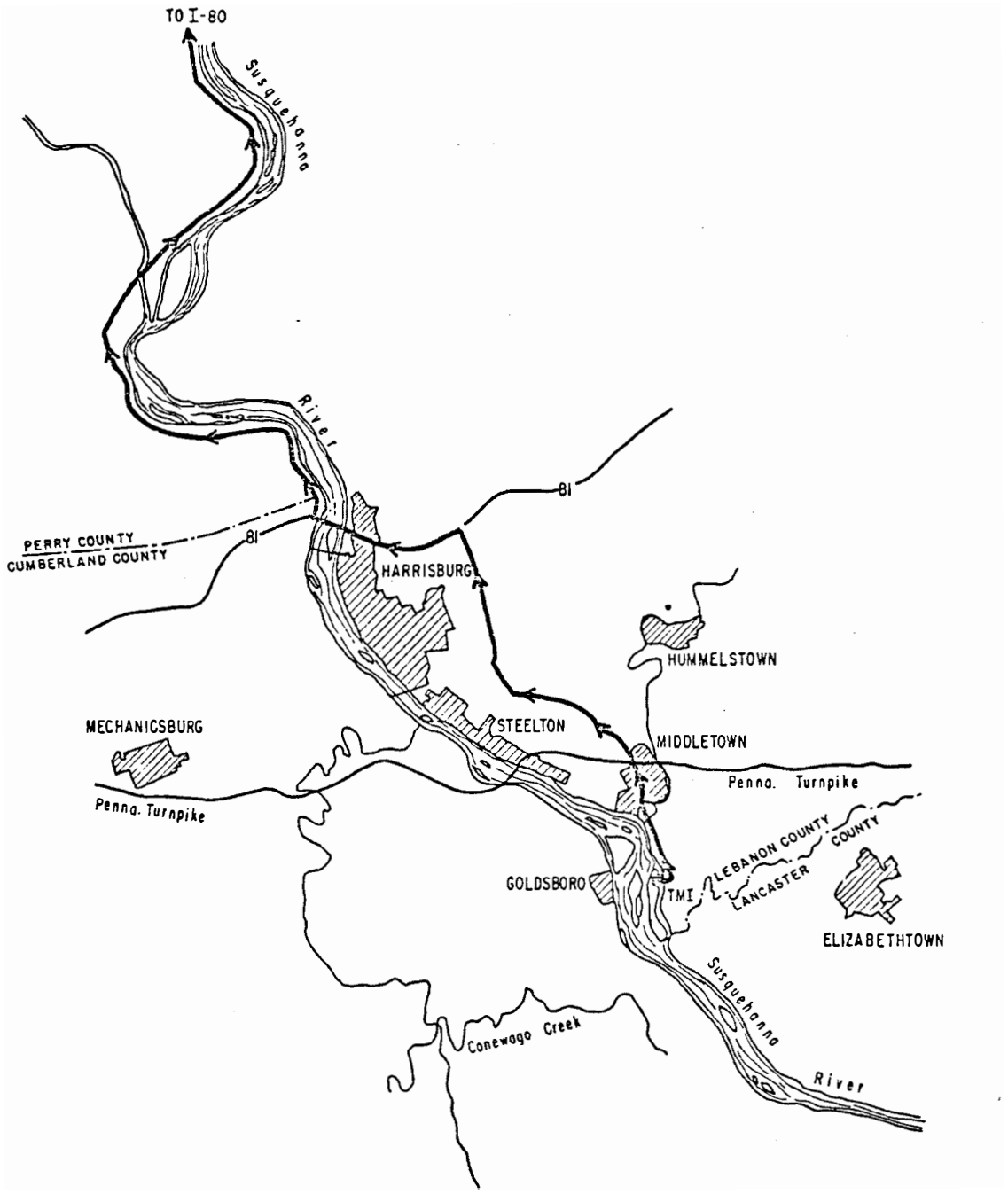

FIGURE 3.6.[7] Local Routing in the Vicinity of the TMI Site for the Route to the Hanford Site

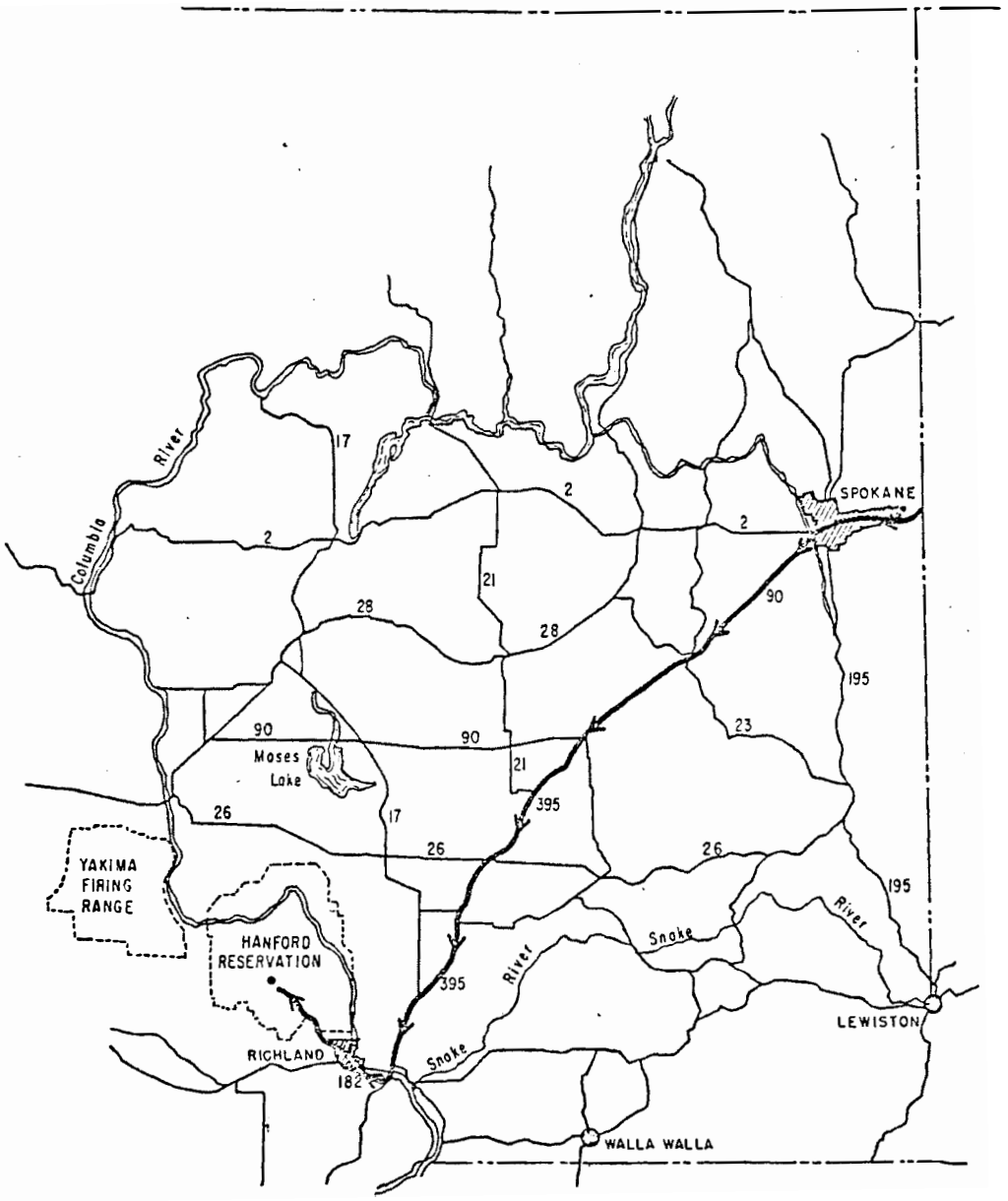

FIGURE 3.7.[7] Local Routing in Washington to the Hanford Site

3.4.1 Temperature Effects

The analysis described in section A.1 indicates that, of the 346 W of decay power generated by the radioactivity in the zeolite, 265 W are absorbed inside the liner. The remaining 81 W are absorbed by the lead shielding in the cask. Since the power generation varies axially in the liner-cask system, a two-dimensional thermal analysis is performed to obtain the temperature profile in the system. Heat conduction and radiation phenomena are modelled directly, while convective effects are incorporated indirectly into the model. The details of the analysis are presented in section A.2.1.

The average temperature of the zeolite, water, and water vapor inside the liner is estimated to be 294°F. The maximum potential temperature in a localized region is estimated as 482°F, occurring in the center of the zeolite region most heavily loaded with Cs. Since zeolite is structurally stable up to 1300°F, no threat to its stability is anticipated.[1] The temperature inside the cask walls is around 120°F, well below the melting point of lead (621°F). Since the CNS 1-13C cask is licensed to hold heat sources up to 600 W, this relatively low temperature is expected.[6]

3.4.2 Pressure Effects

Each zeolite liner will presumably be dewatered subsequent to its removal from service in the SDS and prior to its sealing inside the shipping cask. This is necessary to reduce its unbound water content to the specified 112 lb_m. Presumably, the liner will be vented during this dewatering process to prevent any pressure buildup from the decay heat. This venting is assumed to expel any air originally present such that only water vapor will remain during the shipment phase. Any buildup of radiolytic hydrogen and oxygen gases is presumed to be negligible compared to possible steam buildup.

Prior to emplacement inside the CNS 1-13C cask for shipment, the zeolite liner will be sealed and will remain unvented throughout transport. An equilibrium temperature of 294°F will be established during shipment. Although the volume available for two-phase steam inside the liner is not known precisely, a reasonable estimate can be made, as discussed in section A.2.1.4.4. There it is shown that the 112 lb_m of unbound water inside the liner will form a

saturated mixture at 294°F. The corresponding steam pressure will be 61 psia. This is taken as the equilibrium internal pressure of the zeolite liner. Since it is designed to withstand 350 psig at 400°F, no threat to the liner's integrity is expected from pressure buildup during normal transport.

REFERENCES

1. Evaluation of Increased Cesium Loading on Submerged Demineralizer System (SDS) Zeolite Beds. DOE/NE-0012; U.S. Department of Energy (May 1981).

2. Campbell, D. et al., Evaluation of the Submerged Demineralizer System (SDS) Flowsheet for Decontamination of High-Activity-Level Water at the Three-Mile Island Unit 2 Nuclear Power Station. ORNL/TM-7448; Oak Ridge National Laboratory (July 1980).

3. GPU Service, Submerged Demineralizer System Demineralizer Liner. Reference Drawing 2D-950-29-001, Revision 1 (March 1981).

4. Collins, J., A Report on Acid-Resistant Molecular Sieve Types AW-300 and AW-500. Union Carbide Corp., Linde Division.

5. Code of Federal Regulations, Title 10, Part 71.

6. Procedures, License, and Safety Analysis Report for Chem-Nuclear Systems, Inc. CNSI 1600 (CNS 1-13C) Type-B Radwaste Shipping Cask. Chem-Nuclear Systems, Inc., Bellevue, WA (September 1978).

7. Metropolitan Edison Co., Jersey Central Power and Light Co., and Pennsylvania Electric Co., Draft Programmatic Environmental Impact Statement Related to Decontamination and Disposal of Radioactive Wastes Resulting from March 28, 1979 Accident (at) Three-Mile Island Nuclear Station, Unit 2. U.S. Nuclear Regulatory Commission (July 1980).

4.0 ACCIDENT ANALYSIS

As stated in Section 2, the results from previous transportation risk assessments indicate that potential releases from non-accident situations (e.g., package closure errors) are negligible. Furthermore, the analysis of the equilibrium conditions inside the liner-cask system (see section A.2.1) indicates that no potential release of radionuclides is anticipated. The risk will be dominated by the accident environment. Thus, this study considers only accident situations during transport.

The accident analysis for the transport of the zeolite liners requires estimates of both the probabilities of and the radioactive releases from various accident scenarios in which the liner-cask system can be involved. Reference 1 divides potential truck accidents involving large packages into five categories: fire, impact, puncture, crush, and immersion. As defined, these accident forces are often more severe than those used in analysis of a shipping cask's design integrity for its license application. Neither crush nor immersion is expected to contribute much to the risk relative to the other three forces. Thus, in this analysis, only fire, impact and puncture (and their combined actions, where applicable) are considered.

Released radioactivity can eventually reach man through various environmental-biological pathways (e.g., inhalation and ingestion). For the accidents potentially involving the zeolite shipments, inhalation is expected to be the dominant pathway with respect to the risk. Thus, all radioactive releases will be specified in terms of the amount airborne in the respirable range (10 μm or less).

4.1 ACCIDENT SCENARIOS

Of the three accident forces being considered, only fire can occur concurrently with the others since, by definition in Reference 1, impact and puncture accidents are mutually exclusive. Thus, five accident scenarios can be visualized from these three accident forces:

1. Fire-only
2. Impact-only
3. Puncture-only
4. Impact-with-fire
5. Puncture-with-fire

For the scenarios involving fire, the duration of the fire is an important consideration. A short fire may have little or no effect upon the release, while a longer one could significantly aggravate the release. As will be seen, there is a critical duration above which a fire significantly increases the release for scenarios involving fire. Thus, these scenarios will be further subdivided by the fire duration.

4.1.1 Qualitative Description

As defined for this analysis, the five accident scenarios are mutually exclusive, as necessitated by the nature of the probabilistic analysis performed in section B.1. Each scenario is unique, although the results from one may be applicable to another. Also, for an accident to occur, it is not sufficient for the accident force merely to be imposed. It must exceed some threshold level for failure of the liner-cask system that results in a potential release.

4.1.1.1 Fire-Only

In this scenario, an accident occurs that enables the cask to be engulfed by a 1000°C fire, the thermal environment defined in Reference 1. Further, while the cask may be breached prior to fire engulfment, the liner is assumed to still be intact such that no pathway initially exists for radioactive release. Such a pathway must be created solely by the fire.

Whether or not the cask is already breached, release will occur only if the fire lasts long enough to rupture the liner, presumably by over-pressurization due to aggravated steam generation. It is assumed that if the cask is initially intact, such a fire will melt sufficient lead in the cask's wall to rupture the steel plating, thereby causing loss of the lead. Since this lead serves as a thermal shield for the liner, its loss is

assumed to expose the liner to a severe thermal environment. Even if the cask is breached initially, fire of the same duration as before is assumed necessary to melt sufficient lead to cause loss of this thermal integrity. Thus, both situations (cask initially intact or breached) are assumed equivalent in the analysis.

Upon loss of the thermal shielding provided by the cask, the liner is presumed to undergo immediate exposure to the 1000°C fire. It subsequently overpressurizes at the design pressure (determined in section A.2.3 to be 340 psia at 430°F). Almost instantaneously, two-phase steam and possibly some zeolite are expelled. Subsequent release of airborne radionuclides will occur so long as the fire continues, since all the zeolite (whether expelled or remaining inside the liner) will be exposed to the severe thermal environment.

Should the fire's duration be too short to melt enough lead to constitute a loss of thermal integrity, the liner will not feel the severe thermal environment. It remains intact, and no release occurs. Such a shorter-duration fire is excluded from the fire-only scenario. The determination of this "critical duration" for the fire is a key factor in evaluating this scenario.

4.1.1.2 Impact-Only

Reference 1 defines impact as an accident in which the payload strikes or is struck by an object with no sharp projections (hence, it excludes puncture). For this scenario, the definition is extended to include only such collisions in which both the cask and the liner are breached. Rupture solely of the cask will not cause a release and, thus, is not included in the impact-only scenario. Again, the determination of a failure threshold is essential, that threshold being some minimum impact velocity for dual breach.

As determined in section A.2.1, the internal pressure and temperature of the liner during normal transport have equilibrium values of 61 psia and 294°F. Thus, when breached by impact, the liner will expel two-phase steam at 61 psia plus any zeolite carried along with it. This release will be

essentially instantaneous, although the decay heat will continue to generate steam after the accident. Also, some zeolite may dribble out through the rupture following the initial steam release. Some of the radionuclides could become airborne.

4.1.1.3 Puncture-only

Reference 1 defines puncture as an accident in which the payload strikes or is struck by an object which has the potential for penetration (hence, it excludes impact). In this scenario, the definition is extended to include only such collisions in which both the cask and the liner are breached. Breach solely of the cask will not cause a release and, thus, is not included in the puncture-only scenario. The failure threshold of concern here is the minimum equivalent puncture depth (in terms of the mild-steel thickness) needed to penetrate both the cask and the liner.

The release modes for puncture-only are analogous to those for impact-only, with the possible exception of release magnitude. The size of the breach area will presumably be smaller.

4.1.1.4 Impact-with-Fire

In this scenario, breach of both the cask and the liner are assumed necessary in conjunction with both being subsequently engulfed in the 1000°C fire. It is true that breach solely of the cask with subsequent engulfment in the fire could eventually overpressurize the liner if the fire duration is long enough, as in the fire-only scenario. However, such a scenario has already been included in fire-only. Thus, it is not included here.

Upon impact (at or above the threshold velocity specified for the impact-only scenario), an essentially instantaneous release equivalent to that for the impact-only scenario will occur. Subsequent fire will aggravate this release to a degree dependent upon its duration. As for the fire-only scenario, the critical duration is that needed to melt sufficient lead in the cask's wall to cause loss of thermal shielding for the liner. Thus, as alluded to earlier, this scenario can more conveniently be subdivided into two categories relating to the fire duration. Note that, since the liner has already been breached by impact, no pressure buildup can occur as in the fire-only scenario.

4.1.1.4.1 Subcritical Fire Duration

Since insufficient lead is melted to cause loss of thermal shielding, the liner is assumed not to experience the severe fire environment. Thus, the fire's sole effort will be to volatilize any zeolite already released (some may continue to dribble out and subsequent steam generation may occur, as in the impact-only scenario). The fire will not be a driving force for any subsequent steam or zeolite expulsion from the liner.

4.1.1.4.2 Post-Critical Fire Duration

Upon attainment of the critical duration, enough lead has been melted and lost to expose the liner to the severe fire environment, as in the fire-only scenario. For the time up to the critical duration, the release is that discussed above (section 4.1.1.4.1). Beyond this time, the fire serves as a driving force for continued steam release (so long as unbound or bound water remains). In addition, it will generate an airborne release of radionuclides from the zeolite (whether expelled or inside the liner), all of which is exposed to the severe thermal environment.

4.1.1.5 Puncture-with-Fire

As for the impact-with-fire scenario, breach of both the cask and the liner is assumed necessary in conjunction with both being subsequently engulfed in the 1000°C fire. Breach solely of the cask with subsequent liner overpressurization due to fire engulfment has already been included in the fire-only scenario. Hence, it is excluded here.

As for the impact-with-fire scenario, puncture-with-fire can be subdivided into two analagous categories based upon the fire duration. The release modes are equivalent, except for possible variation in magnitude due to the presumably smaller breach area. The initial release is equivalent to that for the puncture-only scenario.

A qualitative summary of these five accident scenarios, along with the release modes, is provided in Table 4.1.

TABLE 4.1. Qualitative Summary of Accident Scenarios

SCENARIO	ACCIDENT FORCES PRIMARY	ACCIDENT FORCES SECONDARY	RADIONUCLIDE RELEASE (RR) MODES
1. Fire-only	Fire	--	RR from initial S/Z* expulsion from liner due to overpressurization at 340 psia and 430°F. Subsequent RR due to exposure of all Z to 1000°C fire and any continued S generation.
2. Impact-only	Impact	--	RR from initial S/Z expulsion from liner when ruptured with equilibrium pressure = 61 psia and temperature = 294°F. Subsequent RR (minimal) as decay heat generates more steam and some Z dribbles out.
3. Puncture-only	Puncture	--	As above for #2 with possible variation in RR magnitude due to presumably smaller breach area.
4. Impact-with-fire	Impact	Fire	As above for #2 with volatilization of expelled Z by fire during subcritical duration. During post-critical duration, subsequent RR as for #1.
5. Puncture-with-fire	Puncture	Fire	As above for #4 with possible variation in RR magnitude due to presumably smaller breach area.

*S = two-phase steam

Z = zeolite.

4.2 QUANTITATIVE EVALUATION

The quantitative evaluation of the accident scenarios yields their probabilities of occurrence and the release amounts of airborne radionuclides in the respirable range resulting from them. Based upon the qualitative descriptions provided in section 4.1, failure thresholds are estimated in sections A.2 and A.3 for the accident scenarios. These are summarized in Table 4.2.

TABLE 4.2. Failure Thresholds for Accident Scenarios

CRITICAL-DURATION FIRE: 15.3 min. (Section A.2.2)

ZEOLITE LINER OVERPRESSURIZATION LIMITS (SEVERE THERMAL EXPOSURE): 340 psia at 430°F (Section A.2.3)

IMPACT VELOCITY: 30 mph (Section A.3.1)

EQUIVALENT MILD-STEEL PUNCTURE DEPTH: 1.9 in. (Section A.3.2)

These qualitative descriptions are expressed logically through the use of Boolean equations in section B.1.1. From these, probabilistic expressions are derived. These are evaluated based upon the failure thresholds estimated in Appendix A and the data base for transportation accidents from reference 1. The procedure is presented in section B.1.2. The scenario probabilities, which also correspond to the probabilities of airborne, respirable releases occurring, are summarized in Table 4.3. Note that the post-critical duration for scenarios involving fire is subdivided into three intervals as follow:

1. 15.3-30.0 min., with 20.7 min. being the mean duration
2. 30.0-60.0 min., with 39.8 min. being the mean duration
3. 60.0-151 min., with 105.5 min. being the mean duration.

15.3 min. is the critical duration for loss of the cask's thermal integrity. 151 min. is estimated to be the maximum fire duration.

TABLE 4.3. Probabilities of Occurrence of Accident Scenarios

	ACCIDENT SCENARIOS												
	FIRE ONLY			IMPACT ONLY	PUNCTURE ONLY	IMPACT WITH FIRE				PUNCTURE WITH FIRE			
	Fire Duration (min.)					Fire Duration (min.)				Fire Duration (min.)			
	15.3 - 30.0	30.0 - 60.0	60.0 - 151			0-15.3	15.3 - 30.0	30.0 - 60.0	60.0 - 151	0 -15.3	15.3 - 30.0	30.0 - 60.0	60.0 - 151
SCENARIO PROB. (PER ACCIDENT)	.0034	5.3E-4	1.8E-4	.0088	2.4E-5	3.3E-5	9.2E-6	1.5E-6	4.8E-7	9.0E-8	2.5E-8	4.0E-9	1.3E-9
SCENARIO PROB. (PER SHIPMENT)	2.2E-5	3.4E-6	1.1E-6	5.7E-5	1.6E-7	2.1E-7	6.0E-8	9.4E-9	3.1E-9	5.9E-10	1.6E-10	2.6E-11	8.6E-12

In developing the Boolean equations, the scenarios are made mutually exclusive from one another. Thus, the individual scenario probabilities can be summed to give the overall probability of an airborne release in the respirable range (equivalent to the probability of any scenario occurring). This value is .013 per accident, or 8.4E-5 per shipment (1.7E-4 for two shipments). The impact-only and fire-only (15.3-30.0-min. duration) scenarios contribute the most to this probability (68% and 26% respectively).

The release amounts of airborne, respirable radionuclides are derived in Section B.2 for each scenario. The results are summarized in Table 4.4. Note that the eleven radionuclides are identified as being potentially airborne and respirable as a result of release from the accident scenarios. The largest releases for radionuclides in the zeolite are associated with the impact-with-fire scenario. The smallest, those from impact and puncture only, are associated solely with the expulsion of unbound water.

TABLE 4.4. Estimated Airborne Releases in the Respirable Range for All Accident Scenarios

	ACCIDENT SCENARIOS												
	FIRE ONLY			IMPACT ONLY	PUNCTURE ONLY	IMPACT WITH FIRE				PUNCTURE WITH FIRE			
	Fire Duration (min.)					Fire Duration (min.)				Fire Duration (min.)			
	15.3 - 30.0	30.0-60.0	60.0-151			0 - 15.3	15.3-30.0	30.0-60.0	60.0-151	0-15.3	15.3-30.0	30.0-60.0	60.0-151
^{3}H Release (Ci)	.047	.047	.047	.047	.047	.047	.047	.047	.047	.047	.047	.047	.047
^{60}Co Release (Ci)	2.5E-6	2.5E-6	2.5E-6	2.5E-6	2.5E-6	2.5E-6	2.5E-6	2.5E-6	2.5E-6	2.5E-6	2.5E-6	2.5E-6	2.5E-6
^{89}Sr Release (Ci)	3.1E-6	1.3E-5	4.8E-5	2.3E-7	2.3E-7	4.3E-7	3.5E-6	1.4E-5	4.9E-5	2.7E-7	3.2E-6	1.3E-5	4.9E-5
^{90}Sr Release (Ci)	.030	.13	.47	.0016	.0016	.0035	.034	.13	.48	.0020	.031	.13	.48
^{95}Nb Release (Ci)	2.0E-11	2.0E-11	2.0E-11	2.0E-11	2.0E-11	2.0E-11	2.0E-11	2.0E-11	2.0E-11	2.0E-11	2.0E-11	2.0E-11	2.0E-11
^{103}Ru Release (Ci)	1.0E-10	1.0E-10	1.0E-10	1.0E-10	1.0E-10	1.0E-10	1.0E-10	1.0E-10	1.0E-10	1.0E-10	1.0E-10	1.0E-10	1.0E-10
^{106}Ru Release (Ci)	4.3E-5	4.3E-5	4.3E-5	4.3E-5	4.3E-5	4.3E-5	4.3E-5	4.3E-5	4.3E-5	4.3E-5	4.3E-5	4.3E-5	4.3E-5
^{125}Sb Release (Ci)	6.6E-4	6.6E-4	6.6E-4	6.6E-4	6.6E-4	6.6E-4	6.6E-4	6.6E-4	6.6E-4	6.6E-4	6.6E-4	6.6E-4	6.6E-4
^{134}Cs Release (Ci)	.059	.27	.99	7.3E-5	7.3E-5	.0043	.071	.29	1.1	8.8E-4	.062	.27	1.0
^{137}Cs Release (Ci)	.59	2.7	9.9	6.9E-4	6.9E-4	.042	.71	2.9	11.	.0088	.62	2.7	10.
^{144}Ce Release (Ci)	6.3E-6	6.3E-6	6.3E-6	6.3E-6	6.3E-6	6.3E-6	6.3E-6	6.3E-6	6.3E-6	6.3E-6	6.3E-6	6.3E-6	6.3E-6

REFERENCE

1. Dennis, A. et al., Severities of Transportation Accidents Involving Large Packages. SAND77-0001; Sandia Laboratories (May 1978).

5.0 RISK EVALUATION

Estimates for the probabilities and the releases of airborne radionuclides in the respirable range result from the accident analysis. These must be combined with models for the following factors to yield a risk estimate:

1. Atmospheric dispersal of the radionuclides
2. Dose to the critical organs from the radionuclides
3. Population distribution along the transportation route.

This is accomplished, as discussed in Appendix C, through use of the TRECII program.[1] TRECII yields a risk estimate in terms of the 50-year inhalation dose to the exposed population.

The modeling of the above three factors is discussed in sections C.1.1, C.1.2, and C.1.3 respectively. A modification necessary in the use of the TRECII program is the reduction of the eleven radionuclides that are released (see Table 4.4) to five, one of which represents a group of radionuclides. The amounts and the rates of release for these five radionuclides are summarized in Table 5.1 for the accident scenarios.

The 50-year, inhalation dose conversion factors for these five radionuclides are listed in Table 5.2. Four critical organs are identified: total body, bone, lung, and thyroid. The potential impact of ^{90}Sr, especially to total body and bone, is evident.

The population distribution along the shipping route is estimated using PNL's POPCOR program. Thirteen density ranges are defined along the route. The percent of the total route comprised by each range is tabulated for a 10-km corridor width (a band 5-km wide on each side of the route), as listed in Table 5.3.

5.1 RISK ESTIMATES

As described in section C.1, all the preceding information is input into TRECII to generate risk estimates for the transportation of the zeolite liners. Risk can be measured in various terms. The more common

TABLE 5.1. Release Amounts and Release Rates for Radioisotopes (Airborne, Respirable) in Accident Scenarios

		ACCIDENT SCENARIOS												
		FIRE ONLY			IMPACT ONLY	PUNCTURE ONLY	IMPACT WITH FIRE				PUNCTURE WITH FIRE			
		MEAN SCENARIO DURATION (min.)												
		20.7	39.8	105.5	1.0	1.0	7.38	20.7	39.8	105.5	7.38	20.7	39.8	105.5
AMOUNT (Ci)	^{3}H*	.047	.047	.047	.047	.047	.047	.047	.047	.047	.047	.047	.047	.047
	^{90}Sr	.030	.13	.47	.0016	.0016	.0035	.034	.13	.48	.0020	.031	.13	.48
	^{125}Sb	6.6E-4	6.6E-4	6.6E-4	6.6E-4	6.6E-4	6.6E-4	6.6E-4	6.6E-4	6.6E-4	6.6E-4	6.6E-4	6.6E-4	6.6E-4
	^{134}Cs	.059	.27	.99	7.3E-5	7.3E-5	.0043	.071	.29	1.1	8.8E-4	.062	.27	1.0
	^{137}Cs	.59	2.7	9.9	6.9E-4	6.9E-4	.042	.71	2.9	11.	.0088	.62	2.7	10.
RATE (Ci/min)	^{3}H*	.0023	.0012	4.5E-4	.047	.047	.0064	.0023	.0012	4.5E-4	.0064	.0023	.0012	4.5E-4
	^{90}Sr	.0014	.0033	.0045	.0016	.0016	4.7E-4	.0016	.0033	.0045	2.7E-4	.0015	.0033	.0045
	^{125}Sb	3.2E-5	1.7E-5	6.3E-6	6.6E-4	6.6E-4	8.9E-5	3.2E-5	1.7E-5	6.3E-6	8.9E-5	3.2E-5	1.7E-5	6.3E-6
	^{134}Cs	.0029	.0068	.0094	7.3E-5	7.3E-5	5.8E-4	.0034	.0073	.010	1.2E-4	.0030	.0068	.0095
	^{137}Cs	.029	.068	.094	6.9E-4	6.9E-4	.0057	.034	.073	.10	.0012	.030	.068	.095

*Includes ^{3}H, ^{60}Co, ^{89}Sr, ^{106}Ru, and ^{144}Ce.

TABLE 5.2. Dose Conversion Factors for Five Radioisotopes Used in TRECII Dose Analysis

ISOTOPE	DOSE CONVERSION FACTOR** ($rem\text{-}m^3/Ci\text{-}sec$) TOTAL BODY	BONE	LUNG	THYROID
^{3}H*	.032	.056	.087	.026
^{90}Sr	690	2800	6.7	--
^{125}Sb	11.	35.	210	.0070
^{134}Cs	11.	6.6	3.2	--
^{137}Cs	6.0	11.	2.6	--

*This is a group of five isotopes: ^{3}H, ^{60}Co, ^{89}Sr, ^{106}Ru, and ^{144}Ce.

**50-year inhalation dose.

TABLE 5.3. Percentages for Population Density Ranges over the Shipping Route for 10-km Corridor Width

POPULATION DENSITY RANGES (people/km^2)												
0-1	1-10	10-30	30-60	60-100	100-300	300-600	600-1000	1000-1300	1300-1600	1600-2000	2000-2500	2500+
28.	17.	19.	12.	5.8	8.0	6.1	2.2	1.4	.55	.55	0	0

measure is in terms of fatalities. However, this is deemed inappropriate in this study because the anticipated level of such a risk to the public is too small to be statistically meaningful. Thus, the unit selected for measuring the risk is the 50-yr. inhalation dose to the exposed population (along the transport route) resulting from the two shipments. It is measured in terms of man-rems. The risk estimates are presented in two forms: the complementary cumulative density function and the total risk (expected dose). Taken together, these two forms of risk measure provide a meaningful perspective on the overall risk.

5.1.1 Complementary Cumulative Density Function

The complementary cumulative density function presents the probability that the dose exceeds a given value over the entire range of doses that can conceivably result from the accident releases. It is displayed as a curve of the probability of a dose $\geq \chi$ vs. χ. The points along the curve can be viewed as the sums of the probabilities of all scenarios resulting in doses exceeding specific values.

The complementary cumulative density function for the transportation of radioactive zeolite liners from TMI to PNL is shown in Figure 5.1 (base case) for two shipments. Since the risk estimates generated by TRECII are actually more sensitive to the release rates than to the total release amounts, the curve's relatively steep slope indicates that some of the higher-probability scenarios have relatively high release rates comparable to those of lower-probability scenarios. Comparison of Tables 4.3 and 5.1 indicates that this is the case for the fire and impact-only scenarios for several radioisotopes. The curve spans the following range of values: probabilities below 2E-5 and doses below 0.7 man-rem. The largest estimated dose is 0.7 man-rem from the least-likely scenario (probability of 1E-9 for two shipments).

5.1.2 Total Risk (Expected Dose)

The total risk (expected dose) is the mathematical expectation value of the consequence, measured in terms of the 50-yr. inhalation dose to the exposed population (along the transport route). It is a probabilistically-

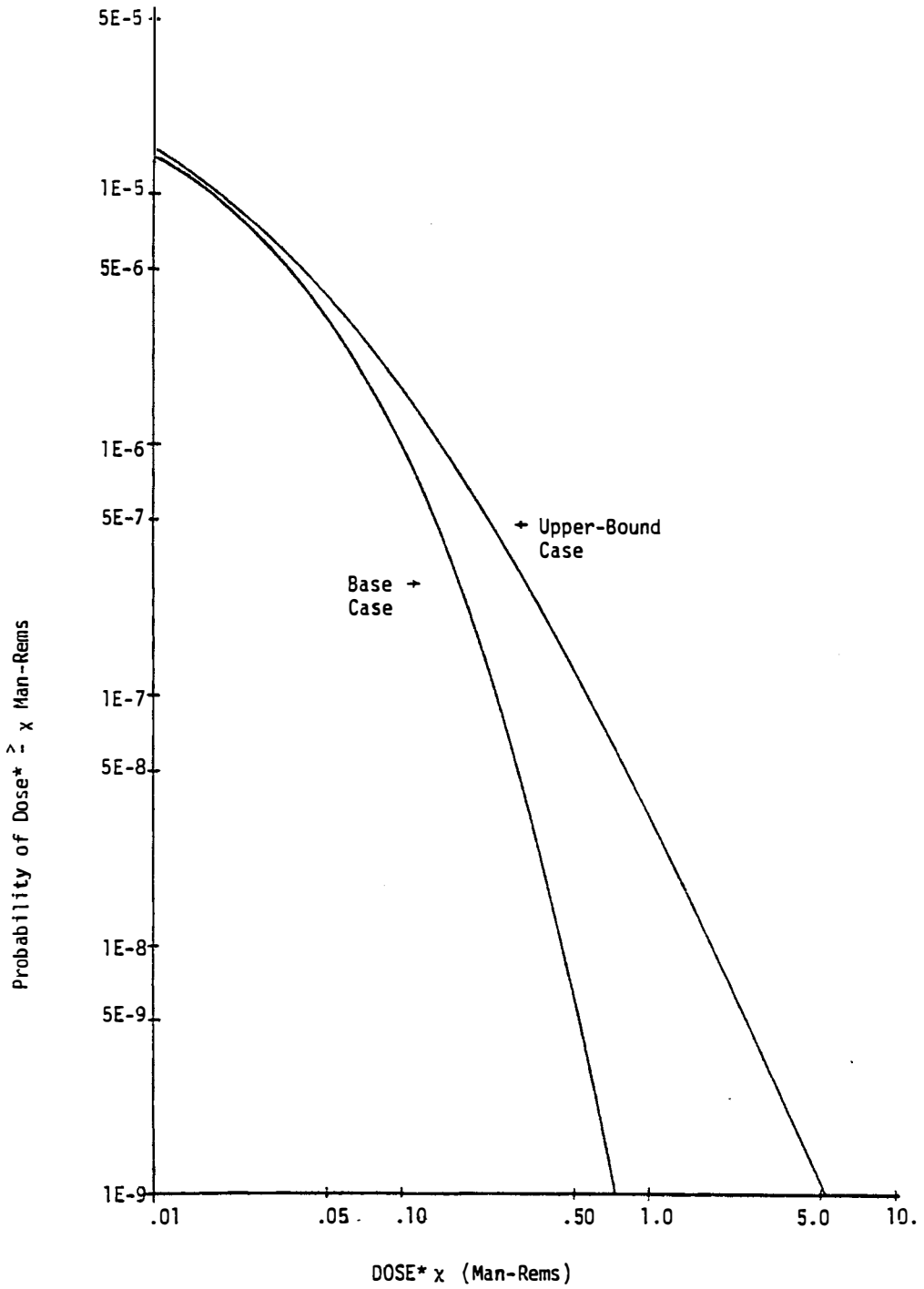

*50-yr inhalation dose to exposed population

FIGURE 5.1. Complementary Cumulative Density Function for Two Shipments

weighted estimate that includes contributions from the full range of probabilities and consequences of all the potential scenarios. It provides a single estimate of the overall risk in contrast to the resolution of the overall risk into specific contributions, as displayed by the complementary cumulative density function.

For the two shipments of radioactive zeolite liners, the probability of occurrence of an airborne, respirable release is 1.7E-4. The total expected dose is 5.3E-7 man-rem; the total expected number of fatalities is negligible.

5.1.3 Dominant Accident Scenarios

As one of its outputs, TRECII lists the contribution made to the total risk by each scenario and radioisotope. These contributions are listed in terms of percent in Table 5.4. The dominant scenario is impact-only with 62% of the contribution, almost exclusively from ^{90}Sr. Second is the 15.3-30.0-min. duration for fire-only with 24% of the contribution, again nearly entirely from ^{90}Sr. Note that there is no significant contribution from puncture-only nor from the scenarios involving two accident forces (impact-with-fire and puncture-with-fire). This is due to their low probabilities relative to those for fire and impact-only.

Ninety-three percent of the contribution to the total expected dose arises from ^{90}Sr. This is not surprising, given its formidable dose impact upon bone and total body (see Table 5.2). Although both ^{134}Cs and ^{137}Cs are released in larger quantities, the lower release amounts and rates for ^{90}Sr are more than compensated for by its dose effect. ^{137}Cs is the next largest contributor, a distant second at 3.9%. However, keeping all of this in perspective, it must be remembered that these scenarios and radioisotopes are dominant contributors to what will be shown to be an insignificant level of risk to the public.

5.2 SENSITIVITY ANALYSIS

The sensitivity of the risk estimates to a variation in release of radionuclides is measured. As discussed in section C.2, the maximum estimable airborne release of radionuclides in the respirable range

TABLE 5.4. Percent Contributions to Total Expected Dose from Each Accident Scenario and Radionuclide

	ACCIDENT SCENARIOS						
	FIRE ONLY			IMPACT ONLY	PUNCTURE ONLY	REMAINING EIGHT SCENARIOS	TOTAL FOR EACH ISOTOPE
	DURATION (min.)						
	15.3-30.0	30.0-60.0	60.0-151				
^{3}H*	.0088	<.001	<.001	.48	.0013	<.001	.49
^{90}Sr	21.	8.1	3.7	60.	.17	.15	93.
^{125}Sb	.034	.0030	<.001	1.8	.0052	<.001	1.9
^{134}Cs	.25	.10	.050	.016	<.001	.0016	.42
^{137}Cs	2.3	.93	.50	.15	<.001	.015	3.9
TOTAL FOR EACH SCENARIO	24.	9.1	4.2	62.	.18	.17	100

*Includes ^{3}H, ^{60}Co, ^{89}Sr, ^{106}Ru, and ^{144}Ce

NOTE: Total Expected Dose = 5.3E-7 man-rem

(.12% of the total radioactivity of each nuclide in the zeolite) is assumed to occur for the longest fire durations. As discussed in section B.2.3, this release is a maximum for zeolite exposure to a 1000°C fire regardless of duration. Note that a fire of duration exceeding 2.5 hrs is extremely unlikely. However, for the sake of performing this sensitivity analysis, the maximum releases estimable for such a fire are postulated to occur. The release amounts and rates for this maximum estimate are listed in Table 5.5. The impact of these can be viewed with respect to the forms of risk estimates used in the "base-case" analysis.

5.2.1 Complementary Cumulative Density Function

As indicated in Figure 5.1 (upper-bound case), the risk curve for the maximum estimable release exhibits an upward shift in probability for a given dose level. This shift increases with the dose. In fact, the largest estimated dose is now increased to 5 man-rem for the least-likely scenario (probability of 1E-9 for two shipments).

This behavior is expected because the releases (and release rates) have been increased for the lowest probability duration interval (60.0-151 min.) in each scenario involving fire. Thus, the upward shift in probability at a given dose level is more pronounced for the higher doses. Nevertheless, even the largest estimated dose of 5 man-rem from the least-likely scenario proves to be insignificant. The curve spans the following range of values: probabilities below 2E-5 and doses below 5 man-rem (wider than in the base case).

5.2.2 Total Risk (Expected Dose)

The 50-yr. inhalation dose to the exposed population (along the transport route) experiences a 28% increase in expected value from 5.3E-7 to 6.8E-7 man-rem as a result of the increase in release. As before, this risk estimate applies to two shipments and represents the probabilistically-weighted mean of all scenario consequences. This value of 6.8E-7 man-rem represents a negligible number of expected fatalaties.

5.2.3 Dominant Accident Scenarios

The percent contribution to the total expected dose from each scenario and radioisotope is listed for this upper-bound case in Table 5.6. As in

TABLE 5.5. Maximum Estimable Release (Airborne, Respirable) Amounts and Rates for Radioisotopes Exposed to Longest Duration Fire

ISOTOPE	MAXIMUM ESTIMABLE RELEASES AMOUNT (Ci)	RATE* (Ci/min)
^{89}Sr	3.4E-4	3.2E-6**
^{90}Sr	3.3	.031
^{134}Cs	7.2	.068
^{137}Cs	71.	.66

*Assumed to occur over 105.5 min.

**This value is not input directly into TRECII because the ^{89}Sr release must first be combined with others in the ^{3}H* radionuclide group.

TABLE 5.6. Percent Contributions to Total Expected Dose From Each Accident Scenario and Radionuclide for Maximum Estimable Releases

	ACCIDENT SCENARIOS						
	FIRE ONLY			IMPACT ONLY	PUNCTURE ONLY	REMAINING EIGHT SCENARIOS	TOTAL FOR EACH ISOTOPE
	DURATION (min.)						
	15.3-30.0	30.0-60.0	60.0-151				
^{3}H*	.011	<.001	<.001	.58	.0016	<.001	.59
^{90}Sr	17.	6.3	22.	47.	.13	.17	92.
^{125}Sb	.026	.0023	<.001	1.4	.0040	<.001	1.5
^{134}Cs	.20	.078	.29	.013	<.001	.0019	.57
^{137}Cs	1.8	.73	2.7	.12	<.001	.018	5.4
TOTAL FOR EACH SCENARIO	19.	7.1	25.	49.	.14	.19	100

*Includes ^{3}H, ^{60}Co, ^{89}Sr, ^{106}Ru, and ^{144}Ce

NOTE: Total Expected Dose for Maximum Estimable Releases = 6.8E-7 man-rem.

the base case, the impact-only scenario is dominant, but its contribution has dropped from 62% to 49%. This is readily attributed to the fact that the maximum estimable releases have been applied to the longest duration intervals of the scenarios involving fire. The release amounts and rates from the impact-only scenario remain the same. Thus, since the total risk increases, this scenario contributes proportionately less to the overall value.

The 15.3-30.0-min. duration for the fire-only scenario is no longer second, having been replaced by the 60.0-151-min. duration with its contribution of 25%. This is expected since the release amounts for this latter duration in the fire-only scenario have been raised. In both scenarios, ^{90}Sr is again the dominant isotope by far. The overall ^{90}Sr contribution is about the same (92%), while that from the second-largest contributor, ^{137}Cs, has risen to 5.4%. However, as for the base case, it must be remembered that these scenarios and radioisotopes are dominant contributors to a level of risk that will be shown to be insignificant.

5.3 CONCLUSIONS

To place the risk estimates into perspective, comparisons are made with natural background radiation along the shipping route and with the total risk from postulated accidents involving spent fuel shipment.

5.3.1 Natural Background Radiation Comparison

A comparison is made with the average level of natural background radiation (0.1 rem/person/yr) to the appropriate population along the transport route. This is done for both the total expected dose and the maximum dose from the least-likely scenario in the upper-bound case.

The total risk incorporates the estimates of all the isopleth areas corresponding to the various wind speeds and atmospheric stability classes employed in TRECII. For all these isopleths, the average area is 90.6 km^2. For an average population density of 141 people/km^2 over the entire route (see section C.1.3, 10-km width), the number of people exposed over the average isopleth area is 1.3E+4. If each receives the average level of

natural background exposure (0.1 rem/yr), the population dose over one year is estimated as 1300 man-rem from natural background.

The total expected dose to the exposed population has been estimated at 6.8E-7 man-rem for the upper-bound case. While this is a 50-year inhalation dose, it is compared with the population dose over one year from natural background for the people in the average isopleth area (1300 man-rem). The total risk is clearly an insignificant fraction (5.2E-10) of the natural background.

The maximum dose from the least-likely scenario in the upper-bound case (5 man-rem at a probability of 1E-9 for two shipments) results from the pairing of a wind speed and an atmospheric stability category corresponding to an isopleth area of 207 km^2. Also, this dose results from exposure over this area when the population density is in the maximum range (an upper limit of 2000 people/km^2 for a 10-km width, see Table 5.3). Using this upper limit, the number of people exposed over this isopleth area is estimated to be 4.1E+5. If each receives the average level of natural background exposure (0.1 rem/yr), the population dose over one year is estimated as 4.1E+4 man-rem from natural background.

Again, the maximum dose from the least-likely scenario in the upper-bound case (5 man-rem) is a 50-year inhalation dose. As before, it is compared with the population dose over one year from natural background for the people in the appropriate isopleth area (4.1E+4 man-rem). As for the total expected dose, this maximum dose for the least-likely scenario is also an insignificant fraction (1.2E-4) of the natural background.

5.3.2 Spent Fuel Shipping Comparison

Reference 2 reports population doses (50-yr., inhalation) from postulated transportation accidents involving spent fuel. The doses, listed by accident category and critical organ, for truck shipment of long-cooled spent fuel are reproduced from reference 2 in Table 5.7. To provide another perspective on the comparative risk to the public from two zeolite shipments, these values must be normalized to a base consistent with that for this zeolite risk assessment.

TABLE 5.7.[2] 50-Year Inhalation Doses to Population from Postulated Transportation Accidents Involving Truck Shipment of Long-Cooled Spent Fuel

	POPULATION DOSES ($\frac{\text{man-rem}}{\text{shipment-km}}$)			
	Critical Organ			
Accident Category	Total Body	Bone	Lung	Thyroid
Impact (small breach)	3E-9	6E-8	1E-9	3E-10
Severe Impact	3E-10	4E-9	1E-10	1E-11
Long Fire	2E-9	2E-8	6E-10	3E-11
Impact plus Fire	4E-13	2E-12	1E-13	4E-14
Severe Impact plus Fire	2E-12	1E-11	1E-12	2E-14

All 20 dose values in Table 5.7 are summed to yield a total expected dose of 9.1E-8 man-rem/shipment-km from spent fuel truck transportation accidents. Multiplying this by the number of zeolite shipments (2) and the distance from TMI to PNL (2600 miles or 4200 km) yields a total risk of 7.6E-4 man-rem. When the total risk for the zeolite upper-bound case (6.8E-7 man-rem) is compared to this total risk for spent fuel shipments, it is found to be a very small fraction (8.9E-4) of it. Thus, on a comparative basis, the total risk from potential accidents in the transport of the two zeolite liners is less than .001 of that from spent fuel.

Based upon the assumptions used and the analysis performed in this study, it is concluded that the transport of radioactive zeolite liners from TMI to PNL by truck can be accomplished at an insignificant level of risk to the public.

REFERENCES

1. Franklin, A., TRECII: A Computer Program for Transportation Risk Assessment. PNL-3208; Pacific Northwest Laboratory (May 1980).

2. Greenborg, J. et. al., Application of ALARA Principles to Shipment of Spent Nuclear Fuel. PNL-3261; Pacific Northwest Laboratory (May 1980).

APPENDIX A

PHYSICAL ANALYSIS OF ZEOLITE LINER AND SHIPPING CASK

APPENDIX A

PHYSICAL ANALYSIS OF ZEOLITE LINER AND SHIPPING CASK

A.1 GENERATION AND ABSORPTION OF DECAY POWER IN THE LINER

The zeolite liners are conservatively assumed to have a total radioactive loading of 70,000 Ci as of July 1, 1981 (the assumed loading date). Upon shipment, assumed to occur on January 1, 1982, the total loading has decayed to 68,180 Ci with the following composition:

^{89}Sr	=	.28 Ci
^{90}Sr	=	2,757 Ci
^{134}Cs	=	6,012 Ci
^{137}Cs	=	59,410 Ci

A.1.1 Beta Decay

All four radioisotopes release β particles, their energies and abundances as follow:[1]

^{89}Sr:	1.463 MeV	(100%)	
^{90}Sr:	.546 MeV	(100%)	
^{134}Cs:	.089 MeV	(28%)	composite = .499 MeV
	.410 MeV	(1%)	
	.662 MeV	(71%)	
^{137}Cs:	.511 MeV	(94.6%)	composite = .547 MeV
	1.176 MeV	(5.4%)	

Each value represents the maximum β-particle energy per disintegration. However, the particles actually possess energies over a wide spectrum. A more accurate estimate of the average β-particle energy is 1/3 of the maximum value. Given the Ci loadings for the four radionuclides, the power generated by β decay is estimated as follows:

ISOTOPE	ACTIVITY (Ci)	ACTIVITY (dis/sec)	AVERAGE PARTICLE ENERGY (1/3 max.) (MeV/dis)	ENERGY GENERATION RATE (MeV/sec)
^{89}Sr	.28	1.04E+10	.488	5.07E+9
^{90}Sr	2757	1.02E+14	.182	1.86E+13
^{134}Cs	6012	2.22E+14	.166	3.69E+13
^{137}Cs	59410	2.20E+15	.182	4.00E+14

The power generated by β decay of each element is 1.86E+13 $\frac{MeV}{sec}$, or 2.98 W, from Sr and 4.37+14 $\frac{MeV}{sec}$, or 70.0 W, from Cs. Thus, the total power generated by β decay is 73.0 W.

In the process of decaying to ^{137}Ba in its ground state, ^{137}Cs also ejects an orbital electron during a small fraction of its transitions following the emission of the .511-MeV β particle. The energy spectrum for this electron ejection is as follows:[2]

$$\left.\begin{array}{l} .624 \text{ MeV } (8.08\%) \\ .655 \text{ MeV } (1.46\%) \\ .660 \text{ MeV } (.48\%) \end{array}\right\} \text{ composite} = .0632 \text{ MeV}$$

Since this occurs only in 94.6% of the ^{137}Cs decays, the power generated by this electron ejection process is $(2.20E+15 \frac{dis}{sec})(.946)(.0632 \frac{MeV}{dis})$ = 1.31E+14 $\frac{MeV}{sec}$, or 21.0 W.

The liner's 3/8-in.-thick walls will ensure that all β particles and the ejected electrons are absorbed within it. Thus, the total β and electron decay power of 94.0 W will be absorbed within the liner.

A.1.2 Gamma Decay

Only the two Cs isotopes emit γ-rays; there are none from ^{89}Sr nor ^{90}Sr. Those from ^{134}Cs are emitted directly during decay, while those from ^{137}Cs are emitted only after emission of the .511-MeV β particle to yield ^{137}Ba in an excited state. The energy spectra and yields (per disintegration) for the γ-rays of these two isotopes are as follow:[2]

^{134}Cs:	1.580 MeV	(.03%)	composite = 1.54 MeV
	1.365 MeV	(3.47%)	
	1.168 MeV	(2.01%)	
	1.038 MeV	(1.04%)	
	.802 MeV	(7.9%)	
	.769 MeV	(87%)	
	.605 MeV	(97.5%)	
	.569 MeV	(13.3%)	
	.563 MeV	(8.6%)	
	.476 MeV	(1.62%)	
^{137}Cs (via ^{137}Ba):			
	.662 MeV	(89%)	composite = .590 MeV
	.032 MeV	(4%)	

The yields shown for the ^{137}Cs γ-rays are applicable only in 94.6% of the disintegrations, i.e. those in which the .511-MeV β particles are first emitted.

The power generated from γ decay of each isotope is $(2.22E{+}14\ \frac{dis}{sec})\ (1.54\ \frac{MeV}{dis}) = 3.42E{+}14\ \frac{MeV}{sec}$, or 54.8 W, from ^{134}Cs and $(2.20E{+}15\ \frac{dis}{sec})\ (.946)\ (.590\ \frac{MeV}{dis}) = 1.23E{+}15\ \frac{MeV}{sec}$, or 197 W, from ^{137}Cs. Thus, the total γ-decay power generated is 252 W, bringing the overall decay power generation to 346 W. However, not all of the γ-rays are absorbed inside the liner. Some will escape and deposit their energy inside the cask's lead walls.

The QAD computer program is used to estimate the amount of γ power escaping from the liner.[3] From this, an estimate can be made of the γ power deposited inside the liner. The zeolite is assumed to form an 8.1-ft^3 cylinder of radius 11 5/8 in. and height 2.75 ft. It is surrounded by steel with a 3/8-in. wall thickness. The zeolite is comprised of 373 lb_m of alumino-silicate, of which 17%, or 63 lb_m, is bound water (of hydration). In addition, there are 112 lb_m of unbound water present inside the liner, bringing the total water content to 175 lb_m.

The amount of alumino-silicate, excluding bound water is 373 lb_m - 63 lb_m, or 310 lb_m. Thus, for the 8.1-ft^3 volume, the densities of each are:

Water: 175 $lb_m/8.1\ ft^3$ = 21.6 lb_m/ft^3

Alumino-silicate: (excluding bound water) 310 $lb_m/8.1\ ft^3$ = 38.3 lb_m/ft^3

Experiments conducted in the evaluation of the SDS's performance indicate that Cs will occupy only about the top 21% of the zeolite cylinder for a Cs loading of 60,000 Ci, or the top 41% at 120,000 Ci.[4] The Sr distribution will be uniform. In the QAD analysis, the 65,400 Ci of Cs are assumed to occupy only the top 25% of the zeolite, while the Sr is uniformly distributed throughout. For γ buildup calculations, the alumino-silicate (excluding bound water) is presumed to be all Al.

QAD yields the γ-energy flux escaping from the zeolite cylinder at various axial and radial positions. These are averaged over their respective surfaces and multiplied by the surface areas to yield the total rate of γ-energy escape from the liner -- 80.5 W. This is assumed to be deposited in the cask's lead walls and represents 32% of the total γ power generated, or 23% of the total decay power generated. The remaining 171 W from γ decay will be absorbed inside the liner, giving a total energy absorption rate of 265 W inside the liner (77% of total power generated). The results are summarized below.

ENERGY ABSORPTION RATE (W)

	Inside Zeolite Liner	Inside Cask's Lead Walls
β Decay:		
Sr	2.98	-
Cs*	91.0	-
γ Decay:		
Cs	171.	80.5
TOTAL	265.	80.5

* Includes electron ejection from ^{137}Ba excited state

A.2 THERMAL ANALYSIS OF THE LINER-CASK SYSTEM

The integrity of the liner-cask system with respect to thermal effects is investigated for two cases: normal transport and fire accident conditions. During normal transport, the dominant effect will be the nonuniform generation of decay heat inside the zeolite. Thus, a two-dimensional (axial and radial) analysis is appropriate. Under fire accident conditions, the 1000°C fire is the dominant effect (decay heat generation is negligible in comparison). Thus, a simpler, one-dimensional (radial) analysis will suffice.

A.2.1 Normal Transport

A two-dimensional model of the liner-cask system is developed for the axial and radial directions. The nonuniform generation of decay power must first be considered.

A.2.1.1 Power Distribution

Because the Cs is located primarily in the upper 25% of the zeolite cylinder, power generation and absorption will not be axially uniform in the zeolite or in the cask's lead walls. To account for this asymmetry, the zeolite cylinder is divided into four stacked cylinders, each of height 2.75 ft./4 = .688 ft., or 8.25 in., for the thermal model. The configuration is shown in Figure A.1, in which the vessel's curved ends have been flattened for ease of modelling. Similarly, the cask's lead walls are divided into four corresponding cylindrical/annular regions as shown in Figure A.2. It remains to estimate the power distribution (265 W inside the zeolite and 80.5 W inside the lead) among these various regions.

A.2.1.1.1 Beta Decay

All power from β decay will be absorbed inside the zeolite. Since Sr is uniformly distributed throughout, it is assumed that each region absorbs 1/4 of the total power from Sr β decay, or 2.98 W/4 = .745 W. The Cs is located mainly in the upper 25% of the zeolite, the top region. Thus, it is assumed that all 91.0 W from Cs β decay (including electron emission from the excited ^{137}Ba nuclei) are absorbed solely in the top region. There is no absorption of β decay energy in the cask's lead walls.

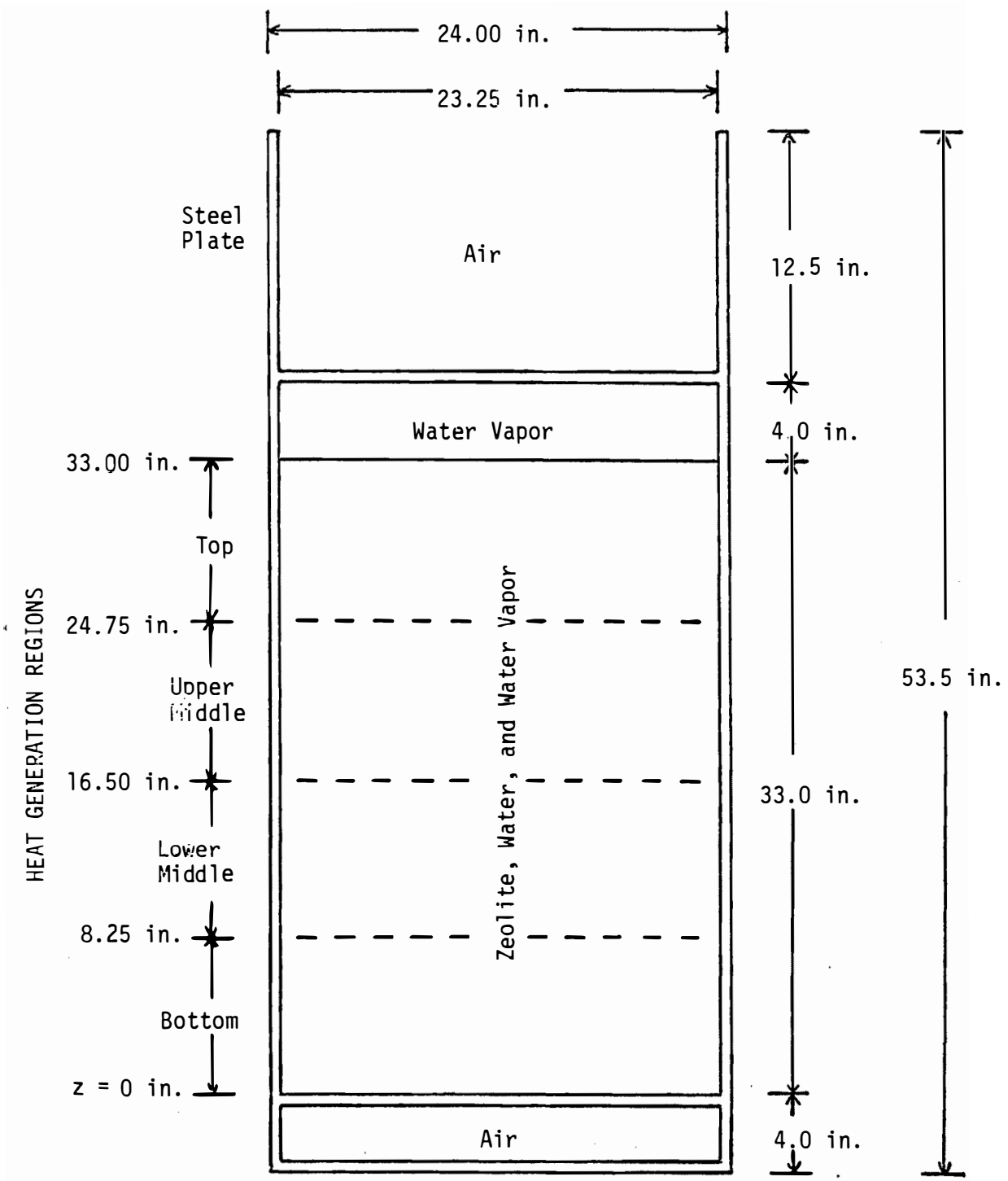

All steel plate thicknesses are 3/8 in.

FIGURE A.1. Schematic Showing Heat Generation Regions Inside Zeolite Cylinder

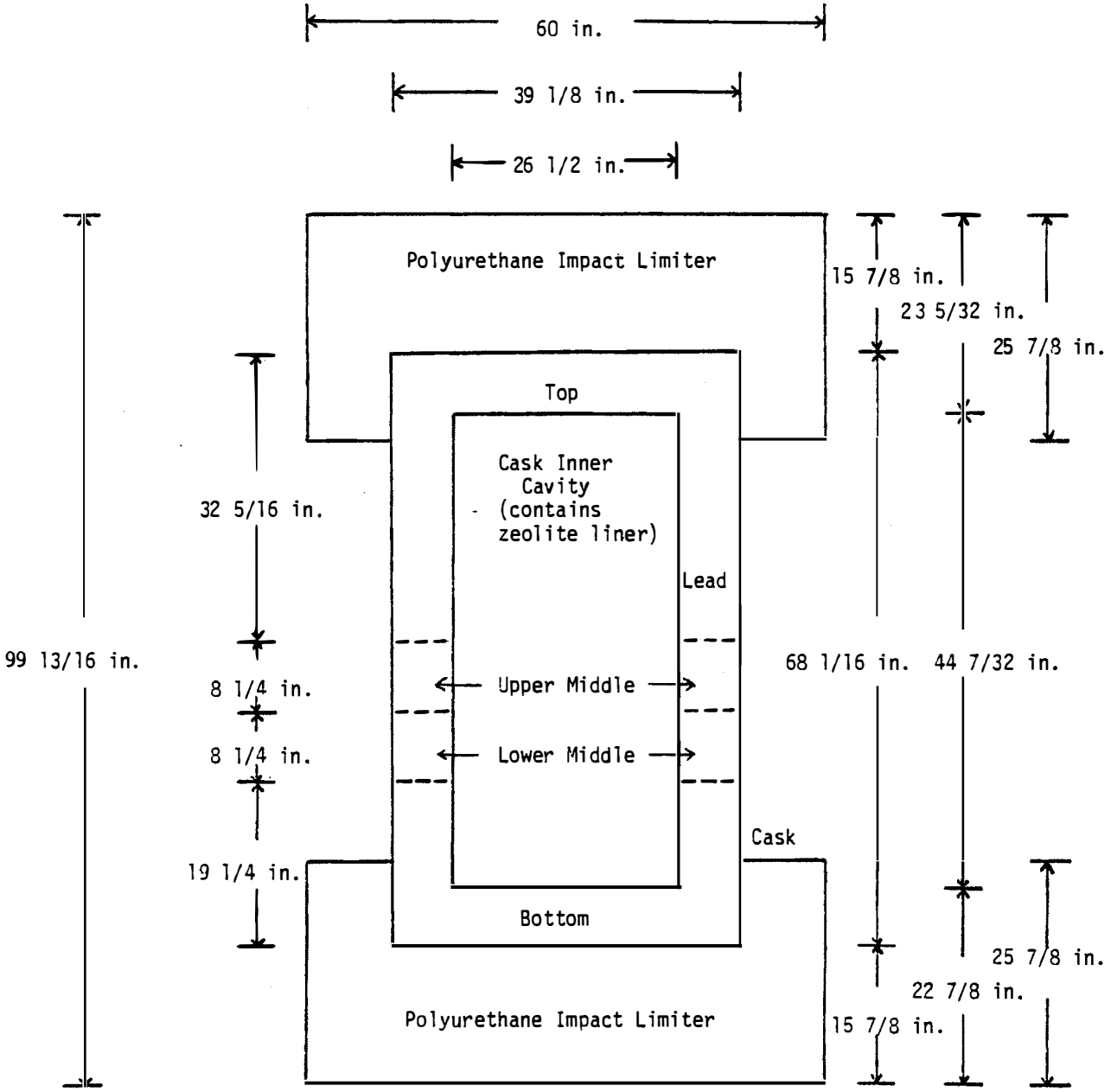

For simplicity, steel plating is not shown.

FIGURE A.2. Schematic Showing Heat Generation Regions Inside Cask's Lead Walls

A.2.1.1.2 Gamma Decay

QAD provides an estimate of the γ flux escaping from the zeolite cylinder at various radial and axial locations. The γ-energy escape rate from each zeolite region can be calculated to yield the distribution of γ power absorbed inside the lead walls. The proportions of γ power escaping radially from each zeolite region can also be used to estimate the proportions of γ power being absorbed in each zeolite region. (The axial power escape is neglected for this latter estimate since there is none from the middle two regions. Including this axial escape from the top and bottom regions would overestimate the proportions used to calculate the γ-power absorption for these regions inside the zeolite).

The γ power escaping from the zeolite cylinder in the radial and axial directions for each region is summarized below:

γ POWER ESCAPING FROM ZEOLITE CYLINDER (W)

Zeolite Region	Radial	Axial	Total
Bottom	.271	.217	.488
Lower Middle	1.81	--	1.81
Upper Middle	14.3	--	14.3
Top	33.5	30.4	63.9
Total	49.9	30.6	80.5

From this, the fraction escaping radially is calculated for each zeolite region. The γ power absorbed within each zeolite region is then assumed to be distributed according to those fractions. The results are summarized below:

Zeolite Region	Radial Escape Fraction	γ Power Absorbed Inside Zeolite (W)
Bottom	.00543	.930
Lower Middle	.0364	6.24
Upper Middle	.287	49.2
Top	.671	115.
Total	1.0	171.

The γ contribution is now combined with that from β to yield the decay energy absorption rate inside each zeolite region. The γ-energy escape rates from the regions represent the absorption inside the cask's lead walls. The results are shown in Table A.1.

TABLE A.1. Energy Absorption Rates for Thermal Analysis of Liner-Cask System During Normal Transport

		Region			
		Bottom	Lower Middle	Upper Middle	Top
Zeolite Height Range (in.)		0-8.25	8.25 - 16.50	16.50 - 24.75	24.75 - 33.00
Power Absorption Inside Zeolite (W)	Sr β	.745	.745	.745	.745
	Cs β*	--	--	--	91.0
	Cs γ	.930	6.24	49.2	115.
	TOTAL	1.68	6.99	49.9	207.
Cs γ Power Absorbed Inside Cask's Lead Walls (W)		.488	1.81	14.3	63.9

*Includes electron emission from excited ^{137}Ba nuclei.

A.2.1.1 Geometric Model

For the two-dimensional thermal analysis, both the axial and the radial geometry of the liner-cask system must be specified. This is done in the detailed schematic shown in Figure A.3. Note the inclusion of a pipe located along the liner's centerline not shown in earlier schematics (Figures 3.2 and A.1). It is included here because it can act as a conductive fin to reduce the temperature in the zeolite. The steel pipe is 1.5 in. wide and extends to within one inch of the uppermost rim of the liner. It is assumed to be 1/16 in. thick.

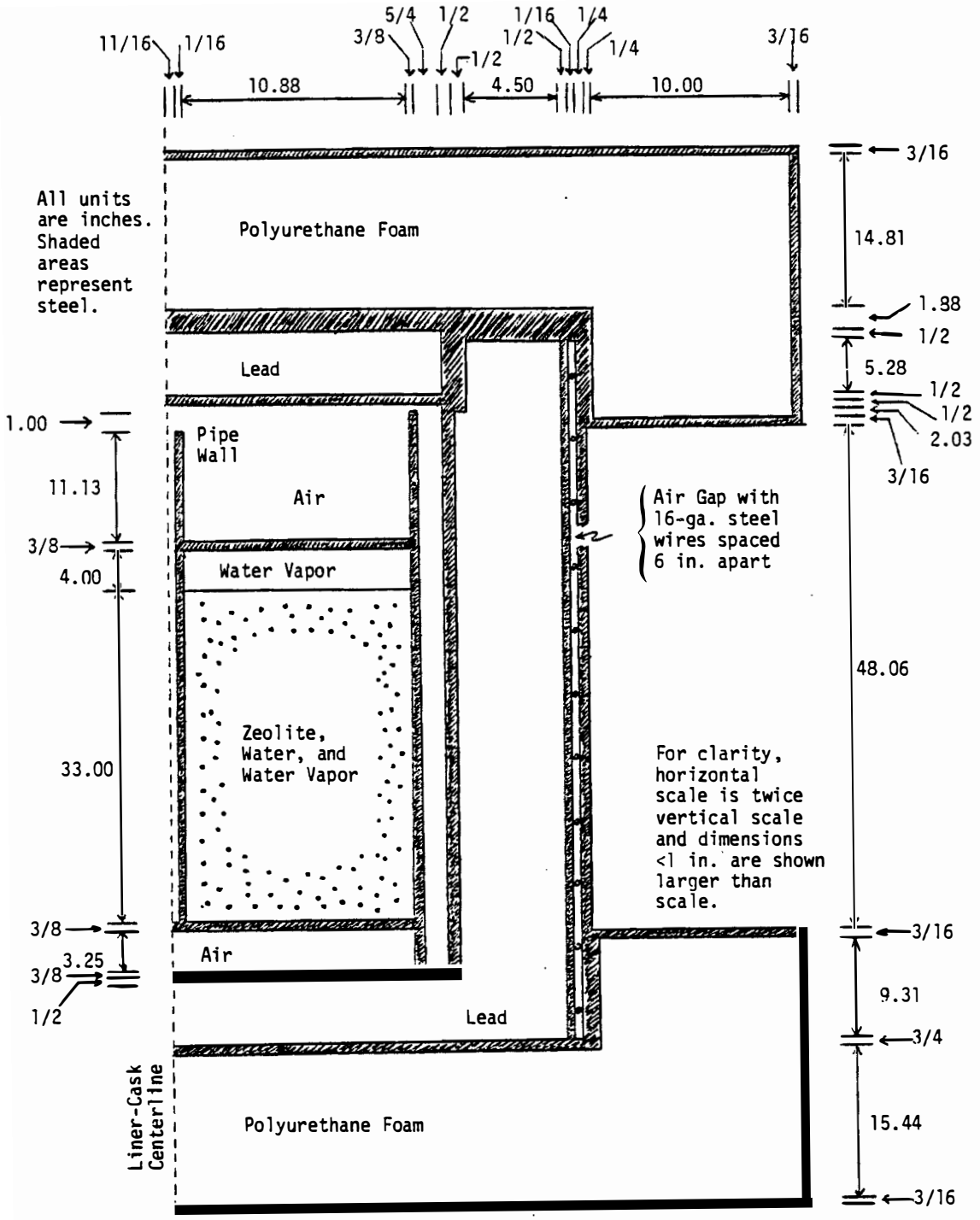

FIGURE A.3. Two-Dimensional Axial and Radial Model of Liner-Cask System Used in Thermal Analysis

A.2.1.3 Thermal Properties

The two-dimensional thermal analysis considers heat conduction and radiation in the liner-cask system plus convection for the various air gaps and for the ambient air. Thermal conductivities and radiative emissivities are specified for the zeolite matrix (including water and/or water vapor) and for the various structural materials in the liner-cask system. Convection coefficients are specified for the ambient air and the air gaps, with thermal conductivities also being assigned to the latter.

A.2.1.3.1 Zeolite Matrix

Swift gives the effective thermal conductivity of dried zeolite as .092 BTU/hr-ft-°F.[5] Since the zeolite is porous, its matrix contains spaces filled with water and/or water vapor. Its effective thermal conductivity will therefore be higher than for the dried condition. Regions where the matrix contains water as opposed to water vapor will exhibit a greater thermal conductivity.

To calculate the effective thermal conductivity, a model is used which views the medium as granular.[6] The zeolite matrix is assumed to consist of zeolite spheres packed in a cubic lattice, the arrangement of which results in a porosity of 42%. This agrees with the value given in reference 7 for the internal porosity of alumino-silicates (40-55%). Based upon the dried zeolite conductivity of .092 BTU/hr-ft-°F, the following values are calculated for the zeolite matrix:

Region	Thermal Conductivity (BTU/hr-ft-°F)
Zeolite + Water	.304
Zeolite + Water Vapor	.110

Note that since the conductivity for the dried zeolite also incorporates convective and radiative effects, the values obtained above also reflect these phenomena.

Heat radiation between the zeolite and the liner's steel walls is modelled by assuming the emissivity between their surfaces to be 0.5. Heat convection inside the liner is not modelled, except as incorporated above in the effective conductivities.

A.2.1.3.2 Structural Materials

The following thermal conductivities are selected for the liner-cask structural materials:

Steel $\longrightarrow$ $10 \frac{BTU}{hr\text{-}ft\text{-}°F}$ (8)

Lead $\longrightarrow$ $20 \frac{BTU}{hr\text{-}ft\text{-}°F}$ (9)

Polyurethane Foam $\longrightarrow$ $1E\text{-}6 \frac{BTU}{hr\text{-}ft\text{-}°F}$

The very low value selected for the polyurethane foam reflects the assumption that it is essentially an ideal thermal insulator.

Radiative effects are accounted for between the following surfaces:

1. liner walls and walls of cask inner cavity
2. Bottom of liner vessel and bottom of liner itself (see Figures 3.2 and A.1)

and for the cask's outer wall. The emissivities for the first two pairs of surfaces are both taken to be 0.5. For the cask's outer surface, an emmisivity of 0.8 is assumed.

A.2.1.3.3 Air Interfaces

Heat convection coefficients must be specified for the following air interfaces:

1. interface between cask's outer wall and ambient air
2. air gap between the liner and the cask's inner walls

3. air gap between the bottoms of the liner vessel and the liner itself

4. thermal radiation gap between the cask's outer pair of steel plates.

Values for the first three are taken directly from reference 9:

Location	Convection Coefficient (BTU/hr-ft^2-°F)
Cask's Outer Wall	1.0
Liner-Cask Air Gap	.15
Vessel-Liner Air Gap	.15

A convection coefficient for the radiation gap must be derived.

This thermal radiation gap is designed to provide thermal resistance for fire-type environments. It consists of 16-gage steel wires wrapped and spaced on 6-inch centers, thereby creating a 1/16-in. gap between two steel shells. The conduction effect of the steel wires in this gap is estimated by formulating a film resistance based upon the appropriate cross-sectional areas of steel and air in this gap (see Figure A.4). The calculation is as follows for a model of unit surface area (note: subscript "s" represents steel; "a" represents air):

$$q = A_s k_s \frac{\Delta T}{\Delta \chi} + A_a k_a \frac{\Delta T}{\Delta \chi}$$

where: q = heat flow rate (BTU/hr)

A = cross-sectional area (ft^2)

k = thermal conductivity (BTU/hr-ft-°F)

T = temperature (°F)

χ = distance (ft)

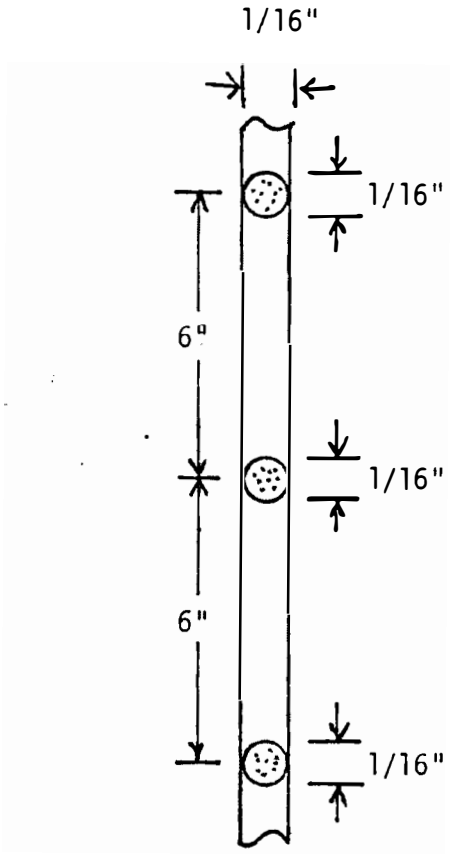

Tangential View
of Radiation Gap
Showing Spacing
of Steel Wires

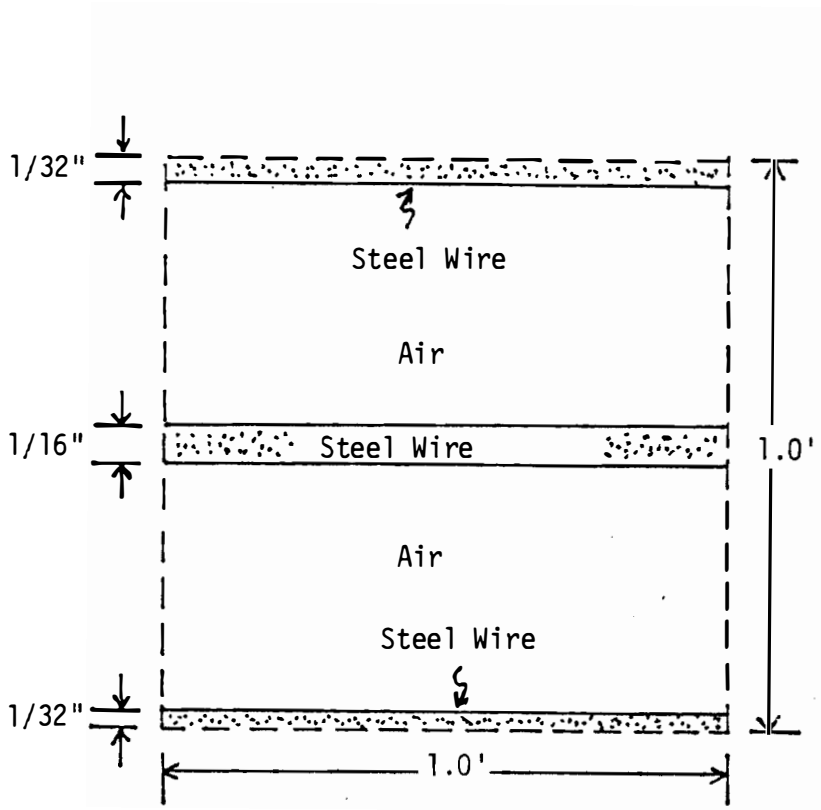

Radial View of Radiation Gap
Showing Spacing of Steel Wires
(1-ft^2 cross-sectional area)

FIGURE A.4. Cross-Sectional Views of Thermal Radiation Gap in Cask Wall

For the gap, the values are:

$$A_s = 2\left(\frac{.0625 \text{ in}}{12 \text{ in/ft}}\right) (1 \text{ ft}) = .0104 \text{ ft}^2$$

$$k_s = 30 \frac{\text{BTU}}{\text{ft-hr-°F}} \text{ (carbon steel)}$$

$$A_a = \left[1 \text{ ft} - 2\left(\frac{.0625 \text{ in}}{12 \text{ in/ft}}\right)\right] (1 \text{ ft}) = .990 \text{ ft}^2$$

$$k_a = .0157 \frac{\text{BTU}}{\text{ft-hr-°F}}$$

$$\Delta x = \frac{.0625 \text{ in}}{12 \text{ in/ft}} = .00521 \text{ ft (gap width)}$$

These values yield the following:

$$\frac{q}{\Delta T} = 63 \frac{\text{BTU}}{\text{hr °F}}$$

For the 1-ft^2 cross-sectional area in the model (see Figure A.4), this corresponds to an equivalent convection coefficient over the gap of 63 BTU/hr-ft^2-°F. For heat conduction through the air gaps, a thermal conductivity of .0157 BTU/hr-ft-°F is used.[8]

A.2.1.4 TEMPEST Computer Analysis

To model the conductive and radiative phenomena in the liner-cask system, the general purpose, three-dimensional hydrothermal code TEMPEST is employed.[10] Convection (except in the air gaps) is not modelled directly, but rather it is incorporated into the effective thermal conductivities of the zeolite matrix. Also, only the axial and radial directions are modelled since no angular dependence is expected.

The zeolite cylinder, which has already been divided into four axial regions of varying power generation (see Figure A.1), is further subdivided radially. Each axial region is separated into three concentric annular volumes as follow (each is 8.25 in. high):

1. an inner annulus of inner radius .75 in. (radius of steel pipe) and outer radius 4.38 in.

2. a central annulus of inner radius 4.38 in. and outer radius 8.00 in.

3. an outer annulus of inner radius 8.00 in. and outer radius 11.63 in. (radius of zeolite cylinder).

Thus, the zeolite cylinder is divided into twelve annular regions with four axial and three radial subdivisions. These are shown in Figure A.5.

The cask and its impact limiters are also divided into various regions. The heat generation rate is assumed uniform within each of the four regions shown in Figure A.2. These regions comprise the lead regions shown in Figure A.3

A.2.1.4.1 Water Liquid-Vapor Interface

Since the thermal conductivities of the zeolite regions depend upon whether or not they contain water or water vapor, determination of the height of the liquid-vapor interface is needed. Initially, the 112 lb_m of unbound water will occupy a volume of 112 $lb_m/64 \frac{lb_m}{ft^3} = 1.79\ ft^3$. Assuming a zeolite porosity of around 50% (consistent with reference 7), the volume available for water and water vapor within the zeolite matrix is $(8.1\ ft^3)(.50) = 4.0\ ft^3$. Thus, water is expected to initally occupy roughly the bottom half of the zeolite cylinder (lower middle and bottom axial regions). The remainder, including the 4.00 in. above the zeolite but within the liner, will hold water vapor (as shown in Figure A.1).

To obtain upper and lower bound on the potential temperatures within the zeolite, two extreme cases are also considered:

1. all water in the vapor form

2. all water in the liquid form.

In addition, the realistic case of half-vapor-half-liquid is analyzed using the TEMPEST code. The ambient air temperature is assumed to be 100°F in all cases.

For each case, the temperature in each of the twelve zeolite regions (refer to Figure A.5) is calculated. Because effective thermal conductivities of the zeolite and water/water vapor are used, these regional temperatures represent average values.

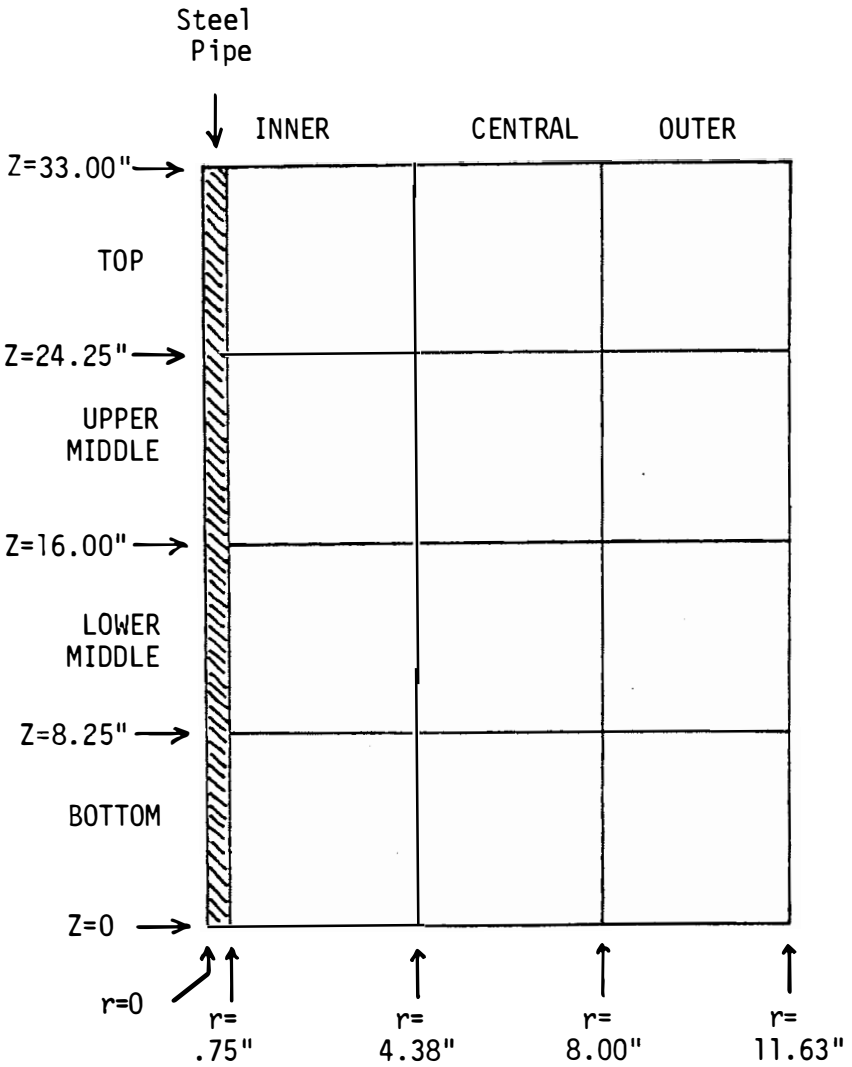

FIGURE A.5. Schematic Showing Cross-Section of Twelve Annular Regions in Zeolite Cylinder

A.2.1.4.2 All-Vapor Matrix

Figure A.6 shows the temperature distribution throughout the zeolite matrix for the all-vapor case. The maximum temperature of 518°F occurs in the inner annulus of the top region as expected. Note that at 518°F, the specific volume of saturated vapor is .57 ft^3/lb_m.[11] Thus, even if none of the bound water has been released at this temperature, the smallest possible volume which the vapor could occupy would be (.57 ft^3/lb_m)(112 lb_m) = 64 ft^3, clearly impossible for the liner under consideration. The all-vapor matrix is an impossibility.

A.2.1.4.3 All-Liquid Matrix

Figure A.7 shows the temperature distribution throught the zeolite matrix for the all-liquid case. The maximum temperature of 274°F occurs in the inner annulus of the top region. At 274°F, saturated liquid has a specific volume of .017 ft^3/lb_m.[11] Since very little, if any, of the bound water has been released at this temperature, the largest possible volume which the liquid could occupy would be (.017 ft^3/lb_m)(112 lb_m) - 1.9 ft^3. Using the lower bound on the zeolite porosity range of 40%, the smallest available volume for the water inside the zeolite matrix would be (8.1 ft^3)(.40) = 3.2 ft^3. Thus, the all-liquid matrix is also an impossibility.

A.2.1.4.4 Half-Vapor-Half-Liquid Matrix

Figure A.8 shows the temperature distribution throughout the zeolite matrix for the more realistic case in which the upper half holds water vapor and the lower holds water. Again, the maximum temperature of 482°F occurs in the inner annulus of the top region. Zeolite is structurally stable up to 1300°F.[4] Thus, no threat is perceived to its stability. Since the top and upper middle regions contain the water vapor, the temperatures are averaged volumetrically throughout these regions to yield an average vapor temperature of 294°F. This volumetric averaging is warranted because the temperature gradients indicated here are somewhat exaggerated. Heat transfer effects would tend to smooth out the temperatures.

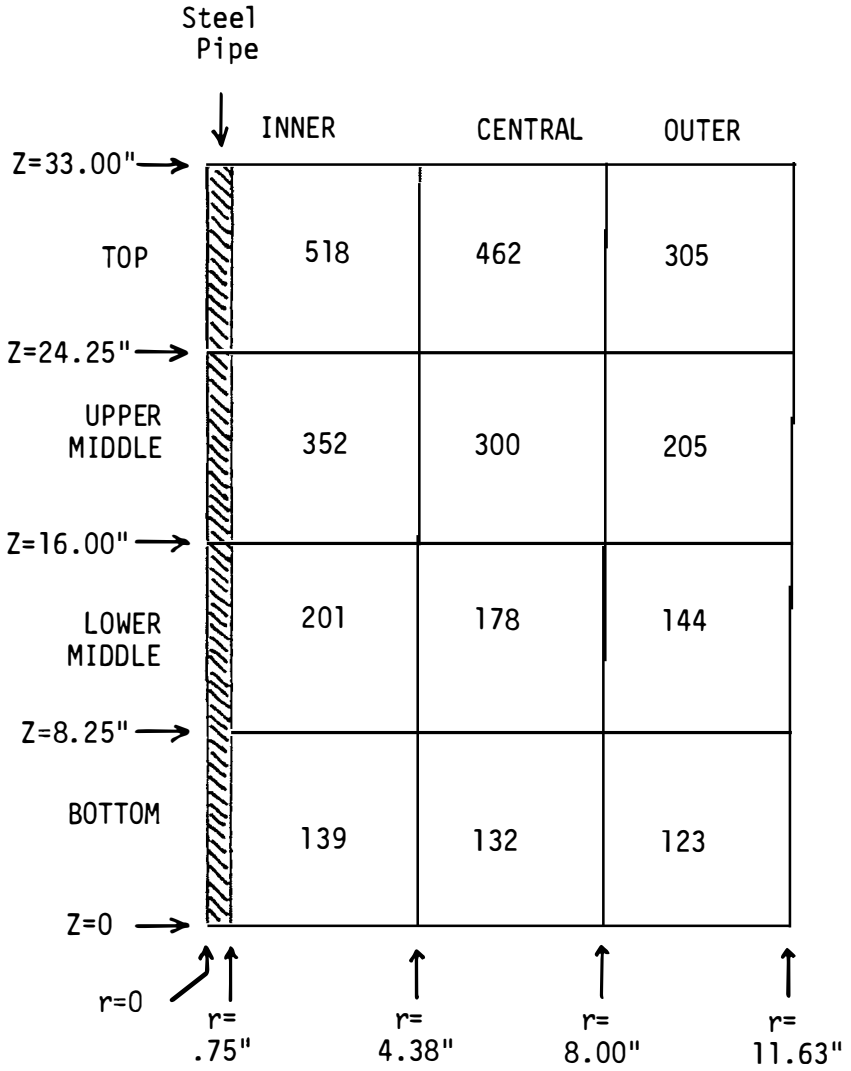

All temperatures are in °F.

FIGURE A.6. Temperature Distribution in Zeolite Matrix for All-Vapor Case

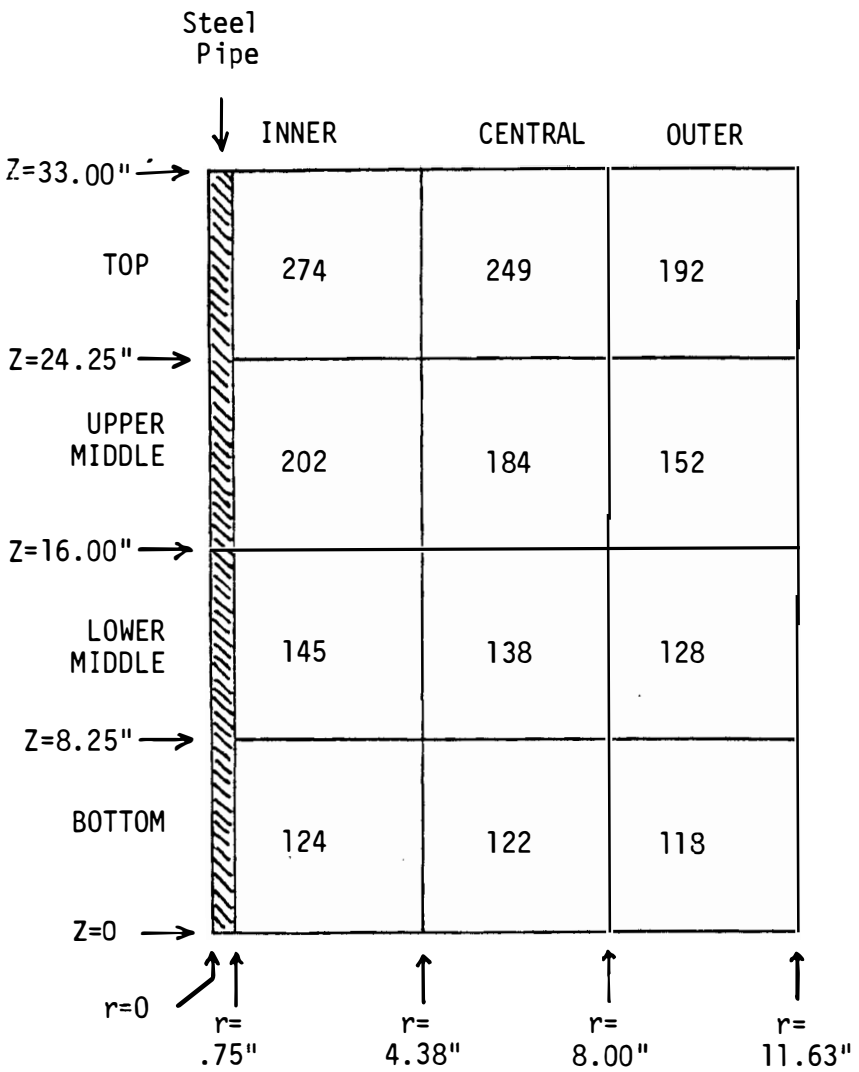

All temperatures are in °F.

FIGURE A.7. Temperature Distribution in Zeolite Matrix for All-Liquid Case

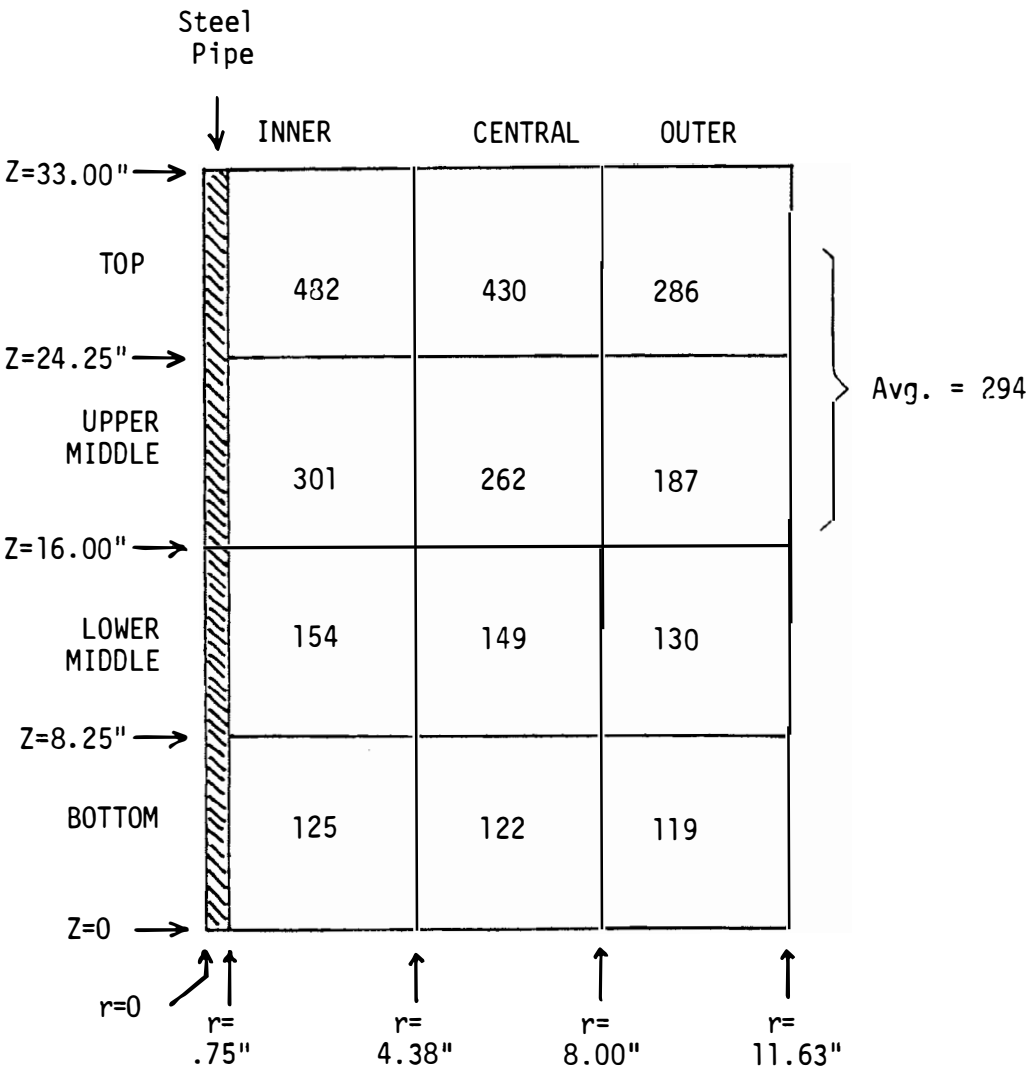

All temperatures are in °F.

FIGURE A.8. Temperature Distribution in Zeolite Matrix for Half-Vapor-Half-Liquid Case

Given the zeolite porosity range of 40-55%, the volume available for water (liquid and vapor) inside the matrix ranges from 3.2 ft^3 to 4.5 ft^3. An additional 1.0 ft^3 is available above the zeolite cylinder, this being the difference between the liner volume (68 gal, or 9.1 ft^3) and the volume occupied by the zeolite matrix (8.1 ft^3). Therefore, the minimum available volume for water is 4.2 ft^3 and the maximum 5.5 ft^3. Very little, if any, bound water has been released at 294°F. Thus, the smallest possible specific volume is 4.2 ft^3/112 lb_m = .038 ft^3/lb_m. On the contrary, the largest possible specific volume is 5.5 ft^3/112 lb_m = .049 ft^3/lb_m. Since both of these lie within the range of specific volumes for saturated steam at 294°F, it is concluded that a saturated mixture exists inside the liner. The corresponding steam pressure is 61 psia.

In section A.2.1.4.1, the zeolite porosity was taken as 50%, giving an available volume within the matrix of 4.0 ft^3 for the water and water vapor. Adding to this the additional 1.0 ft^3 above the matrix yields a total available volume of 5.0 ft^3. Since little, if any, water of hydration has been released at 294°F, the specific volume of the saturated steam is approximately 5.0 ft^3/112 lb_m = .045 ft^3/lb_m. This corresponds to a two-phase mixture which is only .39% vapor. Thus, nearly all of the original 112 lb_m of unbound water remains in the liquid phase and the assumption of a half-vapor-half-liquid matrix remains valid.

A.2.1.4.5 Lead Temperature

In all cases analyzed, the temperature throughout the cask's lead walls rises only slightly (about 20°F) with respect to the ambient air temperature (100°F). Lead melts at 621°F.[9] Thus, at 120°F, no threat to the structural integrity of the cask's lead walls is perceived during normal transport.

A.2.2 Engulfment in Fire

In the thermal analysis for normal transport, it was shown that the temperature of the cask's lead walls rises only slightly to 120°F (for an ambient air temperature of 100°F). The generation of decay power has no effect upon the cask's structural integrity. However, upon engulfment in a

1000°C fire during accident conditions, the lead in the cask's walls could attain the melting temperature of 621°F. The structural integrity of the cask could be lost.

Since the thermal effects of fire engulfment overwhelm those from decay power generation, the latter is ignored in the fire accident thermal analysis. Furthermore, a one-dimensional (radial) analysis including conduction and radiation is deemed sufficient.

A.2.2.1 Geometric Model

Only the cask is modeled for fire engulfment. Upon loss of the thermal shielding which the cask provides for the liner, the liner is presumed to undergo immediate exposure to the 1000°C fire and overpressurize (see section 4.1.1.1). Any thermal insulation provided by the impact limiters is neglected. The cask is assumed to feel the full effects of the 1000°C fire in the radial direction between the limiters. The geometric model of the cask wall is shown in Figure A.9.

A.2.2.2 Thermal Properties

The one-dimensional thermal analysis considers heat conduction and radiation in the cask's walls plus convection in thermal radiation air gap. The values chosen for the thermal conductivities, radiative emissivities, and convection coefficients are the same as those for the two-dimensional analysis, as specified in sections A.2.1.3.2 and A.2.1.3.3. In addition, the fire's emissivity is taken to be 0.9 and the specific heats and densities for steel and lead are chosen as follow:

	Specific Heat (BTU/lb_m-°F)	Density (lb_m/ft^3)
Steel[8]	.11	489
Lead[9]	.031	710

The polyurethane foam impact limiters are not included in the one-dimensional model.

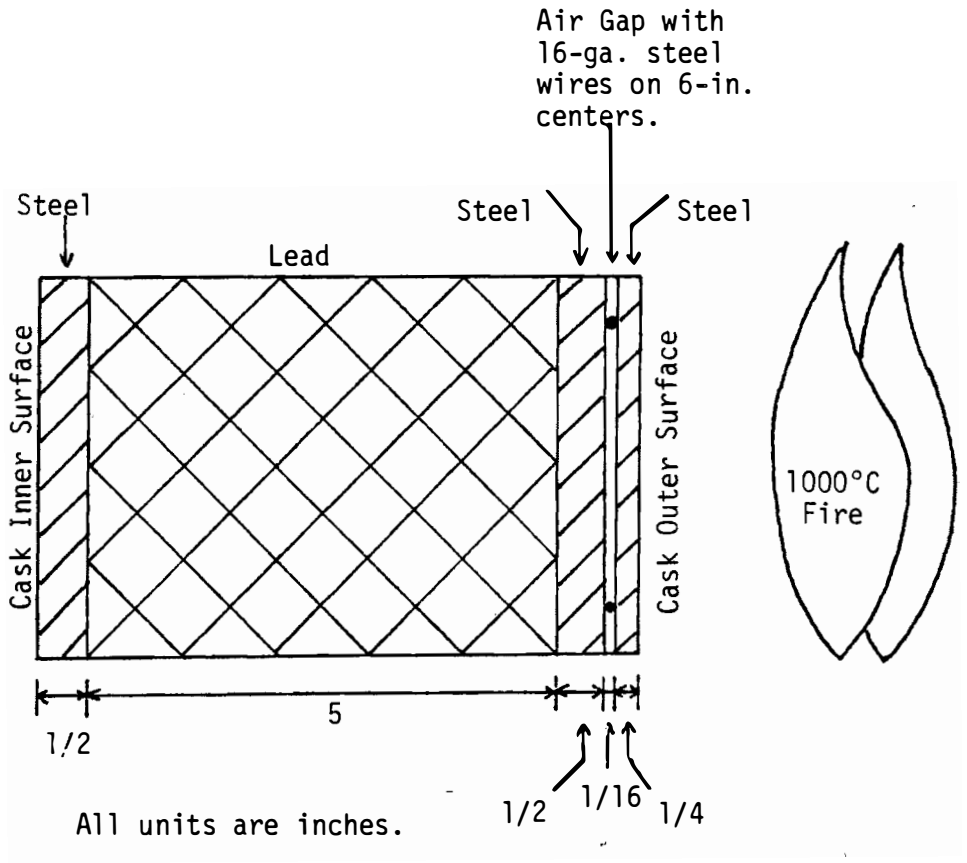

Figure A.9. One-Dimensional Radial Model of Cask Used in Thermal Analysis

A.2.2.3 HEATING4 Computer Analysis

The conductive and radiative phenomena resulting from the cask's engulfment in the 1000°C fire are modelled using the general purpose heat transfer code HEATING4.[12] Only the radial dimension is considered and any convective effects are limited to the air gap. The results of the analysis are displayed as the temperature profile of Figure A.10.

Curve 1 shows the equilibrium temperature of 120°F throughout the cask's walls during normal transport. Curve 2 indicates that, after engulfment in the 1000°C fire for 10.2 min., the outermost portion of the lead in the cask's walls just attains the melting temperature (621°F). Note that the effect upon the liner is negligible. The cask has provided adequate thermal shielding so far.

Lead expands upon melting. Thus, at 10.2 min., the cask's outer steel cladding will begin to experience strain from the lead. As the fire continues, more lead melts, and the strain on the cask's steel plating increases. It is assumed that this strain becomes sufficient to rupture the cladding as soon as 50% of the wall's lead thickness becomes molten. Curve 3 indicates that this occurs after the fire has burned for 15.3 min. Presumably to this point, the fire's effect upon the liner has been negligible, and thermal integrity has been maintained.

However, following breach of the outer cladding at an assumed value of 15.3 min., the remainer of the lead will melt rather quickly. Thermal shielding is lost, and the temperature inside the liner rises quickly. The liner, which is designed to withstand an internal pressure of 350 psig at 400°F, and 15 psig at 850°F, will rapidly overpressurize as its unbound water vaporizes.[13] Rather than speculate as to the time required between rupture of the cask's outer wall and heating of the liner to its failure threshold, it is conservatively assumed that the liner overpressurizes at 15.3 min. It and its contents are further assumed to be exposed fully to the severe 1000°C thermal environment at this time.

A.2.3 Threshold for Liner Overpressurization

Upon exposure to a severe thermal environment, the liner has a potential to overpressurize due to a buildup of steam. The design pressure of the liner is

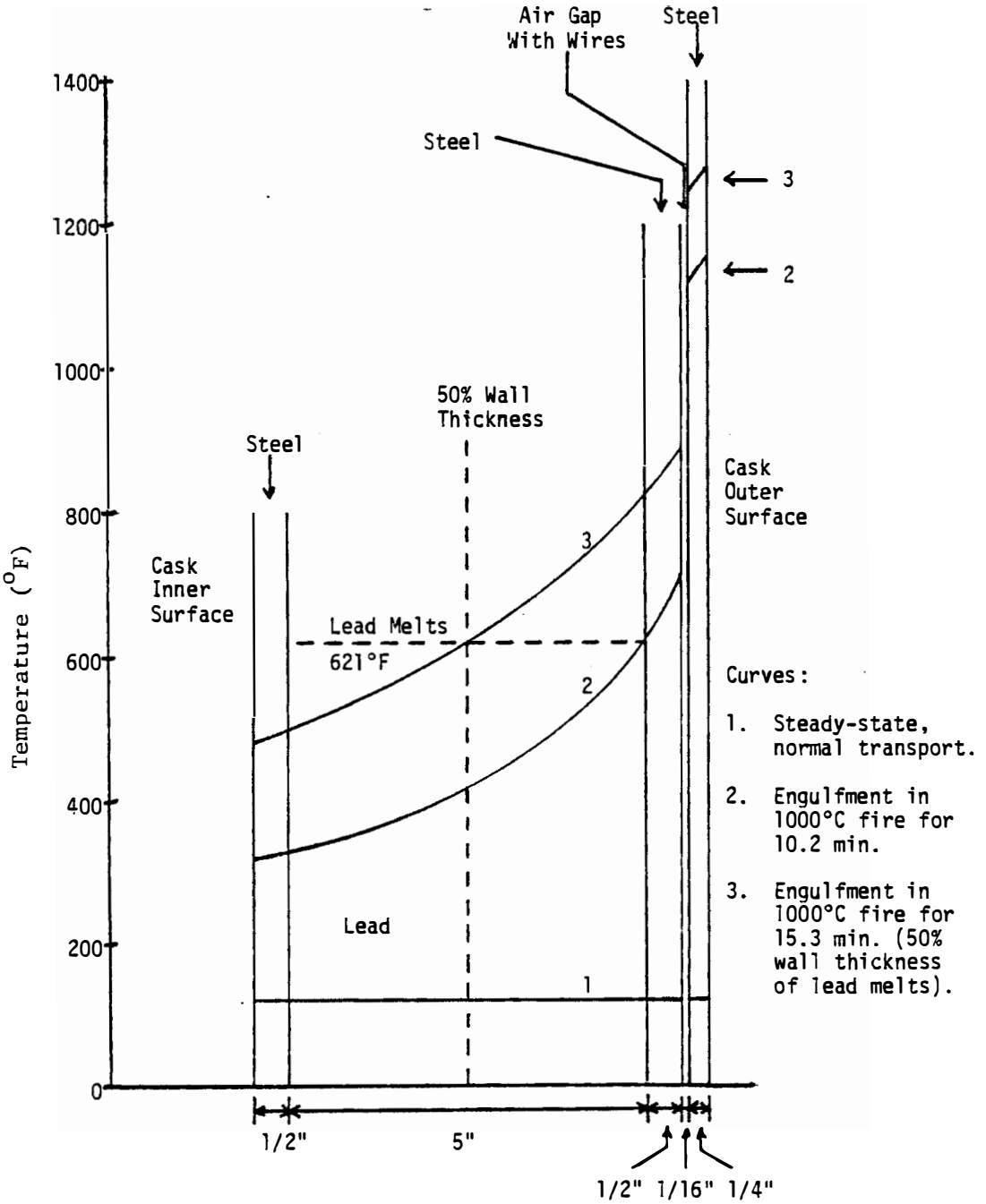

FIGURE A.10. Radial Temperature Profile in Cask Wall for Engulfment in Fire

assumed to decrease linearly from 350 psig (365 psia) to 15 psig (30 psia) over the range from 400°F (860°R) to 850°F (1310°R). The following equation characterizes this temperature dependence of the design pressure:

$$P = 1000 - .744\ T$$

where: $860°R \leq T \leq 1310°R$

P is measured in psia.

While design pressure decreases with temperature increase, internal pressure due to steam buildup rises as the temperature increases. Thus, the temperature at which the internal pressure equals the design pressure represents the critical value for overpressurization of the liner.

The bound water (of hydration) in the zeolite can be driven off over the range from 300°F to 500°F. Assume that all of it has been driven off by the time the temperature reaches 429°F. The available volume required for the two-phase steam to have a specific volume exceeding that of saturated liquid can be estimated. At 429°F, saturated liquid has a specific volume of .019 ft^3/lb_m.[11] For the 175 lb_m of bound and unbound water to form a saturated mixture, the available volume inside the liner must be at least $(.019\ ft^3/lb_m)(175\ lb_m) = 3.3\ ft^3$.

As discussed earlier in section A.2.1.4.4, the volume available for water and water vapor inside the liner is at least 4.2 ft^3. Thus, it is concluded that, even if all bound water is driven off from the zeolite, a saturated mixture will exist at 429°F. The corresponding pressure will be 339 psia. This is due solely to steam since any air originally present is assumed to be expelled from the liner during venting prior to shipment. Furthermore, any buildup of radiolytic hydrogen and oxygen gases during shipment is presumed negligible compared to this steam buildup.

The design pressure at 429°F (889°R) is found from the previous equation to be 339 psia. Thus, it is concluded that, upon exposure to a severe thermal environment, the zeolite liner overpressurizes at approximately 340 psia and 430°F. The size of the breach is not specified since it will be assumed that all the zeolite, whether inside the liner or expelled, will be fully exposed to the 1000°C thermal environment. Further, it will be conservatively assumed

that no retention takes place inside the breached liner for potentially airborne and respirable radionuclides that are released from the zeolite.

A.3 MECHANICAL ANALYSIS OF THE LINER-CASK SYSTEM

Mechanical analysis of the CNS 1-13C shipping cask and its contained zeolite liner is needed to ascertain the failure thresholds for release of airborne, respirable radionuclides from impact and puncture. Breach of both the cask and the liner is required by the definitions of impact and puncture used in this assessment.

A.3.1 Impact

Three impact orientations for cask collisions are considered:

1. Side-on
2. End-on
3. Corner-to-center-of-gravity (the velocity vector upon collision is assumed to be collinear with the point of impact and the cask's center-of-gravity).

The weight of the liner-cask system is as follows:

Zeolite liner (with contents)	= 1,135 lb_m
Shipping cask (empty) with impact limiters	= 24,600 lb_m
Total	= 25,735 lb_m

In all three impact orientations, the energy of collision is presumed to be absorbed by a "crush volume" of the impact limiters (comprised of rigid, polyurethane foam with a crush strength of 1000 psi). Failure is assumed to occur when the body of the cask crushes through the impact limiter and meets the collision target. No credit is given for the cask's structural strength; the impact limiters are assumed to remain affixed to the cask.

A.3.1.1 Side-On

In the side-on collision, a flat target is assumed to collide with the cask's two impact limiters along their radial surfaces. The geometric model for this collision is shown in Figure A.11. The crush volume is:

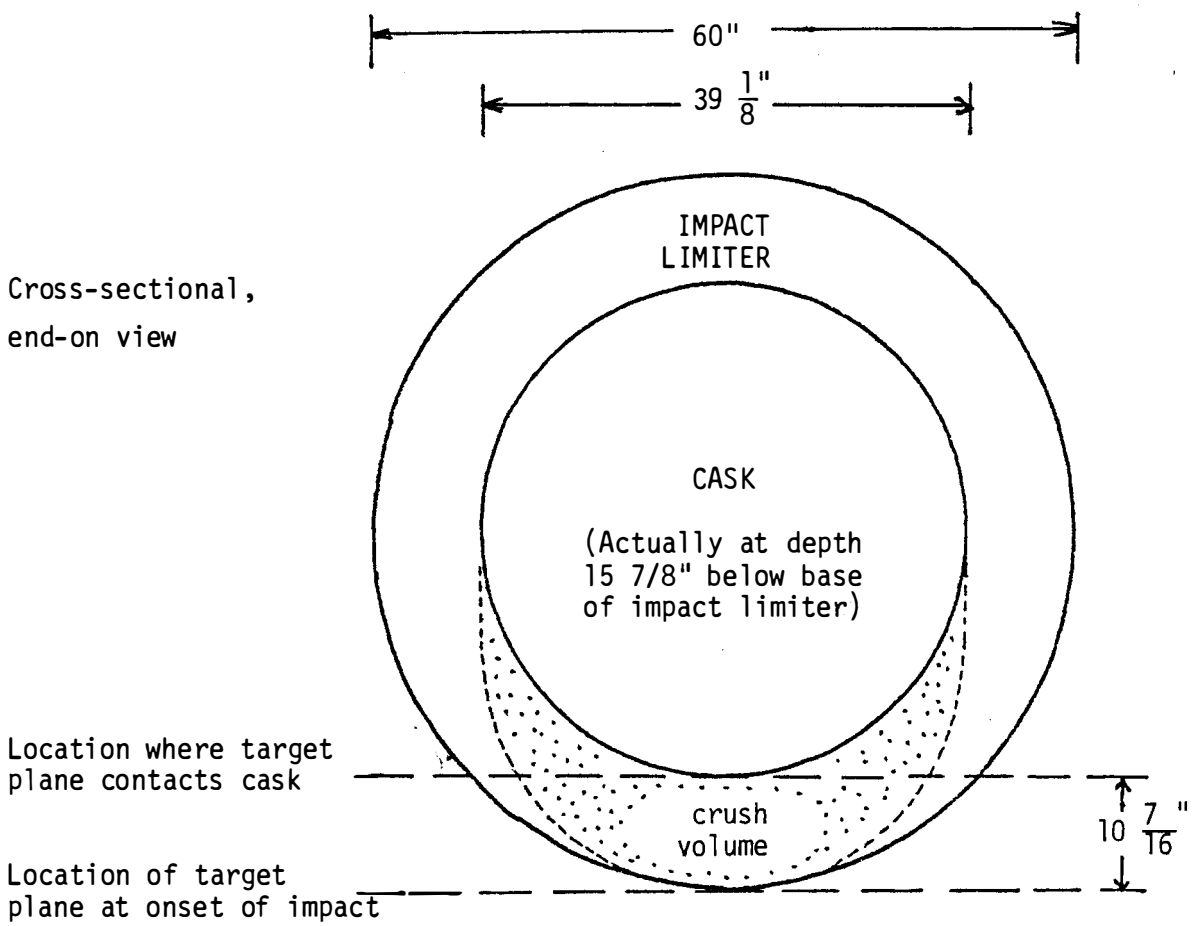

FIGURE A.11. Geometric Model Used in Analysis of Side-On Impact

$$V_{crush} = 2\ (39\ 1/8\ \text{in})\ (10\ 7/16\ \text{in})\ (10\ \text{in})$$

$$= 8170\ \text{in}^3 \text{ for both limiters}$$

The crush strength (σ_{crush}) of the limiters' foam is 1000 psi. Therefore, the energy imparted in the collision over this crush volume is:

$$E_{crush} = V_{crush}\ \sigma_{crush} = 8.17E{+}6\ \text{in-lb}_f$$

The impact velocity needed to produce this energy is calculated as follows:

$$V = \sqrt{\frac{2E_{crush}}{M_{cask\text{-}liner}}}$$

$$= \left[\frac{2(8.17E{+}6\ \text{in-lb}_f)(32.2\ \frac{\text{lb}_m\text{-ft}}{\text{lb}_f\text{-sec}^2})}{(25735\ \text{lb}_m)\ (12\ \frac{\text{in}}{\text{ft}})}\right]^{\frac{1}{2}}$$

$$= 41\ \frac{\text{ft}}{\text{sec}}\text{, or 28 mph}$$

This is an overconservative estimate of the failure threshold velocity for impact breach. The cask itself (without the impact limiters) has been licensed to withstand a 30-ft. drop onto a flat unyielding surface without loss of integrity.[14] This is equivalent to withstanding a 30-mph impact collision. Thus, rather than use the overconservative estimate of 28 mph as the failure threshold for side-on impact, a value of 30 mph is assumed. This is still conservative since both the cask and the liner must be breached for a release, and no credit has been given for the cask's structural strength.

A.3.1.2 <u>End-On</u>

In the end-on collision, a flat target is assumed to collide with the base of one of the cask's impact limiters. The geometric model for this collision is shown in Figure A.12. The failure threshold velocity is calculated as follows:

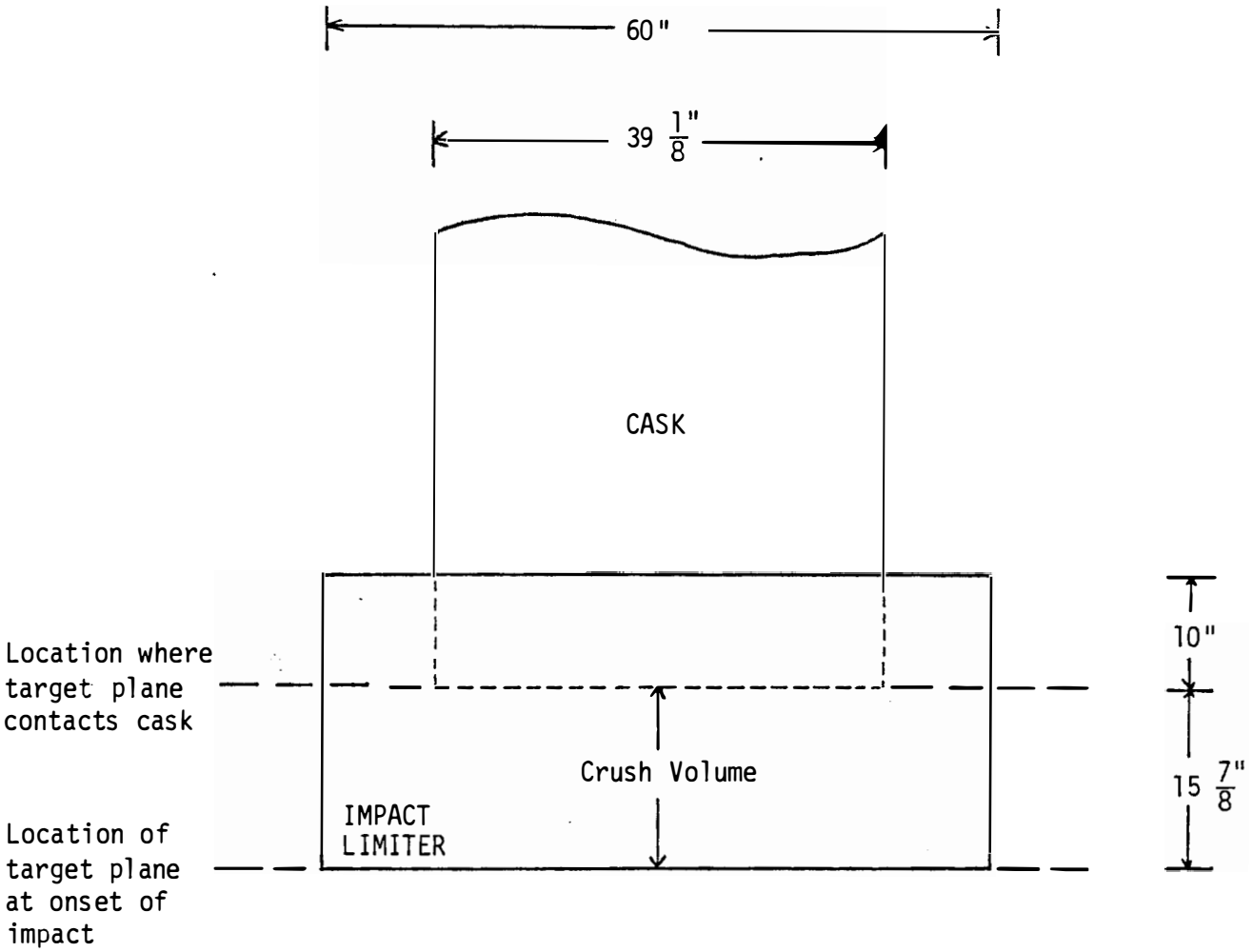

FIGURE A.12. Geometric Model Used in Analysis of End-On Impact

$$V_{crush} = \pi(30\ in)^2\ (15\ 7/8\ in) = 4.49E{+}4\ in^3$$

$$\sigma_{crush} = 1000\ psi$$

$$E_{crush} = V_{crush}\sigma_{crush} = 4.49E{+}7\ in\text{-}lb_f$$

$$V = \sqrt{\frac{2E_{crush}}{M_{cask\text{-}liner}}}$$

$$= \left[\frac{2(4.49E{+}7\ in\text{-}lb_f)(32.2\ \frac{lb_m\text{-}ft}{lb_f\text{-}sec^2})}{(25735\ lb_m)\ (12\ \frac{in}{ft})}\right]^{1/2}$$

$$= 97\ \frac{ft}{sec}\ ,\ \text{or } 66\ mph$$

This is a conservative estimate of the failure velocity needed to breach both the cask and the liner by an end-on impact. Again, no credit has been given for the cask's structural strength.

A.3.1.3 Corner-to-Center-of-Gravity

In the corner-to-center-of-gravity (of the cask) collision, a flat target is assumed to collide with one of the cask's impact limiters along a vector from a corner to the cask's center-of-gravity. The geometric model for this collision is shown in Figure A.13. The failure threshold velocity is calculated as follows:

$$V_{crush} = 1.77E{+}4\ in^3$$

$$\sigma_{crush} = 1000\ psi$$

$$E_{crush} = V_{crush}\sigma_{crush} = 1.77E{+}7\ in\text{-}lb_f$$

$$V = \sqrt{\frac{2E_{crush}}{M_{cask\text{-}liner}}}$$

$$= \left[\frac{2(1.77E{+}7\ in\text{-}lb_f)(32.2\ \frac{lb_m\text{-}ft}{lb_f\text{-}sec^2})}{(25735\ lb_m)\ (12\ \frac{in}{ft})}\right]^{1/2}$$

$$= 61\ \frac{ft}{sec},\ \text{or } 41\ mph$$

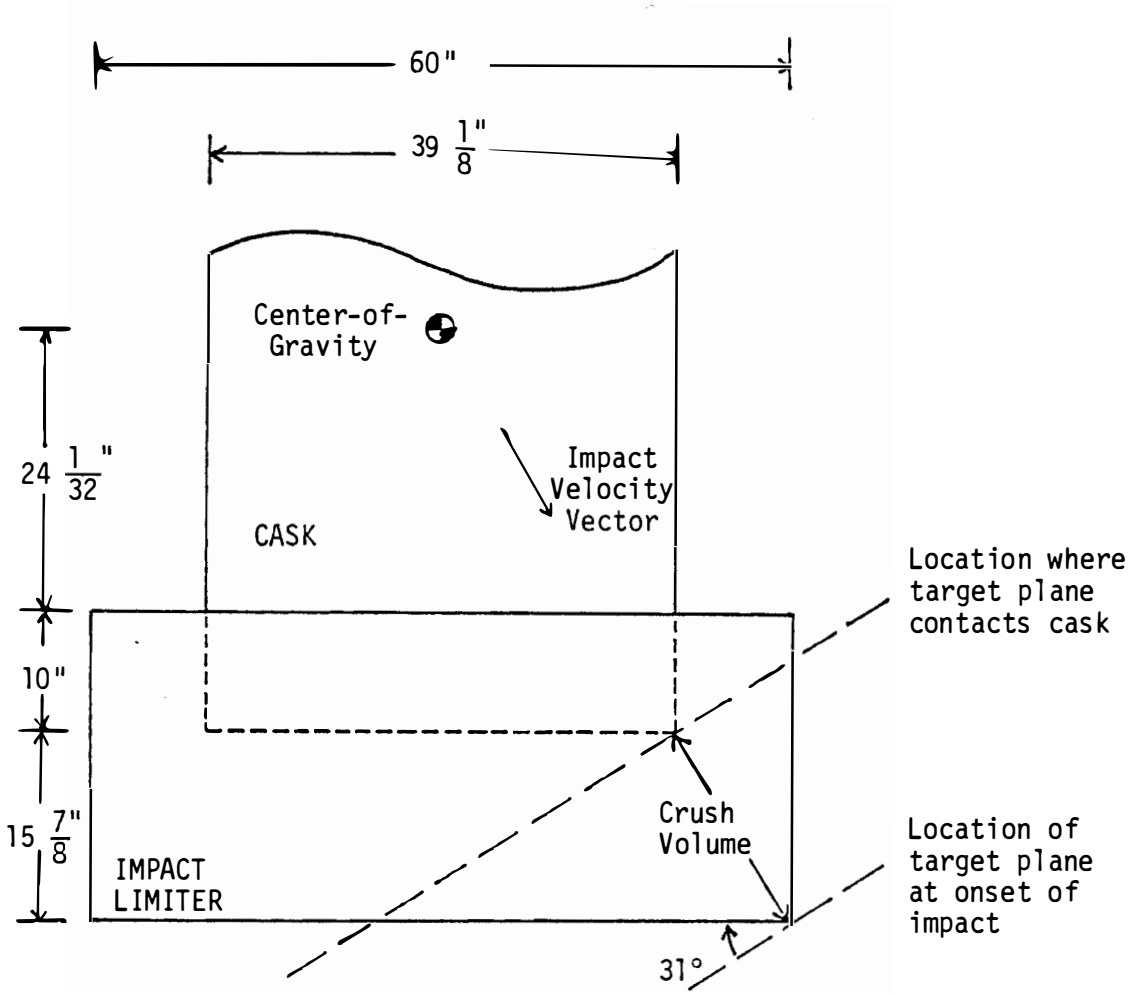

Note: Center-of-gravity is assumed to be at cask's geometric center

FIGURE A.13. Geometric Model Used in Analysis of Corner-to-Center-of-Gravity Impact

This is a conservative estimate of the failure velocity needed to breach both the cask and the liner by a corner-to-center-of-gravity impact. Again, no credit has been given for the cask's structural strength.

A.3.1.4 Estimated Failure Threshold Velocity

The results for the three impact orientations are summarized below:

IMPACT ORIENTATION	FAILURE THRESHOLD VELOCITY (MPH)
Side-on	30
Corner-to-center-of-gravity	41
End-on	66

A collision for the side-on orientation is most likely for the shipping system (cask is mounted upright). This orientation also has the lowest failure threshold. Thus, for an airborne, respirable release of radionuclides to take place due to an impact accident, the failure threshold velocity is estimated as 30 mph. This is conservatively assumed to breach both the cask and the liner.

The size of the breach is not specified. It will merely be assumed sufficient to allow 5% of the zeolite to be expelled from the liner. Further, it is conservatively assumed that no retention takes place inside the liner for potentially airborne and respirable radionuclides that are released from the zeolite when exposed the the 1000°C fire following impact.

A.3.2 Puncture

Breach of both the cask and the liner is required for a potential airborne, respirable release of radionuclides to occur. The presence of the rather large impact limiters at the cask's ends renders the potential for puncture negligible at those locations relative to the puncture potential radially through the cask's wall between the limiters. Thus, only puncture in the radial direction between the impact limiters is analyzed.

The threshold for puncture breach is related probabilistically to the equivalent mild-steel thickness of the package wall.[15] Thus, the equivalent thickness of the cask and the liner walls must be calculated with reference to mild steel. The actual thicknesses and materials of these walls are shown in Figure A.3. All consist of steel except for the cask's 5-in. of lead. Reference 15 estimates that one inch of lead has an equivalent mild steel thickness of 1/16 in., yielding an equivalent mild-steel thickness of 5/16 in. for the cask's lead annulus. The total equivalent mild-steel thickness of the cask and the liner walls is estimated to be:

CASK:	OUTER STEEL PLATES	=	3/4 in.
	LEAD WALL	=	5/16 in.
	INNER STEEL PLATE	=	1/2 in.
LINER:	STEEL PLATE	=	3/8 in.
	TOTAL	=	1 15/16 in.
		≃	1.9 in.

This is estimated to be the failure threshold for potential release of airborne, respirable radionuclides due to breach of both the cask and the liner by puncture.

The size of the breach is not specified, but it is assumed to be smaller than that from impact. It will be presumed sufficient to allow 1% of the zeolite to be expelled from the liner. Further, it is conservatively assumed that no retention takes place inside the liner for potentially airborne and respirable radionuclides that are released from the zeolite when exposed to the 1000°C fire following puncture.

REFERENCES

1. Handbook of Chemistry and Physics, 55th Edition (edited by R. Weast); CRC Press, Cleveland, OH (1973).

2. Engel, R. et al., ISOSHLD--A Computer Code for General Purpose Shielding Analysis. BNWL-236; BNWL (June 1966).

3. Cain, V., A User's Manual for QAD-CG, the Combinatorial Geometry Version of the QAD-PSA Point Kernel Shielding Code. RSIC Computer Code Collection, CCC-307 (May 1979).

4. Evaluation of Increased Cesium Loading on Submerged Demineralizer System (SDS) Zeolite Beds. DOE/NE-0012; U.S. Department of Energy (May 1981).

5. Swift, W., Fission Product and Waste Packaging by Inorganic Zeolite Absorption. HW-73964; Hanford Laboratories Operation, GE, Richland, WA (1962).

6. Crane, R. and R. Vachon, "A Prediction of the Bounds on the Effective Thermal Conductivity of Granular Materials," International Journal of Heat and Mass Transfer. 20:711-23 (1977).

7. Perry, R. (ed.), Chemical Engineer's Handbook (Fifth Edition); McGraw-Hill Book Co., New York, NY (1973).

8. Krieth, F., Principles of Heat Transfer, 2nd Edition; International Textbook Co., Scranton, PA (1965).

9. Holeman., Heat Transfer, 3rd Edition; McGraw-Hill Book Co., New York, NY (1972).

10. Trent, D. et al., TEMPEST: A Three-Dimensional Time-Dependent Computer Program for Hydrothermal Analysis. FATE-80-114; Pacific Northwest Laboratory (September 1980).

11. Zemansky, M. and H. Van Ness, Basic Engineering Thermodynamics; McGraw-Hill Book Co., New York, NY (1966).

12. Turner, W. and M. Simon-Tov, HEATING3--An IBM 360 Heat Conduction Program (with HEATING4 updates). ORNL-TM-3208; Oak Ridge National Laboratory (1971).

13. GPU Service, Submerged Demineralizer System Demineralizer Liner. Reference Drawing 2D-950-29-001, Revision 1 (March 1981).

14. Procedures, License and Safety Analysis Report for Chem-Nuclear Systems, Inc. CNSI 1600 (CNS 1-13C) Type-B Radwaste Shipping Cask. Chem-Nuclear Systems, Inc., Bellevue, WA (September 1978).

15. Dennis, A. et al., Severities of Transportation Accidents Involving Large Packages. SAND77-0001; Sandia Laboratories (May 1978).

APPENDIX B

ACCIDENT SCENARIOS: ANALYSIS OF PROBABILITIES AND RELEASES

APPENDIX B

ACCIDENT SCENARIOS: ANALYSIS OF PROBABILITIES AND RELEASES

B.1 PROBABILISTIC ANALYSIS

The probabilistic analysis of the accident scenarios is performed in two stages. First, a probabilistic description is developed that is consistent with the definitions and the data base associated with the transportation accident environment.[1] This description takes the form of a set of Boolean probabilistic equations for the scenarios identified. The equations are developed such that the occurrence of an accident scenario corresponds directly to the potential for an airborne release of radionuclides in the respirable range. Finally, these equations are evaluated using the data base from reference 1.

B.1.1 Description

Reference 1 identifies five accident forces for large packages involved in truck accidents. Of these five, fire, impact, and puncture are considered potentially significant in this study. These are developed into accident scenarios consistent with the definitions and the data base from reference 1.

Given the occurrence of a truck accident involving a large package (denoted by A), two mutually exclusive accident categories are identified: collision-only (denoted by C) and non-collision-only (denoted by $\bar{C}$). Fires can occur in a truck accident (denoted by F), some when the accident is collision-only (denoted by F_C), the remainder when the accident is non-collision-only (denoted by $F_{\bar{C}}$).

Associated with the three accident forces are failure thresholds required for a release to occur. These can be viewed as the following events:

E = fire occurs with duration sufficient to cause loss of the thermal shielding provided by the shipping cask (the critical duration)

I = impact occurs with velocity sufficient to breach both the liner and the cask.

P = puncture occurs with a probe capable of breaching both the liner and the cask (whose wall thicknesses are measured in terms of their equivalent mild steel thicknesses)

The complements (non-occurrences) of these events are denoted by bar superscripts (e.g., $\overline{E}$).

It is necessary to consider all possible combinations of these events. This is facilitated by the use of a Boolean expression in which terms such as I/A are interpreted as "impact velocity exceeds threshold (for breaching liner and cask) per occurrence of a truck accident (involving a large package)." The reader is referred to reference 2 for a discussion of Boolean algebra.

All possible combinations of these events (per truck accident) may be expressed as:

$$(I/A + \overline{I}/A)\ (P/A + \overline{P}/A)\ [\overline{F}/A + (\overline{E}/F + E/F) \cdot F/A]$$

The latter terms $(\overline{E}/F + E/F) \cdot F/A$ represent the need for a fire to occur before there can be any consideration of its duration.

Reference 1 defines impact as the package "striking or being struck by an object that has no sharp projections." On the contrary, puncture is defined as the package "striking or being struck by an object that has a potential for penetrating the container." Thus, these two events are mutually exclusive. This means that any terms containing $I \cdot P$ must be eliminated.

Bearing this in mind, the above expression is evaluated by the laws of Boolean algebra to yield the following expression:

$$\begin{aligned}
&(I \cdot \overline{P} \cdot \overline{F})/A + [(I \cdot \overline{P} \cdot F)/A \cdot \overline{E}/F] + [(I \cdot \overline{P} \cdot F)/A \cdot E/F] \\
&+ (\overline{I} \cdot P \cdot \overline{F})/A + [(\overline{I} \cdot P \cdot F)/A \cdot \overline{E}/F] + [(\overline{I} \cdot P \cdot F)/A \cdot E/F] \\
&+ (\overline{I} \cdot \overline{P} \cdot \overline{F})/A + [(\overline{I} \cdot \overline{P} \cdot F)/A \cdot \overline{E}/F] + [(\overline{I} \cdot \overline{P} \cdot F)/A \cdot E/F]
\end{aligned}$$

The following two terms do not lead to any possible release by definition:

1. $(\overline{I}\cdot\overline{P}\cdot\overline{F})/A$ = per truck accident, no impact nor puncture threshold is reached, nor does a fire occur

2. $(\overline{I}\cdot\overline{P}\cdot F)/A \cdot \overline{E}/F$ = per truck accident, no impact nor puncture threshold is reached and, while a fire does occur, its duration is less than critical (therefore, no release).

The remaining seven terms potentially lead to a radioactive release. They are divided into five main scenarios according to the accident forces involved:

1. Fire-only: $(\overline{I}\cdot\overline{P}\cdot F)/A \cdot E/F$ = per truck accident, only a fire occurs, and its duration exceeds critical

2. Impact-only: $(I\cdot\overline{P}\cdot\overline{F})/A$ = per truck accident, only impact above the threshold velocity occurs

3. Puncture-only: $(\overline{I}\cdot P\cdot\overline{F})/A$ = per truck accident, only puncture above the threshold limit occurs

4. Impact-with-fire:
   A. fire duration < critical: $(I\cdot\overline{P}\cdot F)/A \cdot \overline{E}/F$ = per truck accident, both impact above the threshold velocity and fire occur, but the fire's duration does not reach critical

   B. fire duration $\geq$ critical: $(I\cdot\overline{P}\cdot F)/A \cdot E/F$ = as above for 4.A, but the fire's duration exceeds critical

5. Puncture-with-fire:
   A. fire duration < critical: $(\overline{I}\cdot P\cdot F)/A \cdot \overline{E}/F$ = per truck accident, both puncture above the threshold limit and fire occur, but the fire's duration does not reach critical

   B. fire duration $\geq$ critical: $(\overline{I}\cdot P\cdot F)/A \cdot E/F$ = as above for 5.A, but the fire's duration exceeds critical.

To enable proper evaluation of these scenario probabilities using the data from reference 1, these expressions must be in terms consistent with those from reference 1. The probability of an event occurring (e.g., I/A) will be denoted as p(event) [e.g., p(I/A)]. Before expanding the expression for each scenario, the following reductions are made for the individual events:

1. $p(I/A) = p(I/C)\ p(C/A) + p(I/\overline{C})\ p(\overline{C}/A)$

   $= p(I/C)\ p(C/A)$ since $p(I/\overline{C}) = 0$

2. $p(\overline{I}/A) = 1 - p(I/A) \simeq 1$ assuming $p(I/A) < 0.1$

3. $p(P/A) = p(P/C)\ p(C/A) + p(P/\overline{C})\ p(\overline{C}/A)$

   $= p(P/C)\ p(C/A)$ since $p(P/\overline{C}) = 0$

4. $p(\overline{P}/A) = 1 - p(P/A) \simeq 1$ assuming $p(P/A) < 0.1$

5. $p(F/A) = p[(F_C + F_{\overline{C}})/A] = p(F_C/A) + p(F_{\overline{C}}/A)$

   $= p(F_C/C)\ p(C/A) + p(F_{\overline{C}}/\overline{C})\ p(\overline{C}/A)$

6. $p(\overline{F}/A) = 1 - p(F/A) \simeq 1$ assuming $p(F/A) < 0.1$

With these results, it is now possible to expand the probabilistic expressions for the scenarios into terms consistent with the data in reference 1.

1. Fire-only:

   $p[(\overline{I}\cdot\overline{P}\cdot F)/A \cdot E/F] = p(\overline{I}/A)\ p(\overline{P}/A)\ p(F/A)\ p(E/F)$

   $\simeq p(F/A)\ p(E/F)$

2. Impact-only:

   $p[(I\cdot\overline{P}\cdot\overline{F})/A] = p(I/A)\ p(\overline{P}/A)\ p(\overline{F}/A)$

   $\simeq p(I/C)\ p(C/A)$

3. Puncture-only:

   $p[(\overline{I}\cdot P\cdot\overline{F})/A] = p(\overline{I}/A)\ p(P/A)\ p(\overline{F}/A)$

   $\simeq p(P/C)\ p(C/A)$

4. Impact-with-fire:

   A. fire duration < critical:

   $$p[(I \cdot \overline{P} \cdot F)/A \cdot \overline{E}/F] = p(I/A)\ p(\overline{P}/A)\ p(F/A)\ p(\overline{E}/F)$$

   $$\simeq p(I/C)\ p(C/A)\ p(F_C/C)\ p(\overline{E}/F)$$

   B. fire duration $\geq$ critical

   $$p[(I \cdot \overline{P} \cdot F)/A \cdot E/F] = p(I/A)\ p(\overline{P}/A)\ p(F/A)\ p(E/F)$$

   $$\simeq p(I/C)\ p(C/A)\ p(F_C/C)\ p(E/F)$$

5. Puncture-with-fire:

   A. fire duration < critical:

   $$p[(\overline{I} \cdot P \cdot F)/A \cdot \overline{E}/F] = p(\overline{I}/A)\ p(P/A)\ p(F/A)\ p(\overline{E}/F)$$

   $$\simeq p(P/C)\ p(C/A)\ p(F_C/C)\ p(\overline{E}/F)$$

   B. fire duration $\geq$ critical:

   $$p[(\overline{I} \cdot P \cdot F)/A \cdot E/F] = p(\overline{I}/A)\ p(P/A)\ p(F/A)\ p(E/F)$$

   $$\simeq p(P/C)\ p(C/A)\ p(F_C/C)\ p(E/F)$$

These expressions represent the probabilities of occurrence of the scenarios (and, thus, of potential releases) per truck accident. Reference 1 defines an accident rate per shipment per mile [denoted by $\lambda(A)$]. To obtain the accident rate per shipment, this value must be multiplied by the total route distance for one shipment. This value also represents (to an extremely close approximation) the probability (per shipment) of an accident involving a large package [denoted by $p(A)$]. When each of the above expressions for the scenarios is multiplied by $p(A)$, the probability (per shipment) of that scenario occurring is found.

B.1.2 Evaluation

Before evaluating the occurrence probabilities of the various scenarios, it is necessary to examine the data from reference 1 to obtain values for the previously derived probabilistic terms. Several terms can be evaluated directly:

1. $\lambda(A)$ = 2.5E-6/shipment-mile. Since the total route distance for one shipment is 2,600 miles, p(A) = .0065/shipment

2. p(C/A) = .80 (probability of a collision-only accident per truck accident). Correspondingly, its complement, $p(\overline{C}/A)$, = .20.

3. p(F/A) = .016 (probability of a fire occurring per truck accident).

4. p(P/C) = 3.0E-5 (probability that a package, the liner with the cask, with an equivalent mild-steel wall thickness of 1.9 in. will be punctured per collision-only accident).

Reference 1 provides the probability of a large package experiencing an impact velocity change below a given value for the "over-the-road" transport vehicle weight. The threshold velocity required to breach both the liner and the cask can be interpreted as an equivalent velocity change. Thus, the probability of the impact velocity exceeding the threshold is equivalent to that of the velocity change exceeding this same threshold.

This probability also depends upon the "over-the-road" vehicle weight. For each shipment, this is estimated to be:

Zeolite liner (with contents)	=	1,135 lb_m
Shipping cask (empty) with impact limiters	=	24,600 lb_m
Truck tractor (5900 kg)[3]	=	13,010 lb_m
Truck trailer (5000 kg)[3]	=	11,025 lb_m
TOTAL	=	49,770 lb_m
	≃	25 tons

For the estimated failure threshold of 30 mph and a vehicle weight of 25 tons, p(I/C) = .011 (probability that the liner and the cask are both breached upon impact per collision-only accident).

$p(F_c/C)$, the probability of a fire occurring in a collision-only accident per collision-only accident, can be estimated from the following equation:

$$p(F_c/C) = \frac{p(F_c/F)\ p(F/A)}{P(C/A)}$$

Reference 1 gives a value of .25 for $p(F_c/F)$, the probability of a fire occurring in a collision-only accident per fire occurrence. Using the previously quoted values for the other terms, $p(F_c/C)$ is estimated to be .0050.

Reference 1 presents a cumulative distribution of fire-accident durations for truck transport of large packages (shown in Figure B.1). This can be used to obtain estimates for $p(\overline{E}/F)$ and $p(E/F)$, the probabilities of a fire duration below and above critical respectively per fire occurrence. For the estimated critical duration of 15.3 min., the following are obtained:

$$p(\overline{E}/F) = .75$$
$$p(E/F) = .25$$

B.1.2.1 Fire Duration Intervals

In developing a risk curve, it is advantageous to consider as many scenarios as possible. Thus, the accident scenarios for fire-only, impact-with-fire, and puncture-with-fire are further subdivided into intervals for fire durations above critical. Reference 1 estimates that the fraction of fires burning less than time t, denoted by F(t), obeys the following equation for t > 60 min.:

$$F(t) = 1 - e^{-(t/.24)^{0.3}}$$

Thus, F(t) does not equal 1 until $t = \infty$. As an approximation, it is assumed that F(t) = 1 at a value of t (denoted by t_{max}) for which F(t) = .999 (equivalent to a probability of .001 that a fire burns longer than t_{max}).

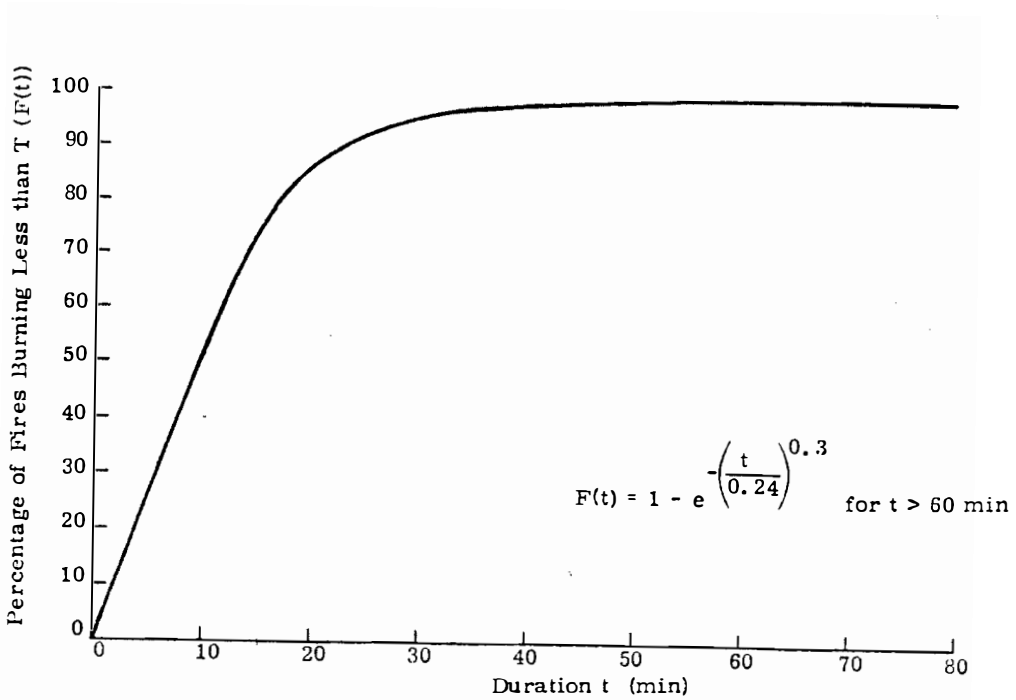

FIGURE B.1.[1] Cumulative Distribution of Fire-Accident Duration for Truck Transport of Large Packages

$$.999 = 1 - e^{-(t_{max}/.24)^{0.3}}$$

$$t_{max} = 151$$

Thus, no fire is assumed to last more than 151 minutes.

The post-critical duration fire scenarios are divided into three intervals:

1. 15.3 - 30.0 min.
2. 30.0 - 60.0 min.
3. 60.0 - 151 min.

The probabilities of a fire duration falling into each interval per fire occurrence are evaluated using Figure B.1:

1. $p(E_1/F) = F(30.0 \text{ min}) - F(15.3 \text{ min}) = .21$
2. $p(E_2/F) = F(60.0 \text{ min}) - F(30.0 \text{ min}) = .033$
3. $p(E_3/F) = F(151 \text{ min}) - F(60.0 \text{ min}) = .011$

B.1.2.2 Scenario Probabilities

All the values needed to calculate the scenario probabilities have now been evaluated. These are summarized in Table B.1. Note that the probability of a scenario occurring is also that for a potential release from that scenario.

The values from Table B.1 are substituted into the probabilistic equations derived for the scenarios in section B.1.1. The scenario probabilities are listed in Table B.2. The sum of these corresponds to the probability of a potential release per accident (.013) or per shipment (8.4E-5). The impact-only scenario contributes 68% of this total probability while fire-only with the 15.3-30.0-min. duration is second with 26%.

TABLE B.1. Input Probabilities for Scenario Evaluation

EVENTS:

A = truck accident occurs per shipment of large package

C = accident type is collision only

$\overline{C}$ = accident type is non-collision-only

F = fire occurs during truck accident

F_c = fire occurs in collision-only accident

E_1 = fire duration lies between 15.3 (critical) and 30.0 min.

E_2 = fire duration lies between 30.0 and 60.0 min.

E_3 = fire duration lies between 60.0 and 151 min.

$\overline{E}$ = fire duration is less than 15.3 min.

I = impact velocity exceeds 30 mph for a 25-ton vehicle (including package)

P = puncture probe pierces an equivalent mild-steel thickness of at least 1.9 in.

PROBABILITIES:

$p(A)$ = .0065/shipment

$p(C/A)$ = .80

$p(\overline{C}/A)$ = .20

$p(F/A)$ = .016

$p(P/C)$ = 3.0E-5

$p(I/C)$ = .011

$p(F_c/C)$ = .0050

$p(\overline{E}/F)$ = .75

$p(E_1/F)$ = .21

$p(E_2/F)$ = .033

$p(E_3/F)$ = .011

TABLE B.2. Probabilities of Occurrence of Accident Scenarios

	ACCIDENT SCENARIOS												
	FIRE ONLY			IMPACT ONLY	PUNCTURE ONLY	IMPACT WITH FIRE				PUNCTURE WITH FIRE			
	Fire Duration (min.)					Fire Duration (min.)				Fire Duration (min.)			
	15.3 - 30.0	30.0 - 60.0	60.0 - 151			0-15.3	15.3 - 30.0	30.0 - 60.0	60.0 - 151	0-15.3	15.3 - 30.0	30.0 - 60.0	60.0 - 151
SCENARIO PROB. (PER ACCIDENT)	.0034	5.3E-4	1.8E-4	.0088	2.4E-5	3.3E-5	9.2E-6	1.5E-6	4.8E-7	9.0E-8	2.5E-8	4.0E-9	1.3E-9
SCENARIO PROB. (PER SHIPMENT)	2.2E-5	3.4E-6	1.1E-6	5.7E-5	1.6E-7	2.1E-7	6.0E-8	9.4E-9	3.1E-9	5.9E-10	1.6E-10	2.6E-11	8.6E-12

B.2 RELEASE ANALYSIS

Since the inhalation pathway has been assumed dominant for this study, only airborne, radioactive releases in the respirable range will be considered. The release amounts discussed shall refer exclusively to this limited category.

B.2.1 Unbound Water

Before proceeding to a scenario-by-scenario analysis, it is worthwhile to consider similarities among the modes of release to facilitate the analysis. In all scenarios, there will be an initial release upon breach of radioactive, two-phase steam from the unbound water. Reference 4 calculates the expected activity concentrations in the SDS process streams following continuous flow of 200 bed volumes through each zeolite bed. These are listed in Table B.3 for the first zeolite columns (corresponding to the liners that will be shipped) as of July 1, 1980. These are corrected for radioactive decay to January 1, 1982, the presumed shipping date. These adjusted concentrations are also shown in Table B.3.

It is conservatively assumed that all 112 lb_m of unbound water will be released from the breached liner (as two-phase steam). All the radioisotopes contained are presumed to become airborne and respirable. Thus, the release for each radioisotope is found by multiplying its concentration (as of January 1, 1982) by the total volume of unbound water. This volume is:

$$\frac{112\ lb_m}{62.4\ \frac{lb_m}{ft^3}}\ (2.83E{+}4\ \frac{cm^3}{ft^3})\ (1\ \frac{ml}{cm^3}) = 5.08E{+}4\ ml$$

These releases are also listed in Table B.3.

B.2.2 Fines

Since all initial releases are energetic due to the buildup of steam pressure inside the liner, some zeolite will also be ejected from the liner. Considering the fines, it is noted that, of the particles that become airborne, only those 10 μm and smaller are respirable. The fines

TABLE B.3. Estimated Airborne Releases in the Respirable Range from Unbound Water

ISOTOPE	CONCENTRATION AS OF 7/1/80 (μCi/ml)	HALF-LIFE (yrs)	CONCENTRATION AS OF 1/1/82 (μCi/ml)	AMOUNT* RELEASED (Ci)
^{3}H	1.0	12.3	.92	.047
^{60}Co	6E-5	5.26	4.9E-5	2.5E-6
^{89}Sr	.0066	.142	4.5E-6	2.3E-7
^{90}Sr	.032	28.1	.031	.0016
^{95}Nb	1.9E-5	.0963	3.9E-10	2.0E-11
^{103}Ru	2.9E-5	.108	2.0E-9	1.0E-10
^{106}Ru	.0024	1.01	8.5E-4	4.3E-5
^{125}Sb	.019	2.70	.013	6.6E-4
^{134}Cs	.0024	2.05	.0014	7.3E-5
^{137}Cs	.014	30.2	.014	6.9E-4
^{144}Ce	4.7E-4	.781	1.2E-4	6.3E-6

*This equals the concentration as of 1/1/82 multiplied by 5.08E+4 ml.

fraction below 10 μm would be minimal at most. The "attribility" of AW-500, a Linde zeolite, has been cited at .25%.[5] The test cited is MIL-D-3716A with the smallest screen size openings being 1000 μm (#18). Clinoptilolite, a similar zeolite, has also been sized.[6] The weight percent below 25 μm is 1E-6% when plotted; any fraction below 10 μm cannot be identified. Thus, the fines are concluded to be above the respirable range, thereby posing no hazard through inhalation.

B.2.3 Heated Zeolite

The remaining zeolite would be too large to become airborne even upon ejection from the liner. Impact and puncture forces would not create additional fines. Thus, the only potential airborne release from these larger particles would result from heating.

Experimental studies of ^{137}Cs releases during zeolite heating have measured total release, not differentiating between bound water and particle releases. Measurement of ^{137}Cs releases from clinoptilolite upon heating indicate minimal release with temperatures below 1200°C (melting point of clinoptilolite).[7] At 1000°C, the release fraction is 4.5E-4 for 4 hours, or 1.9E-6 per minute. Heating for longer periods does not increase the release. Thus, at 1000°C, .12% of the ^{137}Cs is the maximum estimable release regardless of fire duration. A similar study has found no release for Decalso, a zeolite gel , below 1200°C.[8]

Heating releases from the combination of Linde IONSIV IE-96 and A-51 are assumed to be similar to these. The other three radioisotopes (^{89}Sr, ^{90}Sr, and ^{134}Cs) in the zeolite are assumed to have releases similar to ^{137}Cs; i.e., a release rate of 1.9E-6/min. and a maximum total release of .12%, when exposed to a 1000°C fire. No credit is taken for mitigation due to plateout on the liner's interior surfaces.

So long as the thermal integrity of the cask remains intact (less than 50% of its wall's lead thickness is melted), the zeolite inside the liner is assumed not to experience the severe thermal environment. Thus, any radioactive release from the zeolite itself arises solely from that ejected from the liner. However, upon attainment of the critical duration,

the fire is assumed to expose the liner's entire contents to the 1000°C thermal environment (a conservative assumption). Thus, radioactive release arises from all the remaining zeolite, whether inside the liner or ejected. Any radioisotopes released by this heating are assumed to become airborne and respirable. No credit is given for possible retention inside the breached liner.

B.2.4 Scenarios

The analysis presented so far indicates that the airborne, respirable release of radionuclides for any scenario can be viewed in three stages:

1. Initial release (denoted by $I_{x,i}$, where x indicates the scenario and i the isotope)--this is due solely to ejection of the unbound water. Since all the unbound water is presumed lost, this value will be the same for each scenario (eliminating the need for the subscript x).

2. Subcritical-fire-duration release--this is due solely to heating of any ejected zeolite (with a release rate denoted by $C_{x1,i}$).

3. Post-critical-fire-duration release--this is due to heating of both the ejected zeolite (with release rate $C_{x1,i}$) and that remaining inside the liner (with a release rate denoted by $C_{x2,i}$), in effect, all the zeolite.

Clearly, stages two and three do not apply to non-fire scenarios. Stage two is also not part of the fire-only scenario. From this model, it is possible to derive general expressions for the release amount for any scenario:

$$R_{x,i} = I_i \quad \text{(non-fire scenario)}$$

$$R_{x,i}(t) = \left\{ \begin{array}{l} I_i + C_{x1,i}t \quad \text{for } 0<t<t_o \\ I_i + C_{x1,i}t + C_{x2,i}(t-t_o) \\ \quad \text{for } t_o \leq t \leq t_{max} \\ \quad \text{where } t_o = \text{critical duration} \end{array} \right\} \quad \text{(Fire Scenarios)}$$

Note that $C_{x1,i} = 0$ for the fire-only scenario.

B.2.4.1 Fire Duration Intervals

Calculation of $R_{x,i}$ for the non-fire scenarios is straightforward. However, for the fire scenarios, $R_{x,i}(t)$ is a function of the fire duration which is itself probabilistically distributed. Furthermore, the fire scenarios are divided into duration intervals, over which there are as many values for $R_{x,i}(t)$ as there are durations t. Resolution of this difficulty requires consideration of the "expected" (probabilistically-weighted) releases for each duration interval.

It is first necessary to obtain the probability density function for the distribution of fire durations. Figure B.1 is approximated as a series of linear segments whose endpoints are as follow:

t	F(t) (in fractions, not %)
0	0
11.4	.585
15.3	.750
18.4	.830
21.8	.884
26.2	.929
30.0	.957
37.1	.974
60.0	.989
151	1.000 [this is assumed to be $F(t_{max} = 151)$]

With these values, the following equations are derived for the linear segments:

$0 \leq t \leq 11.4$	$F(t) = .0513t$
$11.4 \leq t \leq 15.3$	$F(t) = .0423t + .103$
$15.3 \leq t \leq 18.4$	$F(t) = .0258t + .355$
$18.4 \leq t \leq 21.8$	$F(t) = .0159t + .538$
$21.8 \leq t \leq 26.2$	$F(t) = .0102t + .661$
$26.2 \leq t \leq 30.0$	$F(t) = .00737t + .736$

$30.0 \leq t \leq 37.1$	$F(t) = .00239t + .885$
$37.1 \leq t \leq 60.0$	$F(t) = .000655t + .950$
$60.0 \leq t \leq 151$	$F(t) = .000121t + .982$

F(t) represents the cumulative density function for fires burning for a duration $\leq$ t. In other words, F(t) is the sum of the individual probability densities for fires burning for times τ up to duration t, or:

$$F(t) = \int_0^t f(\tau)d\tau$$

where $f(\tau)$ is the probability density function. f(t) is obtained from F(t) by taking the derivative, as follows:

$$f(t) = \frac{d}{dt} F(t)$$

For the line segments used to approximate F(t), f(t) is merely the slope at t.

t	f(t)
0-11.4	.0513
11.4-15.3	.0423
15.3-18.4	.0258
18.4-21.8	.0159
21.8-26.2	.0102
26.2-30.0	.00737
30.0-37.1	.00239
37.1-60.0	.000655
60.0-151	.000121

If drawn, f(t) would consist of a series of steps starting at (0, 0.513) and ending at (151, 0).

At any time t, the expected release for radioisotope i from scenario x is $[R_{x,i}(t)] = R_{x,i}(t)f(t)dt$. Two situations must be examined: $0 < t < t_o$ (subcritical fire) and $t_o \leq t \leq t_{max}$ (post-critical fire).

B.2.4.1.1 Subcritical

The expected release from all fires within the subcritical duration is:

$$[R_{x,i}(0 < \text{all } t < t_o)] = \int_0^{t_o} (I_i + C_{x1,i}t)f(t)dt$$

$$= (I_i + C_{x1,i}\,\overline{t}_s)\,F(t_o)$$

$$\text{where } F(t_o) = \int_0^{t_o} f(t)dt$$

$$\overline{t}_s = \int_0^{t_o} tf(t)dt/F(t_o) = 7.38 \text{ min}$$

$\overline{t}_s$ is interpreted as the mean fire duration for a subcritical fire. $F(t_o)$ is just the probability that a fire lasts less than 15.3 min., corresponding precisely to the term $p(\overline{E}/F)$ used in the scenario probabilistic expressions. Thus, the term $(I_I + C_{x1,i}\,\overline{t}_s)$ is the release amount for any subcritical fire scenario.

B.2.4.1.2 Post-Critical

The fire durations for the post-critical situation have been divided into three intervals. Denoting the endpoints of any interval as t_- and t_+, the expected release over this interval is as follows:

$$[R_{x,i}(t_- \leq \text{all } t \leq t_+)] =$$

$$\int_{t_-}^{t_+} [I_I + C_{x1,i}t + C_{x2,i}\,(t - t_o)]\,f(t)dt =$$

$$[I_I + C_{x1,i}\overline{t}_+ + C_{x2,i}\,(\overline{t}_+ - t_o)]\,[F(t_+) - F(t_-)]$$

$$\text{where} \quad F(t_+) = \int_0^{t_+} f(t)dt$$

$$F(t_-) = \int_0^{t_-} f(t)dt$$

$$\bar{t}_+ = \int_{t_-}^{t_+} tf(t)dt/[F(t_+) - F(t_-)]$$

$\bar{t}_+$ is interpreted as the mean fire duration over the interval t_- to t_+. For the three duration intervals in the post-critical situation, these values are as follow:

INTERVAL	t_-(min.)	t_+(min.)	$\bar{t}_+$(min.)
1	15.3	30.0	20.7
2	30.0	60.0	39.8
3	60.0	151	105.5

$[F(t_+) - F(t_-)]$ is just the probability that a fire lasts between t_- and t_+. When the values for t_- and t_+ are substituted, this term corresponds precisely to $p(E_1/F)$, $p(E_2/F)$, or $p(E_3/F)$ used in the probabilistic expression for each scenario interval. Thus, for each of the post-critical duration intervals, the term $[I_I + C_{x1,i}\bar{t}_+ + C_{x2,i}(\bar{t}_+ - t_o)]$ is the release amount when the appropriate value of $\bar{t}_+$ is substituted.

B.2.4.2 Release Rates for Scenarios Involving Fire

The release for each radioisotope involved in a fire scenario depends upon the fractional release rate and the amount of zeolite exposed. The fractional release rate for each radioisotope (^{89}Sr, ^{90}Sr, ^{134}Cs, and ^{137}Cs) has been estimated to be the same (1.9E-6/min.). The fire duration had been specified for each duration interval. Thus the amount of zeolite exposed will determine the differences in release rates among the various scenarios involving fire.

B.2.4.2.1 Fire-Only

In the fire-only scenario, all the zeolite, whether it be ejected from or retained within the breached liner, is assumed to experience the 1000°C thermal environment after attainment of the critical duration. Thus, the release rate for any radionuclide i will be:

$$C_{x2,i} = (1.9E\text{-}6/\text{min.})\ (\text{loading of isotope i in zeolite})$$

These are listed in terms of the amount airborne and respirable in Table B.4.

B.2.4.2.2 Impact-with-Fire

In the impact-with-fire scenario, the release rate will vary from the subcritical to the post-critical durations. Assuming 5% of the zeolite is initially ejected into the fire, only this portion is exposed during the subcritical duration. However, once the critical duration is reached, the remaining 95% inside the liner, in addition to the 5% already ejected, is assumed to feel the severe thermal environment. Thus, as in the fire-only scenario, all the zeolite is assumed to be exposed beyond the critical duration. The release rates for any radionuclide i will be:

$$C_{x1,i} = (.05)(1.9E\text{-}6/\text{min})(\text{loading of isotope i in zeolite})$$

$$C_{x2,i} = (.95)(1.9E\text{-}6/\text{min})(\text{loading of isotope i in zeolite})$$

These are listed in terms of the amount airborne and respirable in Table B.5.

B.2.4.2.3 Puncture-with-Fire

The release rates for the puncture-with-fire scenario are analogous to those for impact-with-fire, except for a difference in magnitude. Since the puncture breach is presumed smaller than that for impact, only 1% of the zeolite should be initially ejected into the fire. Thus, the release rates for any radionuclide i will be:

TABLE B.4. Estimated Airborne Release Rates in the Respirable Range for the Fire-Only Scenario

ISOTOPE	LOADING (Ci)	RELEASE RATE*(Ci/min)
^{89}Sr	.28	5.3E-7
^{90}Sr	2757	.0052
^{134}Cs	6012	.011
^{137}Cs	59410	.11

*At 1000°C

TABLE B.5. Estimated Airborne Release Rates in the Respirable Range for the Impact-with-Fire Scenario

ISOTOPE	LOADING (Ci)	RELEASE RATES* (Ci/min)	
		$C_{x1,i}$	$C_{x2,i}$
^{89}Sr	.28	2.7E-8	5.1E-7
^{90}Sr	2757	2.6E-4	.0050
^{134}Cs	6012	5.7E-4	.011
^{137}Cs	59410	.0056	.11

*At 1000°C, assuming 5% of zeolite ejected into the fire initially

$C_{x1,i}$ = (.01)(1.9E-6/min)(loading of isotope i in zeolite)

$C_{x2,i}$ = (.99)(1.9E-6/min)(loading of isotope i in zeolite)

These are listed in terms of the amount airborne and respirable in Table B.6.

Given equal fire durations, the airborne release in the respirable range for each radionuclide in the zeolite (^{89}Sr, ^{90}Sr, ^{134}Cs, and ^{137}Cs) will be largest for the impact-with-fire scenario. In addition to the 100% of the zeolite being exposed should the fire duration exceed critical, there is the additional exposure of 5% of the zeolite during the subcritical phase. Only 1% is so exposed in puncture-with-fire while there is no release during the subcritical phase for fire-only.

B.2.4.3 Scenario Releases

The releases (airborne and respirable) for each radioisotope are calculated for all the scenarios, including the duration intervals for those involving fire. The results are listed in Table B.7. As expected, the largest releases for the radionuclides in the zeolite are associated with the impact-with-fire scenario. The smallest, those for impact and puncture-only, are associated solely with the expulsion of unbound water. Since all 112 lb_m are assumed to be lost upon breach (regardless of breach size or accident force), these amounts are equal.

TABLE B.6. Estimated Airborne Release Rates in the Respirable Range for the Puncture-With-Fire Scenario

ISOTOPE	LOADING (Ci)	RELEASE RATES* (Ci/min) $C_{x1,i}$	$C_{x2,i}$
^{89}Sr	.28	5.3E-9	5.3E-7
^{90}Sr	2757	5.2E-5	.0052
^{134}Cs	6012	1.1E-4	.011
^{137}Cs	59410	.0011	.11

*At 1000°C, assuming 1% of zeolite ejected into the fire initially

TABLE B.7. Estimated Airborne Releases in the Respirable Range for All Accident Scenarios

	ACCIDENT SCENARIOS												
	FIRE ONLY			IMPACT ONLY	PUNCTURE ONLY	IMPACT WITH FIRE				PUNCTURE WITH FIRE			
	Fire Duration (min.)					Fire Duration (min.)				Fire Duration (min.)			
	15.3 - 30.0	30.0-60.0	60.0-151			0 - 15.3	15.3-30.0	30.0-60.0	60.0-151	0-15.3	15.3-30.0	30.0-60.0	60.0-151
^{3}H Release (Ci)	.047	.047	.047	.047	.047	.047	.047	.047	.047	.047	.047	.047	.047
^{60}Co Release (Ci)	2.5E-6	2.5E-6	2.5E-6	2.5E-6	2.5E-6	2.5E-6	2.5E-6	2.5E-6	2.5E-6	2.5E-6	2.5E-6	2.5E-6	2.5E-6
^{89}Sr Release (Ci)	3.1E-6	1.3E-5	4.8E-5	2.3E-7	2.3E-7	4.3E-7	3.5E-6	1.4E-5	4.9E-5	2.7E-7	3.2E-6	1.3E-5	4.9E-5
^{90}Sr Release (Ci)	.030	.13	.47	.0016	.0016	.0035	.034	.13	.48	.0020	.031	.13	.48
^{95}Nb Release (Ci)	2.0E-11	2.0E-11	2.0E-11	2.0E-11	2.0E-11	2.0E-11	2.0E-11	2.0E-11	2.0E-11	2.0E-11	2.0E-11	2.0E-11	2.0E-11
^{103}Ru Release (Ci)	1.0E-10	1.0E-10	1.0E-10	1.0E-10	1.0E-10	1.0E-10	1.0E-10	1.0E-10	1.0E-10	1.0E-10	1.0E-10	1.0E-10	1.0E-10
^{106}Ru Release (Ci)	4.3E-5	4.3E-5	4.3E-5	4.3E-5	4.3E-5	4.3E-5	4.3E-5	4.3E-5	4.3E-5	4.3E-5	4.3E-5	4.3E-5	4.3E-5
^{125}Sb Release (Ci)	6.6E-4	6.6E-4	6.6E-4	6.6E-4	6.6E-4	6.6E-4	6.6E-4	6.6E-4	6.6E-4	6.6E-4	6.6E-4	6.6E-4	6.6E-4
^{134}Cs Release (Ci)	.059	.27	.99	7.3E-5	7.3E-5	.0043	.071	.29	1.1	8.8E-4	.062	.27	1.0
^{137}Cs Release (Ci)	.59	2.7	9.9	6.9E-4	6.9E-4	.042	.71	2.9	11.	.0088	.62	2.7	10.
^{144}Ce Release (Ci)	6.3E-6	6.3E-6	6.3E-6	6.3E-6	6.3E-6	6.3E-6	6.3E-6	6.3E-6	6.3E-6	6.3E-6	6.3E-6	6.3E-6	6.3E-6

REFERENCES

1. Dennis, A. et al., Severities of Transportation Accidents Involving Large Packages. SAND77-0001; Sandia Laboratories (May 1978).

2. Whitesitt, J., Boolean Algebra and Its Applications; Addison-Wesley, Reading, MA (1961).

3. Elder, H. et al., An Assessment of the Risk of Transporting Spent Nuclear Fuel by Truck. PNL-2588; Pacific Northwest Laboratory (November 1978).

4. Campbell, D. et al., Evaluation of the Submerged Demineralizer System (SDS) Flowsheet for Decontamination of High-Activity-Level Water at Three Mile Island Unit 2 Nuclear Power Station. ORNL/TM-7448; Oak Ridge National Laboratory (July 1980).

5. Swift, W., Fission Product and Waste Packaging by Inorganic Zeolite Absorption. HW-73964; Hanford Laboratories Operation, GE, Richland, WA (1962).

6. Ames, L., Zeolite Extraction of Cesium from Aqueous Solutions. HW-62607; Hanford Atomic Products Operation, GE, Richland, WA (1959).

7. Reid, D., The Release of Radiocesium from Clinoptilolite by Elevated Temperature and Water Leaching. HW-74927; Hanford Laboratories Operation, GE, Richland, WA (1962).

8. Hilliard, R. and D. Reid, The Release of Radiocesium from Decalso at Elevated Temperatures. HW-69274; Hanford Laboratories Operation, GE, Richland, WA (1961).

APPENDIX C

ANALYSIS OF DOSE FROM RADIOACTIVE RELEASES

APPENDIX C

ANALYSIS OF DOSE FROM RADIOACTIVE RELEASES

C.1 ANALYSIS REQUIREMENTS

To estimate the dose to the exposed population along the transport route from the release of airborne, respirable radionuclides from potential transportation accidents, the following must be considered:

1. Atmospheric dispersal of the radionuclides
2. Dose to the critical organs from the radionuclides
3. Population distribution along the transportation route

Parameters for these are then combined with the results from the accident scenario analysis (probabilities and releases) to yield an estimate of the risk to the exposed population in terms of dose.

C.1.1 Atmospheric Dispersal

The atmospheric dispersal of airborne radionuclides is analyzed using the TRECII program.[1] It employs the Gaussian plume model to determine the isopleths downwind from the release. The diffusion climatology is specified for the inhalation pathway through the following variables: wind direction, wind speed, and atmospheric stability (Pasquill categories). Values for these have been incorporated directly into TRECII by averaging over reactor sites throughout the U.S. These default values are assumed for this assessment.

The height at which the release occurs can affect the population dose. A release height of 0 meters (ground level) is found to give the maximum dose. Thus, this value is conservatively assumed (a release originating near the ground is expected anyway). Another parameter affecting the dose is the minimum distance to the point of release allowed for the general public. A value of 20m. is assumed to be representative since it is expected that the general public would not be allowed very near to the accident site.

The release duration varies for each scenario, but TRECII allows for only one value to apply to all. The results are found to be insensitive to this so long as the actual release rates are used for each scenario. Thus, the maximum expected release time for any scenario (105.5 min. for the longest-duration fire) is assumed. Also, the minimum dose to an individual that will be considered is set at 100 mrem/yr, the average for natural background.

C.1.2 Critical Organs and Radioisotopes

The results from the accident scenario analysis indicate that eleven radionuclides are potentially released (Table B.7). However, TRECII allows a maximum of only five radioisotopes for dose analysis. Thus, these eleven isotopes must somehow be grouped into five categories for input into TRECII.

The dose depends upon both an organ's uptake of a radionuclide and the isotope's concentration. Thus, a reasonable measure of the relative effect of each isotope is the product of its released radioactivity (airborne and respirable) and its dose conversion factor (for 50-year inhalation dose) for each critical organ. TRECII allows for a maximum of five critical organs. Based on studies performed in previous transportation risk assessments, four are selected: total body, bone, lung, and thyroid.

The products of these two parameters are listed in Table C.1 for each radioisotope and critical organ. Since several isotopes (^{89}Sr, ^{90}Sr, ^{134}Cs, and ^{137}Cs) have releases that vary for different scenarios, the maximum releases that can occur are used in these calculations. The following four radioisotopes contribute most to the cumulative equivalent dose effects (excluding thyroid):

	% CONTRIBUTION TO CUMULATIVE EQUIVALENT DOSE EFFECT		
ISOTOPE	TOTAL BODY	BONE	LUNG
^{90}Sr	81	91	8.9
^{125}Sb	.0018	.0016	.39
^{134}Cs	2.9	.51	9.7
^{137}Cs	16	8.4	81

TABLE C.1. Equivalent Dose Effects to Critical Organs for Inhalation of Released Radioisotopes (Airborne, Respirable)

ISOTOPE	RELEASED* RADIOACTIVITY (Ci)	DOSE CONVERSION FACTORS** (rem-m^3/Ci-sec)				EQUIVALENT DOSE EFFECTS*** (rem-m^3/sec)			
		TOTAL BODY	BONE	LUNG	THYROID	TOTAL BODY	BONE	LUNG	THYROID
^{3}H	.047	.026	--	.026	.026	.0012	--	.0012	.0012
^{60}Co	2.5E-6	2.7	--	1000	--	6.8E-6	--	.0025	--
^{89}Sr	4.9E-5	3.4	30.	61.	--	1.7E-4	.0015	.0030	--
^{90}Sr	.48	690	2800	6.7	--	330	1300	3.2	--
^{95}Nb	2.0E-11	1.9	5.2	21.	--	3.8E-11	1.0E-10	4.2E-10	--
^{103}Ru	1.0E-10	.30	.63	23.	--	3.0E-11	6.3E-11	2.3E-9	--
^{106}Ru	4.3E-5	1.1	8.9	710	--	4.7E-5	3.8E-4	.031	--
^{125}Sb	6.6E-4	11.	35.	210	.0070	.0073	.023	.14	4.6E-6
^{134}Cs	1.1	11.	6.6	3.2	--	12.	7.3	3.5	--
^{137}Cs	11.	6.0	11.	2.6	--	66.	120	29.	--
^{144}Ce	6.3E-6	6.4	120	560	--	4.0E-5	7.6E-4	.0035	--
					CUMULATIVE	408	1427	35.9	.0012

*For radioisotopes whose release amounts vary, the maximum is used.

**50-year inhalation dose (from Reference 2).

***Products of released radioactivities and dose conversion factors.

Of the remaining seven radioisotopes, ^{95}Nb and ^{103}Ru make a negligible contribution to the cumulative equivalent dose effects. The remaining five (^{3}H, ^{60}Co, ^{89}Sr, ^{106}Ru, and ^{144}Ce) can be grouped together and an equivalent dose conversation factor calculated for each critical organ. Of the five radioisotopes, only ^{89}Sr has a variable release. The maximum value is used in these calculations to yield a conservative estimate of the equivalent factors. The results are summarized below for the five radioisotopes:

CRITICAL ORGAN	EQUIVALENT DOSE EFFECT (rem-m^3/sec)	EQUIVALENT DOSE* CONVERSION FACTOR (rem-m^3/Ci-sec)
TOTAL BODY	.0015	.032
BONE	.0026	.056
LUNG	.041	.87
THYROID	.0012	.026

*Calculated by dividing equivalent dose effect by release amount for entire group (.047 Ci)

These equivalent dose conversion factors are input into TRECII along with the dose conversion factors for the four other radioisotopes. These values are summarized in Table C.2. The potential impact of ^{90}Sr, especially to total body and bone, is evident.

With the original eleven radioisotopes now reduced to five, the release fraction and release rate (fraction/min.) are calculated for each isotope in each scenario and input into TRECII. The release rate is assumed uniform over the scenario duration. For the impact and puncture-only scenarios, a duration of 1 min. is assumed. For the remainder, all of which involve fire, the mean fire duration (7.38 min., 20.7 min., 39.8 min., or 105.5 min.) is used for each interval. The results are tabulated in Table C.3. The total amounts of each radioisotope assumed to be present at the start of shipment (January 1, 1982) are as follow:

TABLE C.2. Dose Conversion Factors for Five Radioisotopes Used in TRECII Dose Analysis

ISOTOPE	DOSE CONVERSION FACTOR** (rem-m^3/Ci-sec) TOTAL BODY	BONE	LUNG	THYROID
^{3}H*	.032	.056	.087	.026
^{90}Sr	690	2800	6.7	--
^{125}Sb	11.	35.	210	.0070
^{134}Cs	11.	6.6	3.2	--
^{137}Cs	6.0	11.	2.6	--

*This is a group of five isotopes: ^{3}H, ^{60}Co, ^{89}Sr, ^{106}Ru, and ^{144}Ce.

**50-year inhalation dose.

TABLE C.3. Fractional Releases and Release Rates for Radioisotopes (Airborne, Respirable) in Accident Scenarios

		ACCIDENT SCENARIOS												
		FIRE ONLY			IMPACT ONLY	PUNC. ONLY	IMPACT WITH FIRE				PUNCTURE WITH FIRE			
		MEAN SCENARIO DURATION (min.)												
		20.7	39.8	105.5	1.0	1.0	7.38	20.7	39.8	105.5	7.38	20.7	39.8	105.5
RELEASE FRACTION	^{3}H*	.14	.14	.14	.14	.14	.14	.14	.14	.14	.14	.14	.14	.14
	^{90}Sr	1.1E-5	4.7E-5	1.7E-4	5.8E-7	5.8E-7	1.3E-6	1.2E-5	4.7E-5	1.7E-4	7.3E-7	1.1E-5	4.7E-5	1.7E-4
	^{125}Sb	1.0	1.0	1.0	1.0	1.0	1.0	1.0	1.0	1.0	1.0	1.0	1.0	1.0
	^{134}Cs	9.8E-6	4.5E-5	1.6E-4	1.2E-8	1.2E-8	7.2E-7	1.2E-5	4.8E-5	1.8E-4	1.5E-7	1.0E-5	4.5E-5	1.7E-4
	^{137}Cs	9.9E-6	4.5E-5	1.7E-4	1.2E-8	1.2E-8	7.1E-7	1.2E-5	4.9E-5	1.9E-4	1.5E-7	1.0E-5	4.5E-5	1.7E-4
RELEASE RATE ($min.^{-1}$)	^{3}H*	.0068	.0035	.0013	.14	.14	.019	.0068	.0035	.0013	.019	.0068	.0035	.0013
	^{90}Sr	5.3E-7	1.2E-6	1.6E-6	5.8E-7	5.8E-7	1.8E-7	5.8E-7	1.2E-6	1.6E-6	9.9E-8	5.3E-7	1.2E-6	1.6E-6
	^{125}Sb	.048	.025	.0095	1.0	1.0	.14	.048	.025	.0095	.14	.048	.025	.0095
	^{134}Cs	4.7E-7	1.1E-6	1.5E-6	1.2E-8	1.2E-8	9.8E-8	5.8E-7	1.2E-6	1.7E-6	2.0E-8	4.8E-7	1.1E-6	1.6E-6
	^{137}Cs	4.8E-7	1.1E-6	1.6E-6	1.2E-8	1.2E-8	9.6E-8	5.8E-7	1.2E-6	1.8E-6	2.0E-8	4.8E-7	1.1E-6	1.6E-6

*Includes ^{3}H, ^{60}Co, ^{89}Sr, ^{106}Ru, and ^{144}Ce

$^{3}H^{*}$ = .33 Ci (includes .28 Ci of ^{89}Sr)

^{90}Sr = 2757 Ci

^{125}Sb = 6.6E-4 Ci

^{134}Cs = 6012 Ci

^{137}Cs = 59410 Ci

These are input into TRECII. TRECII allows for a maximum of eight release-rate categories for all the scenarios. Thus, since there are 13 scenarios, it is necessary to regroup the release rates into eight classes. This is accomplished by noting similarities in the sets of release rates for the five radioisotopes among the 13 scenarios. The scenarios are regrouped as follow:

Release-Rate Category	Base Case	Other Scenarios Included
1.	Puncture-with-fire (20.7 min.)	Fire-only (20.7 min.)
2.	Fire-only (39.8 min.)	Puncture-with-fire (39.8 min.)
3.	Impact-with-fire (105.5 min.)	Fire-only (105.5 min.) Puncture-with-fire (105.5 min.)
4.	Impact-only	Puncture-only
5.	Impact-with-fire (7.38 min.)	--
6.	Impact-with-fire (20.7 min.)	--
7.	Impact-with-fire (39.8 min.)	--
8.	Puncture-with-fire (7.38 min.)	--

The probability (per shipment) of an airborne, respirable release is input into TRECII for each accident scenario (these are listed in Table B.2). Also input is the number of shipments (2). The remaining input is related to the population distribution and route.

C.1.3 Population Distribution

The shipping route from TMI to PNL for the two shipments of radioactive zeolite liners is shown in Figures 3.5 through 3.7. An estimate of the population distribution along this route is obtained from PNL's POPCOR program. The shipping route is divided into a series of straight-line segments whose endpoints are specified by their corresponding latitudes and longitudes. Each segment is further subdivided into increments of a specified length. Assignment of an equal distance on either side of the segment completes the description of the corridor over which the population density is to be calculated for that segment. Thus, each increment corresponds to an area determined by its length and the assigned width.

For each area along the route, POPCOR scans a data base of census enumeration districts and records the population density range into which that area falls. These are tabulated for the entire route, yielding percentages for each population density range. POPCOR allows for 13 such ranges, number 1 extending down to 0 persons/km^2 and number 13 extending theoretically to an unlimited number of people/km^2. For the TMI-PNL route, the population density ranges are listed in Table C.4. Two corridor widths are considered for the route--2 km (1 km to either side) and 10 km (5 km to either side). The percent of the total route comprised of each density range is tabulated for both widths, as shown in Table C.4.

The census data used in POPCOR is based on the 1970 census. To compensate for any underestimate this introduces, the upper limit of each density range is presumed to characterize that range. For example, for the 10-km width, 8.0% of the shipping route is presumed to be characterized by a population density of 300 people/km^2. Using these upper bounds for the density ranges, the average population densities over the entire route for the 2 and the 10-km widths are calculated to be 109 and 141 people/km^2

TABLE C.4. Percentages for Population Density Ranges over the Shipping Route

CORRIDOR WIDTH (km)	POPULATION DENSITY RANGES (people/km^2)												
	0-1	1-10	10-30	30-60	60-100	100-300	300-600	600-1000	1000-1300	1300-1600	1600-2000	2000-2500	2500+
2	60.	3.3	7.2	11.	3.6	7.2	5.5	1.9	.83	.28	0	.28	0
10*	28.	17.	19.	12.	5.8	8.0	6.1	2.2	1.4	.55	.55	0	0

* The values for this width are selected for input into TRECII.

respectively. Thus, the 10-km width yields a higher overall route density. It also is more representative of the distance over which an airborne, radioactive release in the respirable range can affect the exposed population. Therefore, the population density ranges over the transport route and their percentages (interpreted as probabilities) for the 10-km width are selected as input into the TRECII program. This represents the population that is assumed to be exposed to any release.

C.2 SENSITIVITY ANALYSIS

A sensitivity analysis is performed by assuming the maximum estimable airborne release of radionuclides in the respirable range (.12% of the total radioactivity of each nuclide in the zeolite) occurs for the longest fire durations. As discussed in section B.2.3, this release is a maximum for zeolite exposure to a 1000°C fire regardless of duration. This release is conservatively presumed to occur for the duration interval of 60-151 minutes.

The maximum estimable releases for ^{89}Sr, ^{90}Sr, ^{134}Cs, and ^{137}Cs are listed in Table C.5. The values for the latter three are substituted directly into the input for TRECII as part of the longest duration intervals for scenarios involving fire. The ^{89}Sr release must be incorporated into the results for the other four isotopes with which it is grouped. Its value of 3.4E-4 Ci does not raise the release amount for the $^{3}H^{*}$ group measurably (.047 Ci). However, it does alter the equivalent dose conversion factors for total body, lung, and especially bone. These are listed below.

Critical Organ	Equivalent Dose Effect (rem-m^3/sec)	Equivalent Dose Conversion Factor (rem-m^3/Ci-sec)
Total Body	.0025	.053
Bone	.011	.24
Lung	.058	1.2

TABLE C.5. Maximum Estimable Releases (Airborne, Respirable) and Fractional Release Rates for Radioisotopes Exposed to Longest Duration Fire

ISOTOPE	TOTAL RADIOACTIVITY (Ci)	MAXIMUM ESTIMABLE RELEASES		
		AMOUNT (Ci)	FRACTION	FRACTIONAL* RELEASE RATE (min^{-1})
^{89}Sr	.28	3.4E-4	.0012	1.1E-5**
^{90}Sr	2757	3.3	.0012	1.1E-5
^{134}Cs	6012	7.2	.0012	1.1E-5
^{137}Cs	59410	71.	.0012	1.1E-5

*Assumed to occur over 105.5 min.

**This value is not input directly into TRECII because the ^{89}Sr release must first be combined with others in the ^{3}H* radionuclide group.

Thus, the increased release of ^{89}Sr does not alter the release amount (or rate) for the ^{3}H* group. Its only effect upon the TRECII input is to raise the equivalent dose conversion factors for total body, bone, and lung in the ^{3}H* group.

REFERENCES

1. Franklin, A., TRECII: A Computer Program for Transportation Risk Assessment. PNL-3208; Pacific Northwest Laboratory (May 1980).

2. Elder, H. et al., An Assessment of the Risk of Transporting Spent Nuclear Fuel by Truck. PNL-2588; Pacific Northwest Laboratory (November 1978).

APPENDIX D

RISK ASSESSMENT OF ALTERNATE SHIPPING ROUTE

APPENDIX D

RISK ASSESSMENT OF ALTERNATE SHIPPING ROUTE

D.1 CENTRAL SHIPPING ROUTE

The risk associated with shipping the two radioactive zeolite liners along a more southerly route than the one specified in section 3.3 is estimated. For convenience, this alternate route will be referred to as the "central" route (since it traverses the central portions of the U.S.) while the former will be called the "northern" route.

The central route is shown in Figure D.1. Its intended use is during wintertime when more adverse weather conditions might beset the northern one. The central route is approximately 200 miles longer than the northern, bringing its total length to about 2,800 miles. This increase is about 8%. As for the northern route, a shipping time of less than one week is anticipated.

D.2 ACCIDENT PROBABILITIES AND RELEASES

The increased length of the central route as opposed to the northern results in a slightly higher probability of a truck accident involving a large package. While the truck accident rate per shipment per mile remains the same as before, $\lambda(A)$ = 2.5E-6/shipment-mile[1], the probability of an accident per shipment increases around 8% due to the longer distance, $p(A)$ = .0070/shipment as opposed to .0065/shipment for the northern route. Since the data base from which these values are derived has already grouped together highway accidents during all weather conditions, any expectation of less adverse weather along the central route during the winter is not directly assimilated into the accident probability. However, it is believed that this value for the central route is conservative.

The accident scenarios are the same as before. Thus, for each scenario, the probability of a radioactive release per accident and the amount and rate of release remain the same as for the northern route [see Tables 4.3 (first row) and 5.1]. However, the release probability per shipment for each scenario increases slightly (about 8%) due to the increased accident probability. These are listed in Table D.1.

FIGURE D.1. Alternate Transportation Route from TMI to PNL

TABLE D.1. Probabilities of Occurrence of Accident Scenarios for Central Route

	ACCIDENT SCENARIOS												
	FIRE ONLY			IMPACT ONLY	PUNCTURE ONLY	IMPACT WITH FIRE				PUNCTURE WITH FIRE			
	Fire Duration (min.)					Fire Duration (min.)				Fire Duration (min.)			
	15.3-30.0	30.0-60.0	60.0-151			0-15.3	15.3-30.0	30.0-60.0	60.0-151	0-15.3	15.3-30.0	30.0-60.0	60.0-151
SCENARIO PROB.* (PER ACCIDENT)	.0034	5.3E-4	1.8E-4	.0088	2.4E-5	3.3E-5	9.2E-6	1.5E-6	4.8E-7	9.0E-8	2.5E-8	4.0E-9	1.3E-9
SCENARIO PROB. (PER SHIPMENT)	2.4E-5	3.7E-6	1.2E-6	6.2E-5	1.7E-7	2.3E-7	6.5E-8	1.0E-8	3.4E-9	6.3E-10	1.8E-10	2.8E-11	9.2E-12

* These remain unchanged from the values for the northern route.

D.3 POPULATION DISTRIBUTION

As for the northern route, the population distribution along the central one is estimated from PNL's POPCOR program. The same 13 density ranges are selected along with the same two corridor widths, 2 km (1 km to either side) and 10 km (5 km to either side). The percent of the total route comprised of each density range is tabulated for both widths, as shown in Table D.2.

Using the upper bound of each density range to characterize that range, the average population densities over the entire route for the 2 and the 10-km widths are calculated to be 108 and 124 people/km^2 respectively. Compared to the corresponding values for the northern route (109 and 141 people/km^2 respectively), that for the 2-km width is found to be virtually the same while that for the 10-km width is approximately 12% less. Thus, within 1 km to either side of the route, the population density is about the same for both routes. However, within 5 km to either side, the central route has a lower population density by about 12%. As before, the population density ranges and percentages (interpreted as probabilities) for the 10-km width are selected as input into the TRECII program[2].

D.4 RISK ESTIMATES

The risk for shipping the two zeolite liners by truck is again estimated through the TRECII program, with appropriate input modifications to reflect the central route. Only the following input parameters change relative to the original analysis of the northern route: shipping distance, accident scenario probabilities (per shipment), and probabilities for population density ranges. All others, including those related to atmospheric dispersal, critical organs, and dose conversion factors, remain the same. TRECII uses data for wind direction, wind speed, and atmospheric stability which are averaged over the entire U.S. Thus, they are not modified for the central route.

The risk is again measured in terms of the 50-year inhalation dose (man-rems) to the exposed population (along the central route) resulting from the two shipments. Both forms are presented for the risk estimates:

TABLE D.2. Percentages for Population Density Ranges over the Central Shipping Route

CORRIDOR WIDTH (km)	POPULATION DENSITY RANGES (people/km^2)												
	0-1	1-10	10-30	30-60	60-100	100-300	300-600	600-1000	1000-1300	1300-1600	1600-2000	2000-2500	2500+
2	60.	3.9	6.7	7.9	5.2	9.4	3.0	1.7	.99	.25	.74	0	0
10*	28.	19.	18.	12.	5.4	8.6	5.4	1.5	.99	.49	.49	0	0

* The values for this width are selected for input into TRECII.

the complementary cumulative density function and the total risk (expected dose). Results are presented for both the base and upper-bound (maximum estimable release) cases.

D.4.1 Complementary Cumulative Density Function

The complementary cumulative density function for the two shipments from TMI to PNL along the central route is shown on Figure D.2 as a dotted line for each case. The previous curve for the northern route is shown for each case as a solid line. As before, the base-case curve spans the following range of values: probabilities below 2E-5 and doses below 0.7 man-rem. The largest estimated dose is 0.7 man-rem from the least-likely scenario (probability of 1E-9 for two shipments). Similarly, the upper-bound-case curve spans the same range of values as before: probabilities below 2E-5 and doses below 5 man-rem. The largest estimated dose is 5 man-rem for the least-likely scenario (probability of 1E-9 for two shipments).

Figure D.2 indicates a slight reduction in risk in both cases for shipment along the central rather than the northern route over nearly the entire dose range (no reduction evident at maximum doses). A quantitative estimate of this reduction is presented in the next section. Qualitatively, this is due to the decrease in population density outweighing the increase in accident probability (per shipment) due to the longer route.

D.4.2 Total Risk (Expected Dose)

For the two shipments of radioactive zeolite liners via the central route, the probability of occurrence of an airborne, respirable release is raised slightly to 1.8E-4 relative to the value of 1.7E-4 for the northern route. This is a result of the increased route distance. However, the total expected doses decrease slightly for the central route in both the base and upper-bound cases relative to the northern route values. Both decreases amount to approximately 6%. In the base case, the central route has a total risk of 5.0E-7 man-rem, compared to 5.3E-7 man-rem for the northern route. In the upper-bound case, the central route has a value of 6.4E-7 man-rem, compared to 6.8E-7 man-rem for the northern.

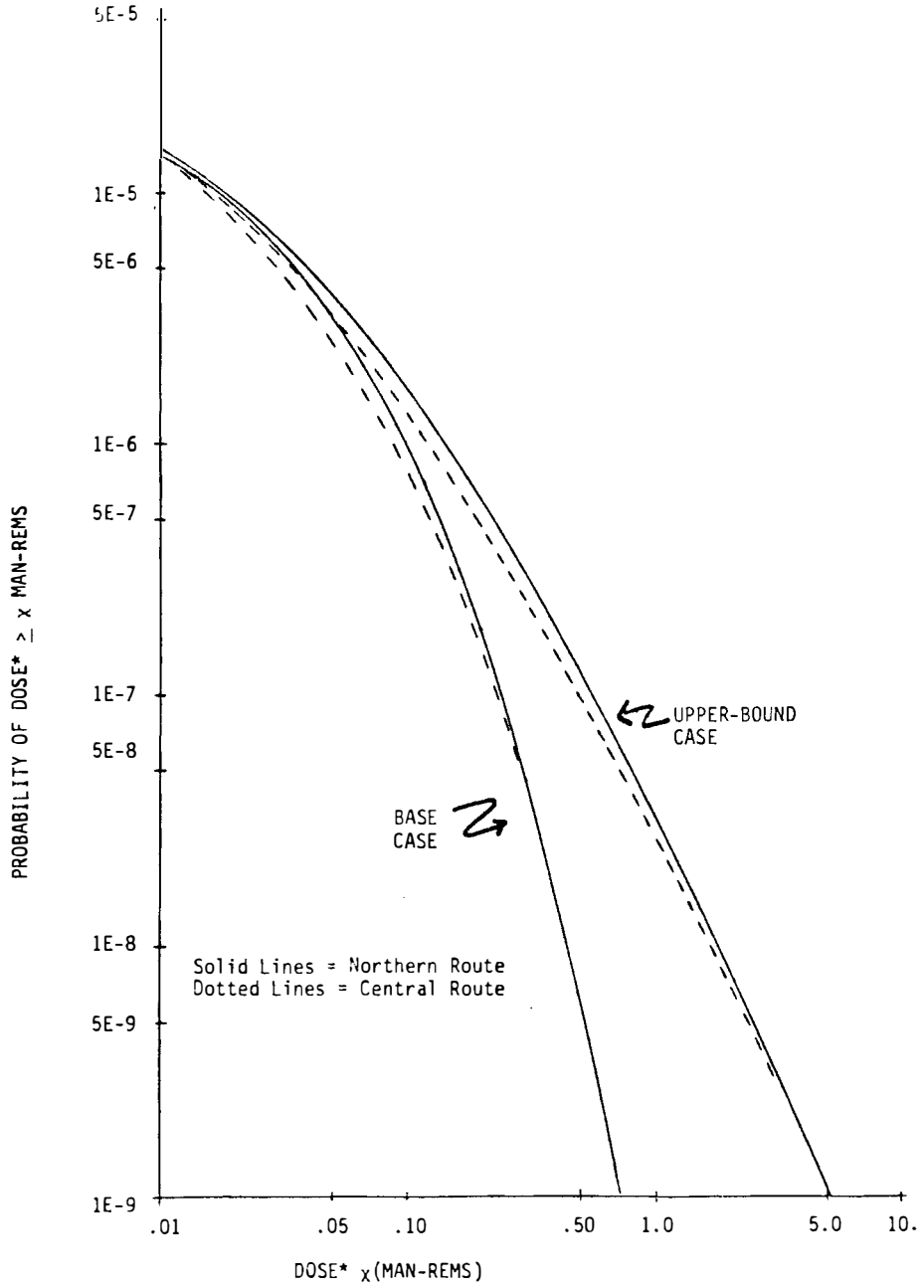

* 50-yr. inhalation dose to exposed population

D-7

FIGURE D.2. Complementary Cumulative Density Function for Two Shipments Showing Results for Both Northern and Central Routes

These decreases can be explained quantitatively as follows. For the central route, the probability of an accident is roughly 8% higher due to the longer distance. However, the average population density along this route is about 12% lower. Since these are combined multiplicatively to estimate the total risk, this value for the central route should be approximately (1.08) (.88) = .95, or 95%, of that for the northern, a decrease of roughly 5%.

D.4.3 Dominant Accident Scenarios

Since the probabilities of occurrence and the release amounts and rates for the various scenarios have not changed relative to one another, the relative contributions to the total risk from each scenario and each radionuclide are not expected to change. This is verified by the TRECII analysis for the central route. Thus, the percent contributions to the total expected dose listed in Tables 5.4 and 5.6 for the northern route are the same for the central. Consequently, as discussed in sections 5.1.3 and 5.2.3, the impact-only scenario and ^{90}Sr release dominate the total risk in both the base and upper-bound cases.

D.5 CONCLUSIONS

To place these risk estimates into perspective, comparisons are made with natural background radiation along the shipping route and with the total risk from postulated accidents involving spent fuel shipment. The analysis follows that of section 5.3.

D.5.1 Natural Background Radiation Comparison

A comparison is made with the average level of natural background radiation (0.1 rem/person/year) to the appropriate population along the central route. This is done for both the total expected dose and the maximum dose from the least-likely scenario in the upper-bound case.

As for the northern route, the average isopleth area for the central one is 90.6 km^2. For the central's average population density of 124 people/km^2 over the entire route (see section D.3, 10-km width), the number of people exposed over the average isopleth area is 1.1E+4. If each

receives the average level of natural background exposure (0.1 rem/year), the population dose over one year is estimated as 1100 man-rem from natural background. This is about 12% less than the natural background estimate for the northern route (1300 man-rem) due to the lower population density.

For the central route's upper-bound case, the total expected dose to the exposed population has been estimated at 6.4E-7 man-rem. Compared to the population dose from natural background for the people in the average isopleth area (1100 man-rem), this total risk is clearly an insignificant fraction (5.8E-10). While this value of 6.4E-7 man-rem is about 6% less than that for the northern route, it does comprise a slightly (about 12%) higher, although still very negligible, fraction of the natural background exposure along the central route (5.8E-10 compared to 5.2E-10 for the northern route). The reason is that the decrease in population density (and, thus, natural background exposure) outweighs the decrease in total risk for the central route.

Corresponding to the maximum dose from the least-likely scenario in the upper-bound case (5 man-rem at a probability of 1E-9 for two shipments) is an isopleth area of 207 km^2 for the central route. This dose results from exposure over this area when the population density is in the maximum range (an upper limit of 2000 people/km^2 for a 10-km width, see Table D.2). Using this upper limit, the number of people exposed over this isopleth area is estimated as 4.1E+5. Attributing the average level of natural background exposure (0.1 rem/year) to each person, the one-year population dose is estimated as 4.1E+4 man-rem from natural background, the same as for the northern route. The maximum dose of 5 man-rem is found to be an insignificant fraction (1.2E-4) of this natural background dose, this fraction being the same as for the northern route.

D.5.2 Spent Fuel Shipping Comparison

As was done for the northern route, the total risk for the central route's upper-bound case is compared to that from postulated accidents involving truck shipment of long-cooled spent fuel. As derived from Table 5.7 (reproduced from reference 3), the total expected dose from spent fuel transportation accidents is 9.1E-8 man-rem/shipment-km (same as

before). While the number of zeolite shipments is the same for the central route (2), the shipping distance is longer (2800 miles or 4500 km). Thus, the total risk for spent fuel shipment becomes 8.2E-4 man-rem on a normalized basis. This is about 8% higher than that for a base normalized to the northern route (7.6E-4 man-rem) due to the longer distance.

The total risk for the zeolite upper-bound case is 6.4E-7 man-rem for the central route. Comparison indicates that the total expected dose from the zeolite shipment comprises a very small fraction (7.8E-4) of that from the spent fuel shipment on a normalized basis. This fraction is approximately 12% less than that for the northern route (8.9E-4) due to the relative decrease in total risk for the zeolite upper-bound case (about 6% compared to the northern route) and the relative increase in the total risk for the spent fuel shipment (around 8% compared to the northern route) when normalized to the central route. As before, the total risk from potential accidents in the transport of the two zeolite liners is less than .001 of that from spent fuel.

As for the northern route, it is concluded that the transportation of radioactive zeolite liners from TMI to PNL by truck along the central route can be accomplished at an insignificant level of risk to the public. Relative to the northern route, the total risk for the central shows a slight decrease. A small decrease in the fraction of the total risk associated with a comparative spent fuel shipment is also evident for the central route. This route does show a small increase in the fraction of natural background dose attributable to it. However, within the limits of accuracy associated with risk assessment, both routes present essentially the same risk -- insignificant.

REFERENCES

1. Dennis, A. et al., Severities of Transportation Accidents Involving Large Packages. SAND77-0001; Sandia Laboratories (May 1978).

2. Franklin, A., TRECII: A Computer Program for Transportation Risk Assessment. PNL-3208; Pacific Northwest Laboratory (May 1980).

3. Greenborg, J. et al., Application of ALARA Principles to Shipment of Spent Nuclear Fuel. PNL-3261; Pacific Northwest Laboratory (May 1980).

DISTRIBUTION

No. of Copies

OFFSITE

S. W. Ahrends
DOE Oak Ridge Operations Office
P. O. Box E
Oak Ridge, TN 37830

A. A. Anselmo
EG&G Idaho
P. O. Box 88
Middleton, PA 17057

A. L. Ayers
EG&G Idaho
P. O. Box 1625
Idaho Falls, ID 83415

J. R. Berreth
Exxon Nuclear Idaho
P. O. Box 2800
Idaho Falls, ID 83401

M. D. Boersma
E. I. Du Pont de Nemours & Company
Savannah River Laboratory
Aiken, SC 29801

J. A. Buckham
Allied-General Nuclear Services
P. O. Box 847
Barnwell, SC 29812

H. M. Burton
EG&G Idaho
P. O. Box 88
Middletown, PA 17057

J. Campbell
Lawrence Livermore Laboratory
P. O. Box 808
Livermore, CA 94550

No. of Copies

W. Carbiener
Battelle Memorial Institute
Office of Nuclear Waste Isolation
505 King Avenue
Columbus, OH 43201

A. A. Churm
DOE Chicago Patent Group
9800 South Cass Avenue
Argonne, IL 60439

J. L. Clark
EG&G Idaho Inc.
P. O. Box 1625
Idaho Falls, ID 83415

C. R. Cooley
DOE Nuclear Waste Management Programs
NE-331, GTN
Washington, D.C. 20545

R. E. Cunningham
Office of Nuclear Safety Materials and Safeguards
Nuclear Regulatory Commission
Room 562, 7915 Eastern Avenue
Silver Springs, MD 20910

G. H. Daly
DOE Nuclear Waste Management Programs
NE-322, GTN
Washington, D.C. 20545

C. P. Deltete
GPU
P. O. Box 480
Middletown, PA 17057

R. F. Garrison
DOE
NE-340
Washington, D.C. 20545

No. of
Copies

J. E. Dieckhoner
DOE Nuclear Waste Management
Programs
NE-321, GTN
Washington, D.C. 20545

27 DOE Technical Information Center

Environmental Protection Agency
Technological Assessment
Division (AW-559)
Office of Radiation Programs
U.S. Environmental Protection
Agency
Washington, D.C. 20460

R. G. Garvin
E. I. Du Pont de Nemours
& Company
Savannah River Laboratory
Aiken, SC 29801

C. H. George
DOE Nuclear Waste Management
Programs NE-330, GTN
Washington, D.C. 20545

P. Hagen
Chemical Operations
Rockwell International
Rocky Flats Plant
P. O. Box 464
Golden, CO 80401

J. P. Hamric
DOE Idaho Operations
Office
550 Second Street
Idaho Falls, ID 83401

S. G. Harbinson
DOE San Francisco Operations
Office
1333 Broadway
Oakland, CA 94612

No. of
Copies

C. A. Heath
DOE Nuclear Waste Management
Programs
NE-330, GTN
Washington, D.C. 20545

L. L. Hench
Department of Materials
Science and Engineering
University of Florida
Gainesville, FL 32611

R. E. Holyworth
EG&G Idaho
P. O. Box 88
Middletown, PA 17057

R. G. Kepler
Organic and Electronic
Department 5810
Sandia Laboratories
Albuquerque, NM 87185

J. H. Kittel
Argonne National Laboratory
Office of Waste Management
Programs
9700 South Cass Avenue
Argonne, IL 60439

D. E. Large
DOE Oak Ridge Operations
Office
P. O. Box E
Oak Ridge, TN 37830

M. L. Lawrence
DOE Nuclear Waste Management
Programs
NE-340, GTN
Washington, D.C. 20545

A. L. Lotts
Oak Ridge National Laboratory
P. O. Box X
Oak Ridge, TN 37830

No. of
Copies

R. Y. Lowrey
DOE Albuquerque Operations
Office
P. O. Box 5400
Albuquerque, NM 87185

P. B. Macedo
Keane Hall
Vitreous State Laboratory
The Catholic University of
America
Washington, D.C. 20017

R. Maher
Waste Management Programs
Savannah River Plant
E. I. Du Pont de Nemours
& Company
Aiken, SC 29801

S. A. Mann
DOE Chicago Operations and
Region Office
Argonne, IL 60439

A. B. Martin
Rockwell International
Energy Systems Group
8900 DeSoto Avenue
Canoga Park, CA 91304

J. B. Martin
Division of Waste Management
Nuclear Regulatory Commission
Washington, D.C. 20555

D. J. McGoff
DOE Nuclear Waste Management
Programs
NE-320, GTN
Washington, D.C. 20545

D. L. McIntosh
E. I. Du Pont de
Nemousr and Company
Savannah River Laboratory
Aiken, SC 29801

No. of
Copies

S. Meyers
DOE Nuclear Waste Management
Programs
NE-340, GTN
Washington, D.C. 20545

W. E. Mott
DOE
EP-142
Washington, D.C. 20545

J. O. Neff
Department of Energy
Columbus Program Office
505 King Avenue
Columbus, OH 43201

G. Oertel
DOE Nuclear Waste Management
Programs
NE-320, GTN
Washington, D.C. 20545

H. Palmour III
2140 Burlington Enginerring
Laboratories
North Carolina State
University
Raleigh, NC 27607

J. W. Peel
DOE Idaho Operations
Office
550 Second Street
Idaho Falls, ID 83401

A. F. Perge
DOE Nuclear Waste Management
Programs
NE-301, GTN
Washington, D.C. 20545

J. H. Pletscher
EG&G Idaho
P. O. Box 88
Middletown, PA 17057

No. of
Copies

R. W. Ramsey, Jr.
DOE Nuclear Waste Management
Programs
NE-301, GTN
Washington, D.C. 20545

B. Rawles
Battelle Memorial Institute
Office of Nuclear Waste
Isolation
505 King Avenue
Columbus, OH 43201

Research Library
Battelle Memorial Institute
505 King Avenue
Columbus, OH 43201

G. L. Ritter
Exxon Nuclear Idaho
P. O. Box 2800
Idaho Falls, ID 83401

R. Roy
202 Materials Research
Laboratory
Pennsylvania State University
University Park, PA 16802

D. B. Rohrer
Division of Waste Management
Nuclear Regulatory Commission
Washington, D.C. 20555

R. Romatowski
DOE Nuclear Waste Management
Programs
NE-30, GTN
Washington, D.C. 20545

T. C. Runion
EG&G Idaho
P. O. Box 88
Middletown, PA 17057

No. of
Copies

R. D. Smith
Division of Waste Management
Nuclear Regulatory Commission
Washington, D.C. 20555

M. J. Steindler/L. E. Trevorrow
Argonne National Laboratory
9700 South Cass Avenue
Argonne, IL 60439

A. L. Taboas
DOE Albuquerque Operations
Office
P. O. Box 5400
Albuquerque, NM 87185

V. Trice
DOE Nuclear Waste Management
Program
NE-30, GTN
Washington, D.C. 20545

E. Vejvoda
Chemical Operations
Rockwell International
Rocky Flats Plant
P. O. Box 464
Golden, CO 80401

D. L. Vieth
DOE Nuclear Waste Management
Programs
NE-332, GTN
Washington, D.C. 20545

R. P. Whitfield
DOE Savannah River Operations
Office
P. O. Box A
Aiken, SC 29801

J. B. Whitsett
DOE Idaho Operations Office
550 Second Street
Idaho Falls, ID 83401

No. of
Copies

A. Williams
Allied-General Nuclear Services
P. O. Box 847
Barnwell, SC 29812

R. Williams
Electric Power Research
Institute
3412 Hillview Avenue
Palo Alto, CA 94304

W. B. Wilson
DOE Savannah River Operations
Office
P. O. Box A
Aiken, SC 29801

ONSITE

DOE Richland Operations Office
J. M. Peterson
P. A. Craig
R. E. Gerton
H. E. Ransom
S. K. Moy
Rockwell Hanford Operations

R. E. Smith

55 Pacific Northwest Laboratory

W. B. Andrews
W. J. Bjorklund
H. T. Blair
W. F. Bonner
D. W. Brite
R. A. Brouns
G. H. Bryan
M. J. Budden
J. L. Buelt
J. R. Carrell
J. G. Carter
L. A. Chick
T. D. Chikalla
R. D. Dierks
L. R. Dodd

No. of
Copies

Pacific Northwest Laboratory (contd)

G. J. Exarhos
J. F. Friley
R. H. V. Gallucci (5)
A. J. Haverfield
L. K. Holton
J. H. Jarrett
D. E. Knowlton
C. A. Knox
L. T. Lakey
D. E. Larson
R. O. Lokken
R. P. Marshall
J. L. McElroy
G. B. Mellinger
J. E. Mendel
T. A. Nelson
J. F. Nesbitt
R. E. Nightingale
R. D. Peters
A. M. Platt
R. E. Rhoads
J. M. Rusin
D. H. Siemens
S. C. Slate
S. L. Sutter
C. L. Timmerman
R. L. Treat
R. P. Turcotte
J. W. Wald
Technical Information (5)
Publishing Coordination (2)